THE UNIVERSITY OF MICHIGAN

INDUSTRY PROGRAM OF THE COLLEGE OF ENGINEERING

HEAT TRANSFER FROM GAS FLAMES IN COOLED TUBES

Donald W. Sundstrom

A dissertation submitted in partial fulfillment
of the requirements for the degree of
Doctor of Philosophy in the
University of Michigan
1958

June, 1958

IP-296

Doctoral Committee:

Professor Stuart W. Churchill, Chairman
Professor Jay A. Bolt
Assistant Professor Edward E. Hucke
Assistant Professor Don E. Rogers
Professor Robert R. White

ACKNOWLEDGEMENTS

I wish to express my appreciation to:

The doctoral committee for their advice and assistance during this investigation.

Dr. S. W. Churchill, the chairman of the doctoral committee, for his interest, suggestions, and encouragement.

Esso Research and Engineering Company for its financial support of this research.

General Electric Company for providing fellowships for two years.

The Industry Program of the College of Engineering, for its help in reproduction of this report.

TABLE OF CONTENTS

TABLE OF CONTENTS (CONT'D)

TABLE OF CONTENTS (CONT'D)

LIST OF FIGURES

LIST OF FIGURES (CONT'D)

LIST OF FIGURES (CONT'D)

NOMENCLATURE

a = speed of sound, ft/sec.

A = area, ft.^{2}

b = constants in temperature integration

B = constants in frequency derivation

c_x = constants in convective equation

C = constants in frequency derivation

C_{ps} = heat capacity of species S, Btu/lb. °F.

$\overline{C}_p$ = mean heat capacity of mixture, Btu/lb. °F.

D = diameter, ft.

Db = sound level, decibels

E = combustion efficiency, fraction of available heat released by chemical reaction.

f = sound frequency, cycles/sec.

F = real constant in conformal transformation

F_D = drag of flame holder and tube walls, lb. force

g_c = conversion factor, ft (lb. mass)/(lb. force) sec.^{2}

G = mass velocity, lbs/hr. ft.^{2}

h = heat transfer coefficient, Btu/hr. ft.^{2} °F.

k = thermal conductivity, Btu/hr. ft. °F.

l = integer in frequency equation for radial modes of oscillation

L = length, ft.

L_b = burning length between flame holder and test object exit, ft.

L_t = total tube length between plenum chamber and test object exit, ft.

L' = mean beam length, ft.

m = integer in frequency equation for tangential modes of oscillation.

$\overline{M}$ = average molecular weight of mixture, lbs/lb. mol.

n = integer in frequency equation for axial modes of oscillation

N = lb. mols.

Nu = Nusselt number, hD/k, dimensionless

P = absolute pressure, psia

$\overline{P}$ = pressure amplitude of sound wave, psia.

P_D = pressure drop due to drag, of flame holder and tube walls, psia.

Pr = Prandtl number, $C_p \mu/k$, dimensionless

q = heat transfer rate, Btu/hr.

$(q/A)_s$ = heat transfer rate at inside surface of tube, Btu/hr. ft.^{2}

Q_t = heat transfer to tube wall, Btu/lb.

$Q_r(T_o)$ = heat released due to chemical reaction at reference temperature, T_o, Btu/lb.

$Q_R(T_o)$ = heat released by complete combustion at reference temperature To, Btu/lb.

r = radius, ft.

R_o = gas law constant

Re = Reynolds' number, DG/μ dimensionless

S = complex constant in conformal transformation

t = time, hr.

t = temperature (when used with subscribt), °F

T = absolute temperature, °R

u = linear velocity, ft/hr.

U = overall heat transfer coefficient, Btu/hr.ft.^{2} °F.

U,U',U'' = ordinates of points in W, W', and W" planes, respectively

v = particle velocity, ft./sec.

$|v|$ = maximum particle velocity, ft./sec.

V, V', V'' = abscissas of points in W, W', and W" planes, respectively

w = weight rate of flow, lbs./hr.

W, W', W'' = points in transformed complex plane.

x = longitudinal coordinate of cylinder, ft.

y = particle displacement in x direction

α_G = absorptivity of gas, dimensionless

γ = ratio of specific heat at constant pressure to specific heat at constant volume

ϵ_G = emissivity of gas, dimensionless

ϵ_S' = effective emissivity of surface, dimensionless

θ = angular coordinate, radians

φ = actual fuel to air ratio in inlet mixture divided by the stoichiometric fuel to air ratio

μ = coefficient of viscosity, lb./ft. hr.

μ' = second coefficient of viscosity, lb./ft.hr.

π = ratio of circumference to diameter of circle, dimensionless

ρ = density, lbs/ft.^{3}

Subscripts

av = average

b = bulk of fluid

c = convection

g = gas

o = outside surface of test object

r = radiation

s = inside surface of test object

w = water

x = distance from flame holder, in.

1,2 = arbitrary states or positions

Abbreviations

Db = decibels

gpm = gallons per minute

lb = pound

log = common logarithm (base = 10)

ln = natural logarithm (base = e)

mil = 0.001 inch

psia = absolute pressure, $lb./in.^2$

psig = gauge pressure, $lb/in.^2$

SCFM = standard cubic feet per minute (at 70°F and 1 atm.)

INTRODUCTION

Heat transfer from flames has been investigated extensively for specific applications, such as furnaces and ramjet combustors. General studies of heat transfer from flames, however, are scarce. In particular, very few data are available on the rate of heat transfer from burning gases to the walls of a cylindrical enclosure.

In addition to the experimental difficulties involved in high temperature studies, basic investigations in chambers are hampered by the multiplicity of variables required to define the system, and the lack of adequate understanding of the combustion process itself. In a ramjet, for example, a flame generally burns from some type of bluff body inserted in the path of the air flow. A partial list of variables involved in the burning process includes mass flow rate, inlet air temperature, inlet velocity distribution of air and fuel, inlet turbulence conditions, proportion of fuel to air, combustor operating pressure, flame holder type and geometry, and chamber length and geometry. Important dependent variables frequently encountered in combustion systems are the nature and amplitude of flame generated oscillations which, in some cases, considerably influence the burning rate and heat transfer. The phenomenon of screeching combustion, for example, is reported to greatly increase the heat transfer rate.

The complexity and unsolved problems of turbulent combustion processes made theoretical analysis difficult. The structure of turbulent flames is incompletely understood. The mechanism by which a flame is anchored on a bluff body flame holder is unresolved. The

chemical kinetics of combustion reactions at high temperatures are virtually unknown. These and many other problems often combine to hinder the generalization of experimental results through application of theoretical considerations.

Convective and radiant heat transfer usually constitute the most significant portion of the total heat transfer from flames and high temperature combustion products. Some studies have been made which separate the convective and radiant heat transfer. Timofeev and Uspenskii[70] investigated heat transfer from hot combustion products to the water cooled walls of a 4-inch diameter chamber. Gas temperature and radiant heat transfer were measured at positions along the length of the tube. The radiant contribution gave only fair agreement with a theoretical expression. The convective heat transfer coefficients were scattered about an empirical curve for low temperature heat transfer. Tailby and Saleh[69] studied local heat transfer rates from a laminar, luminous diffusion flame burning in the inlet of a water cooled tube of 2 inch diameter. The convective and radiant transfer were determined as a function of tube length, gas pressure in the jet, diameter of the gas jet, and distance separating the gas jet from the lower end of the tube. No comparison was made with empirical literature values for heat transfer from unburned gas.

Other investigations of the effect of operating variables and geometry on the rate of heat transfer from flames in a tube are of less general significance.

Kilham[31] investigated heat transfer to a rotating cylinder immersed in a carbon monoxide-air flame and stated that his experimental heat transfer coefficients agreed closely with values predicted for non-burning gases. Differences between experimental and predicted results, however, were noted with a hydrogen-air flame.

Many types of flame-generated oscillations have been identified in combustion systems. When burning a homogeneous mixture of fuel and air from a suitable flameholder, in a cylindrical enclosure, resonance of the complex gases can be related to the geometry of the burner. By solving the classical wave equation, these oscillations can be shown to occur in axial, radial, or transverse modes. The axial, or "organ-pipe" mode, and transverse or "screeching" mode are frequently encountered in tubular burners. The characteristics of flame-generated oscillations have been studied by many investigators. The effect of these oscillations on burning rate and heat transfer, however, has been largely neglected.

It is apparent that many aspects of heat transfer from flames are insufficiently understood and require experimental investigation. No fundamental studies appear to have been conducted on heat transfer between flames, propagating from a bluff body flame holder, and the cooled walls of an enclosing circular tube. With certain geometries and flow conditions, flame-generated oscillations would be produced, which would be expected to influence the rate of heat transfer. An experimental investigation of this problem seemed warranted.

The objectives of the experimental study were defined as:

1) To design an apparatus suitable for studying heat transfer rates from bluff body stabilized flames within a cooled tube.
2) To determine the effect of some of the important process variables on local rates of heat transfer.
3) To determine the effect on heat transfer of any acoustical oscillations generated in the tube by the burning process.

Because of the large number of independent variables involved in the combustion process, it was necessary to specify many variables, including some that are expected to exert an important influence on rates of heat transfer. For example, the studies were limited to one type of fuel and a single tube diameter.

The present investigation considers the effect of flow rate, fuel to air ratio, inlet air temperature, flame holder blockage and length of tube upstream and downstream of the flame holder. The frequencies and relative amplitudes of any flame-generated oscillations are measured. The measurement of local gas temperatures in the burning mixture, and the resolution of total heat transfer into the radiant and convective contributions are considered beyond the scope of this study.

Experimental data are presented for local heat transfer rates downstream from the flame holder, both in the presence and absec downstream from the flame holder, both in the presence and absence of flame-driven acoustical oscillations.

LITERATURE SURVEY

The rate of heat transfer from flames has received extensive study for specific applications. Considerable information, for example, is available on heat transfer within industrial furnaces. Some data are also available in the declassified literature on heat transfer from rocket chambers. Fundamental investigations of the effect of process variables on rates of heat transfer in cylindrical chambers, however, are scarce. In particular the effect of flame generated oscillations on heat transfer in an enclosure is relatively unknown.

The literature survey will review topically the experimental and theoretical aspects of direct interest in this study. A brief review of the theories on the structure and mechanism of turbulent flames is included to illustrate the complexity and lack of understanding of a combustion process.

Mechanisms of Heat Transfer

The important mechanisms of heat transfer from flame gases to a solid wall are forced convection and radiation. Other mechanisms which are usually of minor importance include catalytic combination of free radicals and atoms on the surface of the solid, catalytic combustion on the surface of the solid, transference of excess energy by collision of high energy gas molecules with the solid, and exothermic displacement of chemical equilibria. With cold walls and flame temperatures below 3000°F, only heat transfer by forced convection and radiation are usually considered.

In many combustion chambers, the combustion gases are highly turbulent, and heat is partly transferred by the movement of eddies of gases. The rate of this convective process can often be expressed as a function of Reynolds' and Prandtl's numbers. Under some situations, it may be possible to estimate the convective heat transfer coefficient from the flame to the wall from one of the familiar relations developed for fluids flowing in a pipe.

Summerfield[66] reviews recent theories of turbulent heat transfer by convection with special reference to high temperature combustion chambers. Zellnik[84] found that local rates of convective heat transfer from a high temperature air stream to a cold tube wall could be correlated in the form of

$$Nu = 0.023 Re^{0.8} \; Pr^{1/3} \left(T_b / T_s \right)^m \qquad (1)$$

where m is zero or 0.33, depending upon whether physical properties are evaluated at bulk or surface temperatures. For gas film convective heat transfer coefficients in rocket motor combustion chambers and nozzles, Greenfield[16] recommends the expression

$$h_g = 0.029 \frac{G^{0.8}}{D^{0.2}} \; C_p \, \mu^{0.2} \qquad (2)$$

Superimposed on the convective process is that of thermal radiation. Since radiation increases rapidly with increase in temperature level, thermal radiation may account for a large part of the total energy transfer from flames. The radiation from hydrocarbon flames can be classified as luminous or non-luminous. The non-luminous radiation

consists of emission in certain regions of the infrared spectrum as well as some visible and ultraviolet radiation. Non-luminous radiation is due principally to carbon dioxide and water vapor. The luminous radiation is a continuous emission from such molecules as CH, C_2, and OH, and from incandescent soot particles.

The thermal radiation from non-luminous flames can be estimated from the methods and data presented by Hottel in McAdams[42]. Radiation from luminous flames can range up to several times the value of non-luminous radiation. Topper[72] found that the intensity of luminous radiation increased rapidly with an increase in combustor inlet pressure and was affected to a lesser degree by variations in fuel to air ratio and air mass flow. In his experiments, the flame emissivity varied from 0.09 to 0.79.

Kilham[31] devised an interesting technique to study heat transfer from flames to a solid. He exposed a rotating refractory tube to carbon-monoxide-air and hydrogen-air flames, and measured the radiant heat flux from the tube to the surroundings. He assumed that at equilibrium the rate of heat transfer from flame gases to solid by forced convection and by radiation was equal to the heat loss by radiation. Experimental heat transfer coefficients for the carbon-monoxide air flame agreed closely with values predicted from McAdams[42] for pure convection. The lack of agreement with the hydrogen-air flame was attributed to recombination of radicals at the surface of the tube.

In a continuation of the above studies, Jackson and Kilham[24] investigated heat transfer by forced convection from the combustion products of a hydrogen-air flame. With the cylinder removed from the flame

cone, the experimental and predicted heat transfer coefficients agreed.

Experimental Studies in Chambers

Although of great practical significance, experimental data on heat transfer rates in rocket combustion chambers are scarce.

Sutton[68] presents a general discussion of some of the more significant applications of heat transfer theory in the field of rocketry. Boden[7] discusses the distribution of heat transfer in rocket motors and a number of factors which influence it. Gordon[15] states that the expermental convective heat exchange for radically different propellants and rocket-type combustion chambers fall consistently higher than the values predicted from low temperature empirical expressions. From experiments on heat transfer in small scale rocket combustion chambers, Ziebland[85] also indicated average experimental heat transfer coefficients up to 2.9 of the computed value. The difference between experimental and computed values was attributed mainly to the unestablished flow pattern near the inlet of the combustor. He also noted that extrapolation of low pressure emissivity data to high pressures and temperatures yield low results for the emissivity.

Winter[82] studied the heat transfer conditions at the air cooled tube walls of a 6-inch diameter gas turbine combustion chamber. By assuming a flame temperature and gas emissivity, he approximated the radiant and convective heat transfer. For a kerosene fuel, he found that 50 to 80 percent of the heat was transferred by radiation.

Shorin and Pravoverov[63] measured local heat transfer rates from a laminar diffusion flame in a sectionally water cooled combustion

chamber. The location and nature of radiating objects placed in the gas stream strongly influenced the rate of heat transfer. The highest heat transfer rates were achieved with a ceramic flame stabilizer and radiating mantle in the chamber. The correlation of data in terms of a "furnace criterion" indicated that radiant heat transfer predominated.

Hammaker and Hampel[18] studied heat transfer from gas flames burning inside several feet of straight 1/2 inch and 1 inch outside diameter tubes immersed in still air and running water. The burner was removed from the immediate tube entrance to minimize oscillations and to reduce secondary air velocity past the burner head. The tube surface quickly approached a maximum temperature within a few inches of the inlet. Temperatures then remained fairly constant near the maximum up to about 43 inches from the inlet of the one inch diameter tube. Tube surface temperatures then decreased with tube length. No attempt was made to estimate inside flame temperatures and internal heat transfer coefficients.

Timofeev and Uspenskii[70] investigated heat transfer from hot gases to water cooled walls in a chamber of 100 mm. diameter and 800 mm. length at Reynolds' numbers up to 9000. Products of combustion entered the chamber with an established velocity and temperature field. Gas temperatures and radiant heat transfer were determined by a pyrometer at positions along the length of the tube. The radiant contribution gave fair agreement with a theoretical expression which was derived for the case of a flowing gas with radial temperature gradients. The convective heat transfer coefficients, obtained from the difference between overall and radiant heat transfer rates, were scattered about an empirical curve from the literature. A linear plot of total heat transfer

coefficient against Reynolds' number gave excellent correlation. This result indicated that the dominant factor is the hydrodynamic properties of the flow.

Tailby and Saleh[69] studied local heat transfer rates from a luminous diffusion flame burning in a sectioned, water-cooled tube of 2 inch inside diameter. The variables studied were tube length, gas pressure in the jet, diameter of the gas jet, and distance separating the gas jet from the lower end of the tube. The effect of these four variables on air entrainment, visible flame length, total radiant and convective heat ttansfer, thermal efficiency, flame temperature, and emissivity was investigated and linear empirical equations formulated.

They found that radiation was the most important factor in the heat transfer from the lower portion of the tube, but that convective heat transfer increased in the upper sections. Luminous radiation from the flame constituted a significant portion of the total radiation. The results were not compared with any of the usual empirical heat transfer expressions.

Effect of Pulsations on Heat Transfer

When pulsations are imposed on a fluid, heat transfer from the fluid might be expected to change due to an altered thickness of the boundary layer. In the laminar region, Richardson[55] showed that the velocity profile for pulsating flow is steeper near the wall than for smooth flow. The heat transfer would be expected to increase under such conditions. A similar process might occur for turbulent flow also, but the equations are too cumbersome for analytical solution.

The experimental information is meager and often conflicting. Working with water in the turbulent region and at low frequencies, Martinelli et al.[41] reported no difference in heat transfer between steady unidirectional flow and pulsating flow whereas West and Taylor[77] found that heat transfer could be increased up to 70% by increasing the amplitude of pulsation. Linke[35] found an increase in heat transfer from oil of up to 4 times in the laminar region and up to 1.35 times in the turbulent region. Havemann and Rao[20] investigated the effect of frequency, wave amplitude, Reynolds' number and wave form on heat transfer to air. In general, the change in heat transfer was negative below a certain frequency and positive above it. Only a negative change could be detected when the amplitude of the pulsation was very low.

In all of the investigations mentioned above, pulsations have been produced mechanically and have frequencies below 50 cycles per second. Considerably less heat transfer information is available for higher frequencies.

Havemann[19] studied heat transfer from rapidly compressed and oscillating gases in a cylinder. He found that the increase in heat transfer over a gas at rest was dependent on the amplitude of the pressure fluctuations and to a lesser extent, on the frequency of oscillation. Lemlich[34] measured the effect of vibration on natural convective heat transfer from a wire and observed an increase in heat transfer with an increase in amplitude or frequency. Kubanskii[33] applied acoustic waves to cylinders in still and moving air and observed an increase in heat transfer in both cases. He reported increases in heat transfer up to

50% for sound waves with mean vibration velocities exceeding the velocity of air flow past the tube.

Summarizing the available information, the effect of pulsation on heat transfer from fluids is dependent on the amplitude of the oscillation, and, to a lesser extent, on the frequency. Heat transfer appears to increase with both increasing amplitude and frequency.

Quantitative experimental data on heat transfer from oscillating flames appears to be completely lacking. Berman and Cheney[4] conducted a study of combustion instability in a three inch rocket chamber. They observed no abnormal heat transfer rates from flame generated sinusoidal-type oscillations with amplitudes up to 100 psi peak to peak. Shock-type instability, with peak to peak amplitudes up to 500 psi, was accompanied by heat transfer rates up to 2.5 of the normal values. Tischler and Male[71] state that the combustion-driven oscillation known as screeching can cause abnormally high heat transfer rates. They mention an engine which had as much as 1/4 inch of solid stainless steel metal eroded from the chamber in runs of less than one second total duration. Screeching at frequencies from 200 to 16,000 cycles per second has been reported in the literature.

Flame-Generated Instabilities

Several types of flame-generated instabilities have been isolated and identified in a variety of combustion devices. Resonance of the gases in a ramjet burner, for example, are usually of three general types[13]: (1) oscillations associated with failure of the flames to stabilize properly on the ignitor (2) oscillations depending on the

existence of a time lag between the injection of propellants into the burner and their transformation into high temperature gases and (3) oscillations, initiated or amplified by the combustion process, having frequencies corresponding to the resonant frequencies of the gas in the burner. By burning a homogeneous fuel-air mixture from a suitable flame holder, the oscillations due to ignitor and injection system can be eliminated.

Theory of Acoustical Oscillations

The classical wave equation applies to acoustical oscillations of small amplitude in a fluid medium. Although oscillations related to combustion instability are frequently of very large amplitude, experimental observations have often been found to be adequately described by classical acoustics.

Rayleigh[54] has determined the most general solution of the wave equation in a cylindrical cavity. Each possible acoustic mode has a particular frequency, which is usually different from that of any other mode. Morse[44] shows that the frequency of any particular mode may be computed from the formula

$$f_{m,l,n_z} = \sqrt{\frac{a}{2} \left(\frac{n_z}{L}\right)^2 \left(\frac{\alpha_{ml}}{r}\right)^2} \qquad (3)$$

Any choice of the wave numbers m, l, n_z, as positive integers or zero corresponds to a possible natural mode of acoustical oscillation within the cylinder. When two of these are zero, the remaining mode is called pure. Pure modes with m = l = 0 are the axial or organ pipe modes. The waves with m = n_z = 0 are called radial modes; those

with $l = n_z = 0$ are called tangential or "sloshing" modes. Combination acoustic modes result when there are more than one non-zero wave number.

Organ-Pipe Oscillations

The organ pipe is usually considered as a long tube, in relation to its diameter, open at either one or both ends. For small amplitudes of oscillation, wherein the thermodynamic equations can be linearized, the mode of oscillation is sinusoidal, both in time, and along the tube in space. Pressure and gas particle velocity are sinusoidal functions of distance and time inside the tube. For the fundamental mode inside a tube open at both ends, the standing pressure wave has a node at each end and an antinode at the center. The standing velocity wave has a node at the center and an antinode at each end. By adding sections of tube to obtain higher modes of oscillation, and realizing that any of these modes is possible in any length of tube, a general equation relating possible frequency to tube length is obtained:

$$f = \frac{na}{2L} \qquad n = 1, 2, 3, \ldots\ldots \qquad (4)$$

An intermittent source of energy is required to drive the oscillation and overcome the ever present damping forces in the system. In the case of a self-sustaining flame driven oscillation, Rayleigh's[54] hypothesis states that the period of energy release must be in phase with the pressure fluctuations at the point of heat release. Putnam and Dennis[49] have justified experimentally the validity of this criterion. They found further that the energy must be released near a point of maximum effectiveness. Energy in the form of a pressure disturbance, for example, must be added near a velocity antinode. In the case of flame

generated oscillations, energy is added in the form of periodic velocity disturbances. The maximum effect is obtained in the region of maximum amplitude of the oscillating pressure (as is the case with vibrating reed type instruments).

Dunlap[12][13] studied resonance of a propane-air flame in a 1"x1"x12" square cross section combustion chamber, acoustically open at both ends. Agreement was obtained between experimentally observed frequencies and frequencies predicted by assuming an organ-pipe type of resonance of hot and cold gases. Resonance was found to be most severe in slightly rich mixtures. The flame was not prone to resonate at extreme rich or lean mixtures. The first overtone was occasionally observed in rich mixtures.

Dunlap noted that the oscillations of any particular mode occurred when the flame holder was in the region of a pressure antinode for that mode. He postulated the following driving mechanism which satisfies Rayleigh's hypothesis. Standing sound waves in the combustion chamber produce a variation in pressure and temperature at the flame front with time. The dependence of flame speed on temperature and pressure results in a cyclic variation of burning rate, which is in phase with the pressure fluctuations.

Kaskan[29] measured the position and shape of a flame in a tube with time and concluded that there was no over-all change in flame speed due to oscillations. On the other hand, the area of the flame front varied by extension of the edges, in phase with pressure, as required by Rayleigh's hypothesis. He postulated a driving mechanism based on a periodic change in the area of the flame.

Putnam and Dennis[50] investigated a system consisting of a 0.3 in. diameter disc flame holder in a 7/8 in. diameter tube. In agreement with Dunlap, they found that oscillations were most likely to occur when the flame-holder was near a pressure antinode.

With longer downstream sections on the tube, Putnam and Dennis[52] encountered a low frequency flame-driven oscillation. The observed frequency was far lower than the calculated organ pipe frequency of the tube and higher than the corresponding Helmholtz frequency. The low frequency was directly associated with a large, periodic variation in flame shape, which resulted from a periodic blowoff of the flame, and reignition from the central core behind the holder. The driving energy is supplied by the large variations in flame shape, with consequent variations in flame area and burning rate.

Continuing their studies of flame generated oscillations, Putnam and Dennis[53] investigated the stability limits of a flame holding baffle in a 7/8 inch diameter tube. Increases in length of the combustor downstream of the flame holder resulted in decreases in the stability range (the range of fuel to air ratios over which a flame will burn for a given inlet velocity). The stability limits were found to be unaffected by organ-pipe oscillations generated at high combustor velocity. A low frequency oscillation observed at low velocity was concluded to be the cause of premature blowoff. This oscillation occurred whenever it was possible for the flame front to touch the wall. The sound pressure level data for the low frequency oscillation was much higher than would be predicted from an extrapolation of their sound pressure levels for the organ pipe oscillations.

Acoustical Damping

Organ-pipe oscillations can be energetically damped by means of a quarter wave length tube. A pressure pulse fed into the quarter wave tube is reflected back from the end of the tube to the main chamber a half cycle later. At this time, the oscillating chamber pressure is in opposite phase to the reflected pulse, so that a rarefaction now exists at the tube entrance. When the reflected pressure pulse meets the rarefaction, attenuation of the oscillating component of the chamber pressure is obtained.

Putnam and Dennis[51] conducted tests on the suppression of burner oscillations by quarter wave tubes, by drilled holes, and by Helmholtz resonators. The effectiveness of a quarter wave tube was found to be critically dependent on length, but relatively insensitive to location, as long as the tube was placed in the region of a pressure antinode. The quarter wave tube did not have to be placed near the particular antinode where energy was fed into the oscillation. The degree of suppression was approximately proportional to the cross sectional area of the tube.

Screech Combustion

An intense high frequency acoustic disturbance known as "screech" is often encountered in ramjets and afterburners. Screech combustion is accompanied by a marked shortening of the flame zone and an increase in efficiency and heat transfer rates. Truman and Newton[73] showed that the frequencies of screeching combustion observed in burners of various sizes correspond to some simple mode of transverse oscillation. Moore

and Maslen[43] made a theoretical study of transverse oscillations, assuming that the combustion chamber resonance results from amplification of an initially weak wave of transverse type coupled with a pressure-dependent rate of energy release in the combustor. Blackshear, et al.[6] found that the acoustic oscillations accompanying screech in their 6 inch burner consisted of the first transverse mode in the hot gases downstream of the flame holder. Screech was noted to increase combustion efficiency about 35 percent. Kaskan and Noreen[30] studied high frequency oscillations by Schlieren photographs in a 2 in. x 4 in. duct with a v-gutter flameholder. They postulate that the transverse oscillations are driven by a variation in flame area with time. Using a 1" x 4" combustion chamber, Rogers and Marble[57] measured the limits of stable screech, and the amplitude and frequency of pressure oscillations over a range of mixture ratios, inlet air temperatures, and combustor flow rates. From Schlieren photographs and high speed motion pictures of the combustion process, they concluded that the high frequency oscillation is accompanied by a periodic shedding of vortices from the flame holder lip with the same frequency as the oscillation. They suggest that the driving mechanism is a periodic transport of combustible material into the hot wake of the flame holder.

Effect of Flame-Generated Oscillations

Some experimental information is available on the effect of flame generated oscillations in a combustion process.

Loshaek, Fein, and Olsen[40] applied a sound wave with a frequency of 12,700 cycles per second to a laminar propane-air burner

flame. The sound altered the flashback limit so that the flame became more stable, and the blowoff limit so that the flame became less stable. The burning velocity and flow velocity profiles were unchanged.

Kippenham and Croft[32] noted that high frequency sound did not change the magnitude of the normal flame velocity of laminar or turbulent flames burning from tubes. The configuration changed from a cone to a flattened bowl shape for laminar flames, and to a suspended violently agitated zone in the case of turbulent flames. Hahnemann and Ehret[17] observed similar configuration changes in a stationary propane-air flame issuing from a nozzle. They report an increase in the maximum flame speed of about 20 percent.

Havemann[19] studied the effect of oscillations on flames burning inside tubes. He found that the apparent flame velocity increased with amplitude and frequency of oscillation. Schmidt et al.[61] also noted an increase of flame velocity with amplitude for a combustion wave propagating in a tube.

Theory of Flame Propagation

A flame front is a region in the flow field where rapid change in the chemical composition of the fluid occurs with consequent release of chemical energy in the form of heat. In the majority of cases the phenomenon is very complex, involving heat transfer, diffusion, and chemical reaction. The problem of steady state propagation of a laminar one-dimensional deflagration flame through a gas is amenable to mathematical treatment. Boys and Corner[8], and Hirschfelder and Curtiss[23] have shown that the characteristic velocity of propagation of such a flame,

called the burning velocity, corresponds to an eigenvalue of the set of differential equations and boundary conditions describing the system. Even for the simplest kinetic systems, exact solutions can be obtained only by numerical integrations. Hirschfelder[22] has extended the theoretical analysis of laminar flames to the problem of heat transfer in chemically reacting gas mixtures.

The first attempt to predict the turbulent burning velocity in terms of the laminar burning velocity and the characteristics of turbulence was made by Damkohler[10]. For large scale turbulence, he postulated that the turbulence merely causes a wrinkling of the flame front and that the individual sections of the wrinkled flame continue to propagate at the laminar flame speed. When the scale of fluctuations is small compared to the thickness of the reaction zone, he assumed that the flame front is not distorted, but that the detailed processes of heat transfer and diffusion are increased. Karlovitz et al.[28] found agreement between experimental values of turbulent burning velocity and theoretical values based on the concept of a wrinkled laminar flame.

Longwell, et al.[38] suggested that within a given volume, an insufficient number of laminar flame sheets can be obtained to yield the probable local heat release rates that have been observed in a 1 7/8 inch ramjet by Mullen et al.[45]. The application of the wrinkled laminar flame theory appears to be limited.

Summerfield et al.[67] postulate that a turbulent flame is a zone of reaction distributed in depth, having smooth spatial variations in the time average values of temperature and concentration. The transport properties within the combustion zone are controlled by the stream

turbulence. The treatment suggests a close analogy between a turbulent and a laminar flame. In order to compute a turbulent flame velocity from this theory, a knowledge of the approach stream turbulent diffusivity, and the thickness of the turbulent reaction zone is required.

In the case of intense mixing, the concept of discrete flame fronts is abandoned, and the reaction is assumed to take place homogeneously. Under such conditions, reaction kinetics, rather than mixing, control the rate of the burning process. Avery and Hart[1] made a theoretical analysis for instantaneous homogeneous mixing and heat transfer for a combustor in which the controlling rate process is a reaction kinetic rate.

Application of homogeneous reactor theory requires a knowledge of the kinetic constants of the combustion reaction at usual combustion temperatures. Such data is almost completely lacking. Weiss and Longwell[39] investigated lean mixture blowout data from insulated spherical reactors under conditions of homogeneous burning. The results indicate that the high temperature combustion of hydrocarbons in air can be empirically described by a second order rate equation with an activation energy of about 40,000 cal per mole. Heat losses from the combustion zone reduce the rate of reaction by reducing the reaction temperature.

Mechanism of Flame Stabilization

In order for a mixture of fuel and air to react rapidly, the mixture must be raised to a high temperature or come in contact with active particles from a nearby reaction zone. Bluff body flame stabilization depends on the existence of a sheltered wake behind the body in

which hot gas recirculates. If conditions are properly selected, a flame will exist in the wake of the baffle and will eventually spread throughout the total inflammable mixture. The hot gas in the wake, acting as a pilot burner, ignites fresh combustible mixture flowing past in the external stream. Flame stabilization by small scale bluff bodies of various geometries has been studied by many investigators, including De Zubay[11] on discs, Longwell[36] on parallel cylinders, gutters and cones, Scurlock[62] on normal cylinders, and Weir et al.[75] on spheres.

A number of flow models have been proposed as an aid in interpreting stability data. Longwell[38] suggested that the region behind a baffle is a zone of intense stirring and can be treated with the homogeneous reactor theory of Avery and Hart[1]. Another model divides the wake into a precombustion zone, in which the reaction rate is negligible and heat conduction predominates, and a combustion zone in which heat conduction is small compared to the chemical heat release. Spalding[65] has postulated three models: recirculation of a part of the reacting mixture, stabilization by two standing vortices, and mixing of hot and cold jets of gas. Using simple chemical reaction laws, all models predict the effect of stability parameters in qualitative agreement with experimental results.

Detailed measurements of the conditions existing in the wake of a baffle are scarce. From tracer studies, Nicholson and Field[46] noted a low ratio of mixing time to residence time in the baffle wake. Longwell[38] made detailed efficiency traverses which indicated a zone

of high efficiency in the wake of the baffle, and a lack of complete mixing. The existence of a recirculating flow towards the baffle was established with a salt probe.

Westenberg et al.[78] made helium tracer and combustion efficiency measurements in the wake of a conical one inch flameholder. The data is interpreted as showing the lack of violent mixing existing in the recirculation zone. Instead, there exists a relative calm with a definite reverse flow of hot gas directed upstream. They suggest that the stabilizing mechanism is one of interchange of fresh combustible and hot gases by turbulent and molecular diffusion across the wake boundary. This is similar to the jet mixing model of Spalding. Zukoski and Marble[86] and Williams et al.[81] also conclude that combustion is restricted mainly to the narrow shear layer between the free stream and the recirculation zone.

Flame-Generated Turbulence

Confinement of a bluff body-stabilized flame in a tube produces velocity gradients between burned and unburned gases due to the acceleration from expansion of burning gases. Scurlock[62] calculated flame propagation rates downstream of a flame holder. Since the effective flame velocity was increased over the laminar flame velocity, he concluded that turbulence was generated by velocity gradients across the flame front. The effect of approach stream turbulence intensity on flame velocity was found in most cases to be smaller than the effect due to internally generated disturbances.

Jenson[25] attributes velocity fluctuations in the reactant region upstream of a stabilizer to acoustic phenomena resulting from shear generated turbulence in the flame zone. He concludes that the combustion process, through its effect on the velocity distribution, provides a means leading to better mixing and combustion.

Karlovitz[27] postulates that the high intensity turbulence created by the turbulent flame has a large influence on every mixing and heat transport phenomenon behind the flame front. From mixing length theory he concludes that, immediately behind the turbulent flame, the heat transfer rate should be increased several times above the value that would be expected from approach flow turbulence.

Flame Spreading From Baffles

The burned material in the wake region of a baffle serves as a nucleus from which the flame propagates downstream through the unburned mixture. Combustion efficiency depends on the rate at which the stabilized flame spreads through the remainder of the air and fuel passing through the combustor. In contrast to the fairly extensive studies on the stability of baffles, there is little quantitative information available on the rate of flame spreading from baffles.

Scurlock[62] and Tsien[74] have theoretically examined the effect of heat release on velocity distribution and flame width. They assumed a line flame source in a two-dimensional duct, no momentum transfer in a radial direction, an initially uniform velocity distribution, and constant static pressure at any cross section. By employing one-dimensional conservation equations, they calculated velocity profiles in the duct as a

function of fraction burned. The assumptions of a line source and no radial momentum transfer limit the usefulness of the analysis. Also, the correlations give no information as to the variation of combustion efficiency with downstream distance.

Wilkerson and Fenn[79] studied flame spreading in a 1 7/8 in. ramjet, the effectiveness of flame spreading being represented by the combustion efficiency at the burner outlet. An increase in efficiency occurred with an increase in pilot heat input from an independent pilot flame. For each flameholder configuration, a mixing factor was obtained, which measured the rate of mixing of the pilot heat with the main stream. A simple correlation between the mixing factor and the combustion efficiency was presented. Evaluation of the self-piloting effect of a baffle would be one of the major problems encountered in extending the results.

Mullen et al.[45] determined combustion efficiencies for hydrocarbon fuel burning in a 2 inch diameter tube. They studied the effect of combustion chamber length, ignitor geometry, fuel-to-air ratio, air velocity, and air temperature. Combustion efficiencies increased with increased length, increased inlet air temperature, and decreased air velocity. A fuel-air mixture near stoichiometric proportions gave maximum combustion efficiency. Most of the data was taken at air rates sufficiently high to cause choking at the exit.

Scurlock et al.[80] studied flame widths downstream of a variety of stabilizers in a 1 in. x 3 in. rectangular combustion chamber. For the range of variables studied, they concluded that inlet turbulence level, stabilizer diameter, and stabilizer shape had a negligible effect on flame width. As inlet velocity was increased, flame width decreased

and a longer combustion chamber was required to reach a given combustion efficiency.

Longwell et al.[48] measured combustion efficiencies downstream of baffles in a 9 in. x 5 in. duct. There was no consistent effect of baffle size or blockage on efficiency in the range tested. The influence of fuel to air ratio was small, the fastest burning rates occurring at a stoichiometric mixture. A general conclusion about the effect of velocity could not be drawn. Increased tailpipe length increased the initial flame spreading due to more severe pressure and velocity fluctuations in the duct. No satisfactory flame theory could be formulated to explain the data.

Zelinski et al.[83] studied the burning efficiency of a confined, pre-mixed, rim-stabilized flame jet. They reported that burning efficiency increased with increased pressure, inlet temperature, equivalence ratio, and jet length, and decreased with increased jet velocity, hole diameter, and mass throughput rate. Turbulence inducing screens upstream of the flameholder did not increase the burning rate above that for fully developed pipe turbulence.

Measurement of Local Heat Transfer Rates

The local rates of heat transfer through a tube wall can be determined by 1) measuring the temperature difference between thermocouples inserted in the tube wall and 2) measuring the increase in enthalpy of a fluid flowing through annular sections.

For gas flow outside and transverse to a circular tube, Churchill[9] developed a method of measuring local heat transfer rates at high

gas temperatures and high heat fluxes. He inserted thermocouples at three different radial distances in a thermally insulated annular sector of the tube wall. From the difference in thermocouple readings, the average heat flux through the sector was readily computed. Zellnik[84] applied this technique to the measurement of local heat transfer rates from flowing gases inside a circular tube. He installed flux measuring stations at several points along the length of the tube, thus permitting calculation of the longitudinal heat transfer profile. Since measurements were made for a single tube position, any dissymmetry in the radial temperature distribution could cause an error in the observed local rate.

By measuring the flow rate and temperature rise of a fluid passing through an annulus of the tube, an average heat transfer rate can be computed for the annular section. The length of the annular sections are selected within practical limits to give the desired detail in the longitudinal heat transfer profile. The disadvantages of this method usually result from inaccuracies in measuring small temperature changes and from difficulty in adequately insulating the sections.

Neither method actually gives a true local heat transfer rate. The thermocouple technique gives an average rate over the insulated sector and the annulus method results in an average rate over the length of the external annulus.

Methods of Efficiency Measurement

The heat released by a combustion process within a chamber can be determined by 1) measuring the thrust across the combustion chamber 2) measuring the gas temperature rise in the chamber and 3) chemical

analysis of the combustion chamber exhaust gases.

In the combustion chamber thrust method, the aerodynamic efficiency is determined by comparing the actual thrust, under the given chamber operating conditions, with the theoretical maximum thrust, calculated from fuel and air supply rates, and calorific value of the fuel. The actual thrust is calculated from pressure drop measurements across the combustion chamber. By determining the pressure loss characteristics of the combustion system during cold flow, the combustion efficiency (fraction of fuel burned) can be separated from the aerodynamic efficiency. The advantage of this method is its simplicity. The main disadvantage is the difficulty of estimating the aerodynamic drag of the system from cold flow measurements.

A mean value of the outlet gas temperature, weighted according to velocity distribution, can be obtained by a traverse with a suitable thermocouple and pitot-static instrument. The combustion efficiency is calculated by comparing the actual gas temperature rise to the theoretical rise for complete combustion. The disadvantages of this method result from the difficulty in estimating thermocouple corrections for high temperature gas streams, and from the time required to obtain accurate temperature and pressure traverses.

The heat actually released and the maximum heat available in the combustion chamber can be calculated from chemical analysis of the combustion chamber exhaust gases. When properly applied, this method is capable of giving the greatest accuracy. Since the gas composition at the outlet is usually not uniform, a sampling traverse is required. The

sampling probe should be small to minimize disturbance of the flow pattern. Rapid quenching of the sample is also necessary to prevent additional chemical reaction. The time consumed in accurate analysis of the samples from each traverse is generally considerable.

APPARATUS

The apparatus was designed for the measurement of local heat transfer rates from a stream of burning gas inside a circular tube. Air and propane can be supplied at rates up to 100 SCFM and 5 SCFM, respectively.

The equipment essentially consists of a fuel supply system, an air supply system, a cooling water supply system, and a heat transfer test unit with appropriate instrumentation. The fuel, air, and water supply systems have greater operating ranges than required for the present study. General views of the apparatus are shown in Figures 1 and 2 and a schematic diagram is given in Figure 3. A detailed description of individual equipment items is presented in subsequent sections.

The functional relationship between the major sections of the apparatus follows. Compressed air from a 95 psig building supply system flows through a cleaner and dehumidifier, and then continues through a pressure regulator and rotameter. Simultaneously, a stream of propane vapor is withdrawn from a 400 pound tank, and passed through a surge tank, a pressure regulator, and a rotameter for gas flow measurement. The fuel and air streams are combined and sent through a plenum chamber containing screens to promote mixing. After flowing through a straight length of pipe, the fuel-air mixture enters the heat transfer unit, which has thermocouples imbedded in the wall for measurement of the radial temperature profiles inside six thermally isolated annular sectors. The flame propagates from a bluff body flame holder, which can be located at any position along the length of the

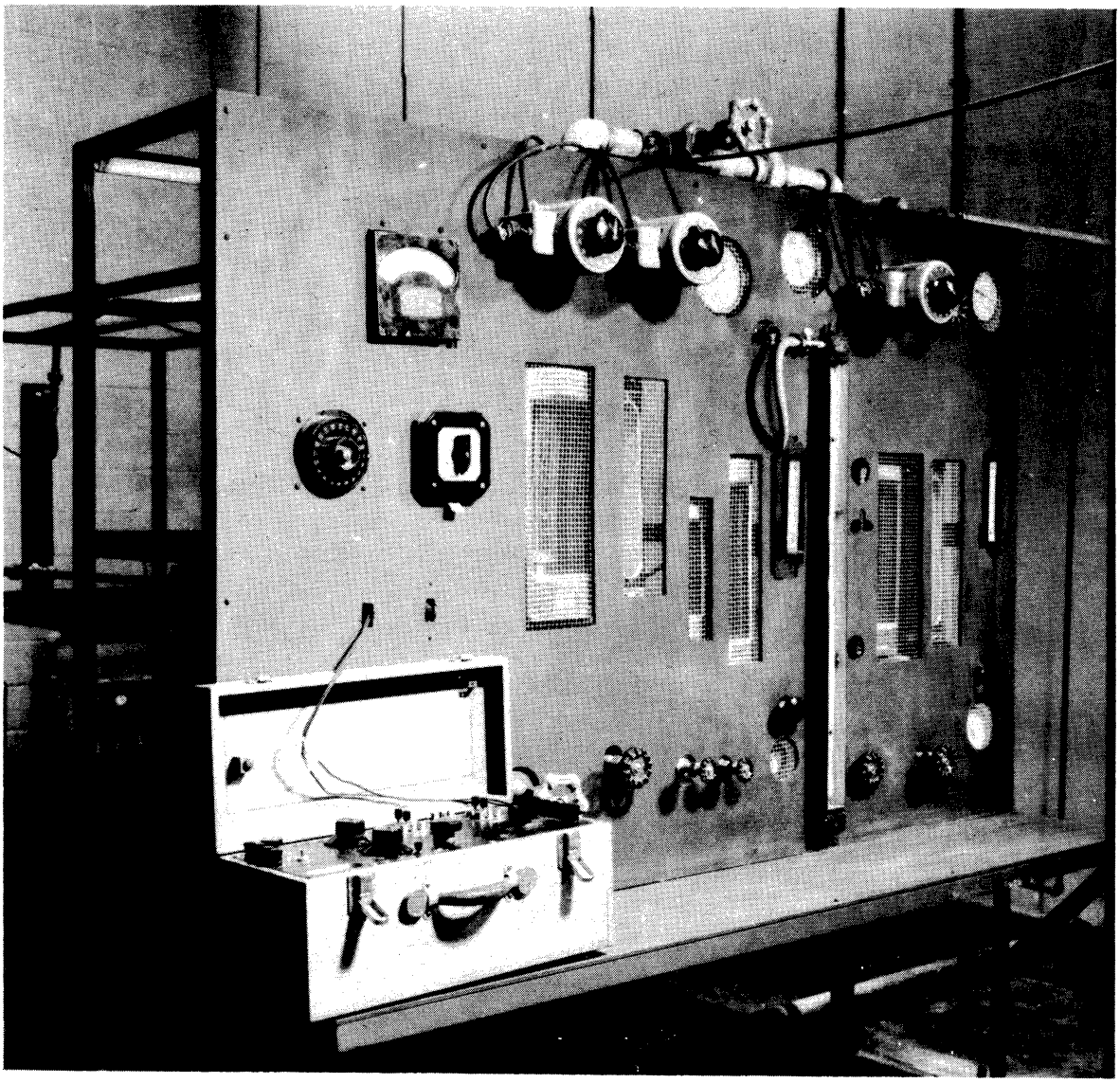

Figure 1. Photograph of Control Panel

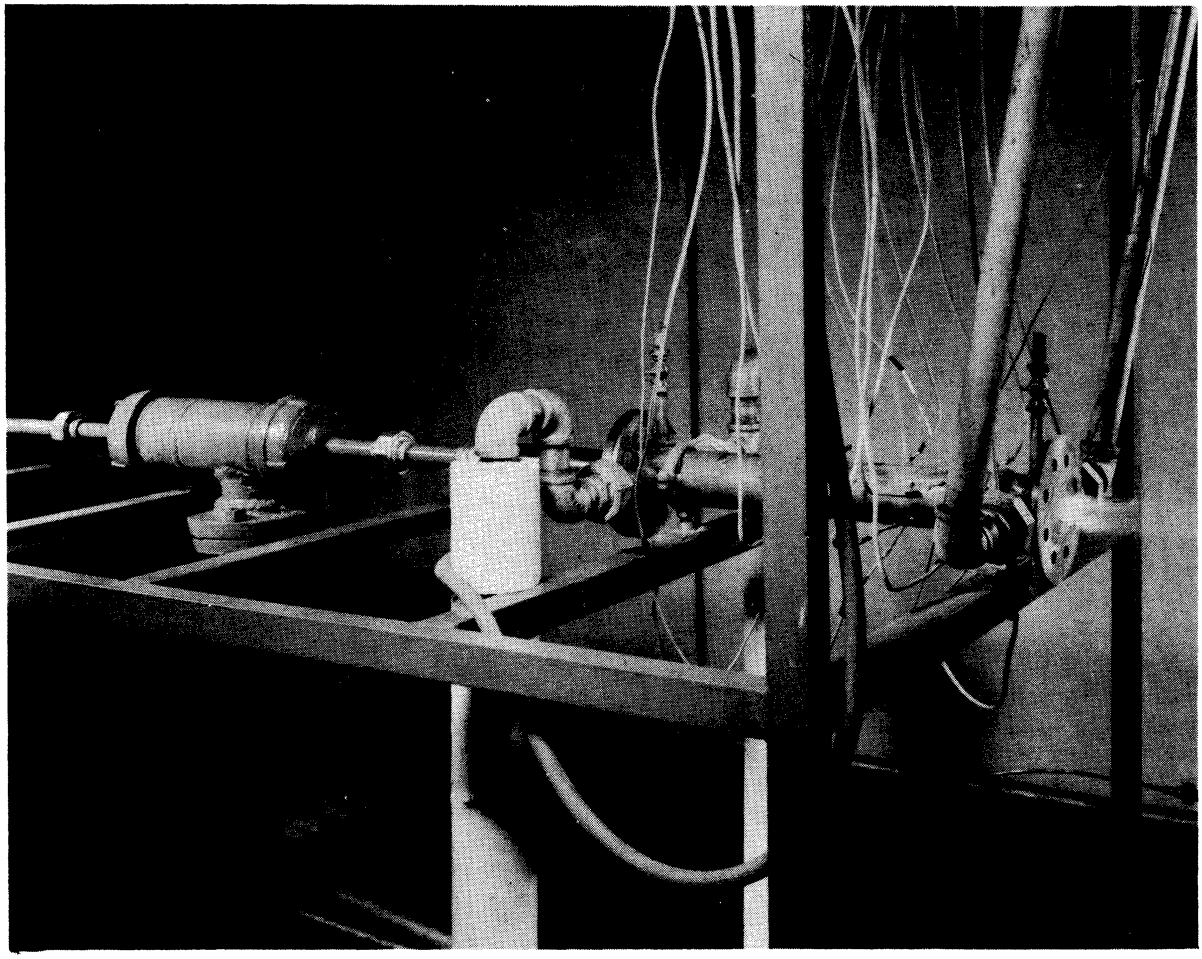

Figure 2. Photograph of Heat Transfer Unit and Plenum Chamber

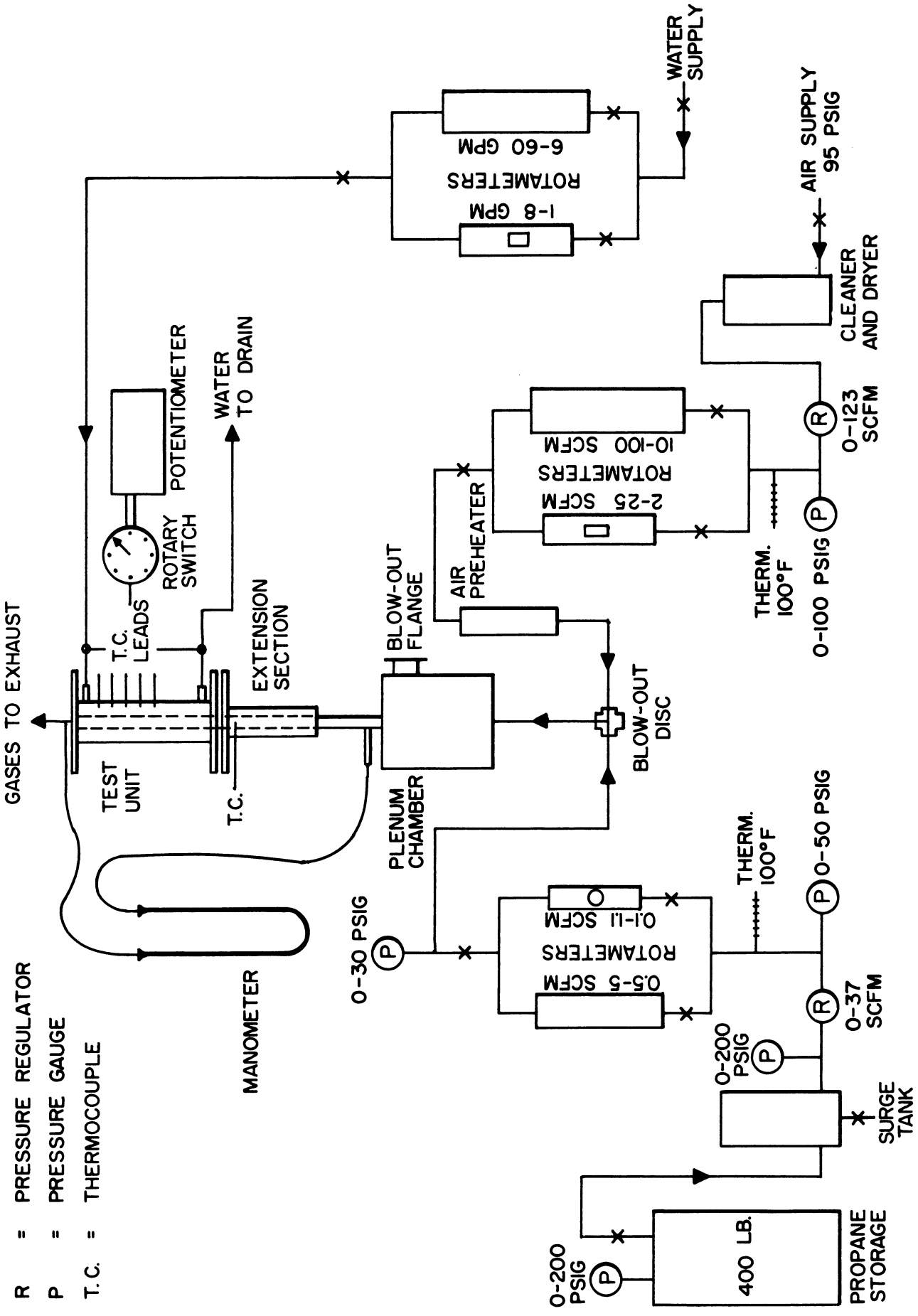

Figure 3. Schematic Diagram of Flow Systems

heat transfer unit. The combustion products from the tube are exhausted through a suction system.

Cooling water is supplied at a constant rate to the annulus of the test unit by the building water system. All thermocouples are connected to a rotary selector switch, and all voltages are measured on a semi-precision portable potentiometer.

Air and Fuel Supply System

The air was furnished by the building supply system at 95 psig. Since humidity of the air is known to affect the rate of combustion, a cleaner and dehumidifier was installed in the line before the metering section and test unit. The cleaner was a metal box made of 1/4 inch steel plate, 1 foot square, and 1 1/2 feet high. The air entered through two diametrically opposed holes near the bottom of the box. A metal plate and a central hole was inserted above the inlet holes to reduce channeling along the sides of the container. About six inches of 3/16 inch diameter ring packing was placed on this plate. On top of the rings was a 1 inch layer of steel wool. The packing and glass served the purpose of filtering out entrained oil and dirt particles from the compressor. Above the steel wool was 8 inches of anhydrous 4 mesh calcium chloride to remove moisture from the air. The air from the compressor at the high pressure possessed a low moisture content, and the dessicant served to reduce it even further. No attempt was made to control the humidity at a specified level. Although the maximum air velocity through the box was less than 1/2 foot per second, the air tended to channel through the calcium chloride. Regular inspection and frequent replacement of the dessicant minimized the

undesirable channeling.

After the air cleaner, the air was reduced in pressure to 35.3 psig (50 psia) by means of a bleed-type pressure regulator with capacity up to 123 SCFM. The outlet pressure was essentially unaffected by small fluctuations in the inlet air supply line. The air from the regulator passed through one of two rotameters in parallel. The low flow rate meter had a range from 2 to 25 SCFM and the high range meter from 10 to 100 SCFM (at 50 psia and 70°F). A needle valve downstream from the rotameter controlled the flow rate. Bourdon-type pressure gages were inserted in the air line before and after the pressure regulator to measure supply pressure and inlet rotameter pressure, respectively. The air temperature was measured by means of a thermometer in the line prior to the rotameter. The air supply system was mainly constructed of 3/4 inch pipe.

The air from the rotameter passed through a 1500 watt electrical heating unit. The outlet temperature from the air heater was controlled by a thermostat with a range of 50 - 250°F.

Commerical propane, consisting of about 97 percent propane and the remainder propylene, was stored in a 400 pound tank. The tank was equipped with a liquid level indicator and a pressure gage. Three Chromalox electric heating elements were inserted near the bottom of the tank. Each heater had a capacity of 750 watts at 115 volts and a surface area of about 100 square inches. Without the heating elements the latent heat of vaporization for the propane would be supplied from the sensible heat of the liquid and heat transfer from the surroundings to the tank. During

rapid and prolonged withdrawal of propane vapor, calculations indicated that heat transfer from the surroundings would only partially supply the latent heat requirements. Hence, the temperature and vapor pressure of the liquid propane would decrease. The heating elements allowed a relatively constant pressure to be maintained during a run. The supply of electric current to each of the heaters was controlled by individual variacs.

The vapor pressure of propane in the tank is mainly dependent upon outside temperature and varied from about 90 to 140 psia during the course of the investigation. The vaporized propane was passed through a 4 inch by 12 inch cylindrical surge tank to a pressure regulator of 37 SCFM capacity. After its pressure was reduced to 50 psia, the propane was sent through one of two rotameters in parallel. The low capacity meter had a range of 0.1 to 1.1 SCFM and the other a range of 0.5 to 5 SCFM (at 50 psia and 70°F). The flow rate was controlled by a needle valve downstream of the rotameter. The supply pressure and rotameter pressure were measured by bourdon-type gages. Rotameter inlet temperature was indicated by a liquid thermometer.

The rotameter calibration curves specified by the manufacturer, together with a few check points obtained with a critical flow prover, appear in Figures 46 to 49 of Appendix D. The rotameter inlet pressure was maintained at the calibration pressure (50 psia) and the inlet temperatures had a maximum deviation of 3°F from the calibration temperature (70°F).

Cooling Water System

Preliminary tests indicated that the building water supply system provided water of reasonably constant pressure and temperature. For this

reason, no controlled water circulation system was installed. During a run, temperature variations usually did not exceed 0.5°F and pressure fluctuations were such that flow did not vary more than 4 percent. The cooling water was metered through one of two rotameters in parallel. The smaller capacity meter had a range of 0.8 to 8 GPM while the larger meter had a capacity up to 60 GPM.

Plenum Chamber

The separate streams of air and propane vapor were combined at a 3/4 inch pipe cross. The fuel and air entered at diametrically opposite ends of the cross. A 3/4 inch union type blowout disc was attached to another outlet of the cross. The union contained a thin aluminum disc designed to rupture at a pressure of 150 psia. The combined stream passed through the opening opposite the blowout assembly to a plenum chamber which was designed to fulfill the following functions: (1) to aid in the mixing of propane and air, (2) to furnish a flame trap and blow-out disc assembly and (3) to provide a sufficient volume to ensure that the exit tube is acoustically "open". This means that a standing sound wave oscillating in the length of tube between plenum chamber and test section exit would have a pressure node at the plenum chamber end of the tube.

The plenum chamber was constructed from a 12 inch length of 4 inch diameter pipe. A 3 inch flange assembly was attached near the exit end. A 0.001 inch piece of brass shim stock inserted between the flanges as a blowout disc was found to rupture at about 50 psia. The flame trap consisted of a 4 inch diameter sintered stainless steel disc

fastened by screws to a 1/2 inch thick stainless steel support plate. The support plate, containing a multiplicity of 1/4 inch holes to allow passage of the gas, was welded in place near the entrance of the plenum chamber. The sintered stainless steel serves to quench any deflagration reaching the plenum chamber, while the blowout assembly relieves any abnormal pressure increase through rupture of the shim stock. Mixing of the gases in the plenum chamber was promoted by a series of three 50 mesh screens. The chamber was closed at either end by a 4 inch cap. A schematic sketch of the plenum chamber appears in Figure 4.

Heat Transfer Unit

The heat transfer test unit was, functionally, a counter-current heat exchanger. High temperature burning gases on the inside transferred heat to cooling water in the annulus. Details of the test object are provided in Figure 5.

The test object was constructed from a 20 inch length of type 304 stainless steel. The outside diameter was 1.940 $\pm$ 0.004 inches while the inside diameter varied in an uneven fashion from 0.970 inches at one end to 0.975 at the other. The internal fluctuations are in part due to variations in surface roughness. Six isolated sectors were provided along the length of the tube by cutting thirty mil longitudinal grooves and chordal slots to within 25 mils of the inside surface. At each sector, the longitudinal grooves were 60° apart whereas the chordal slots were 1 inch from each other. The midpoints of these sectors were located at 2, 4, 6, 8, 10 and 12 inches from the front of the tube. The

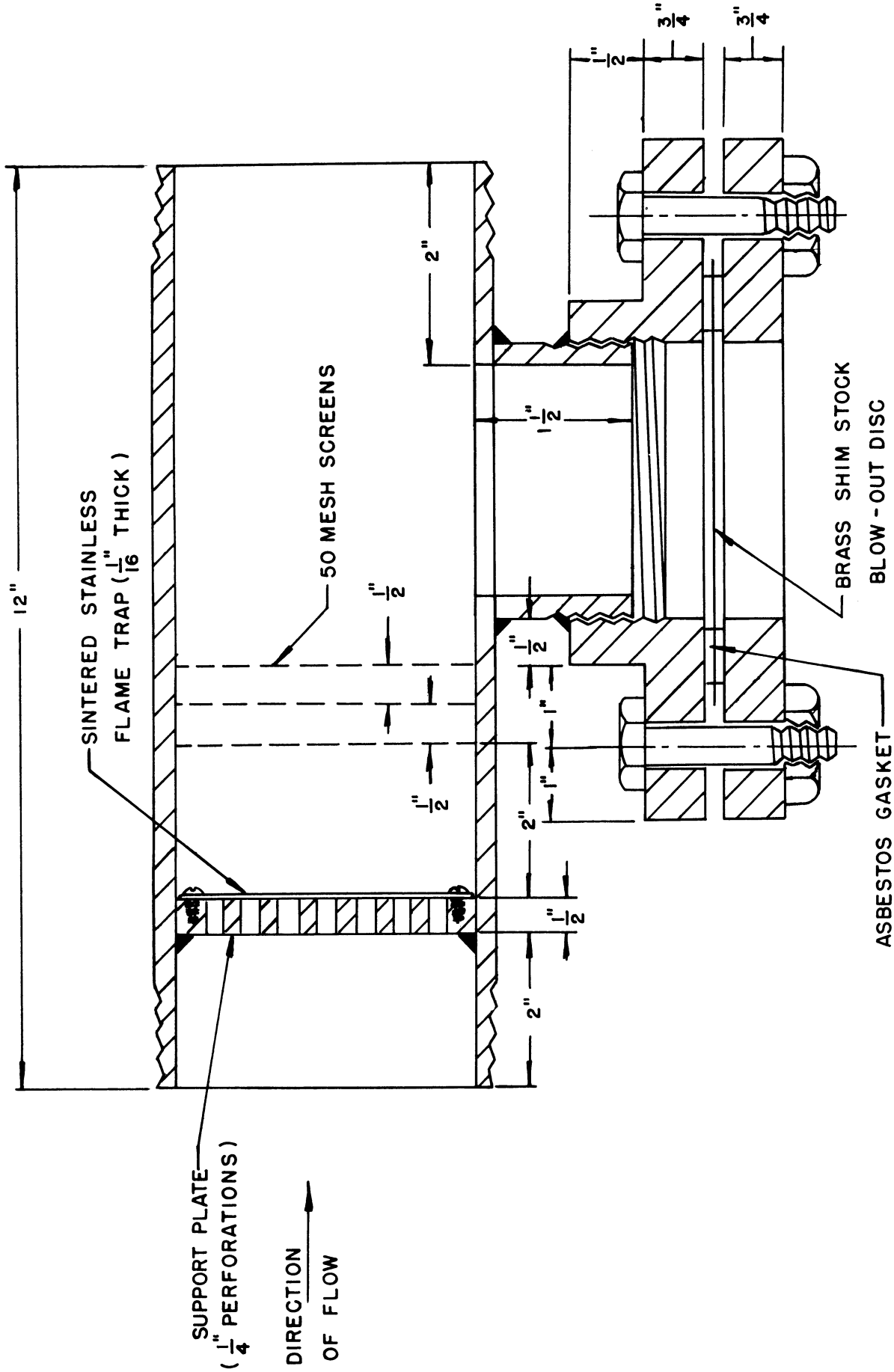

Figure 4. Detail of Plenum Chamber.

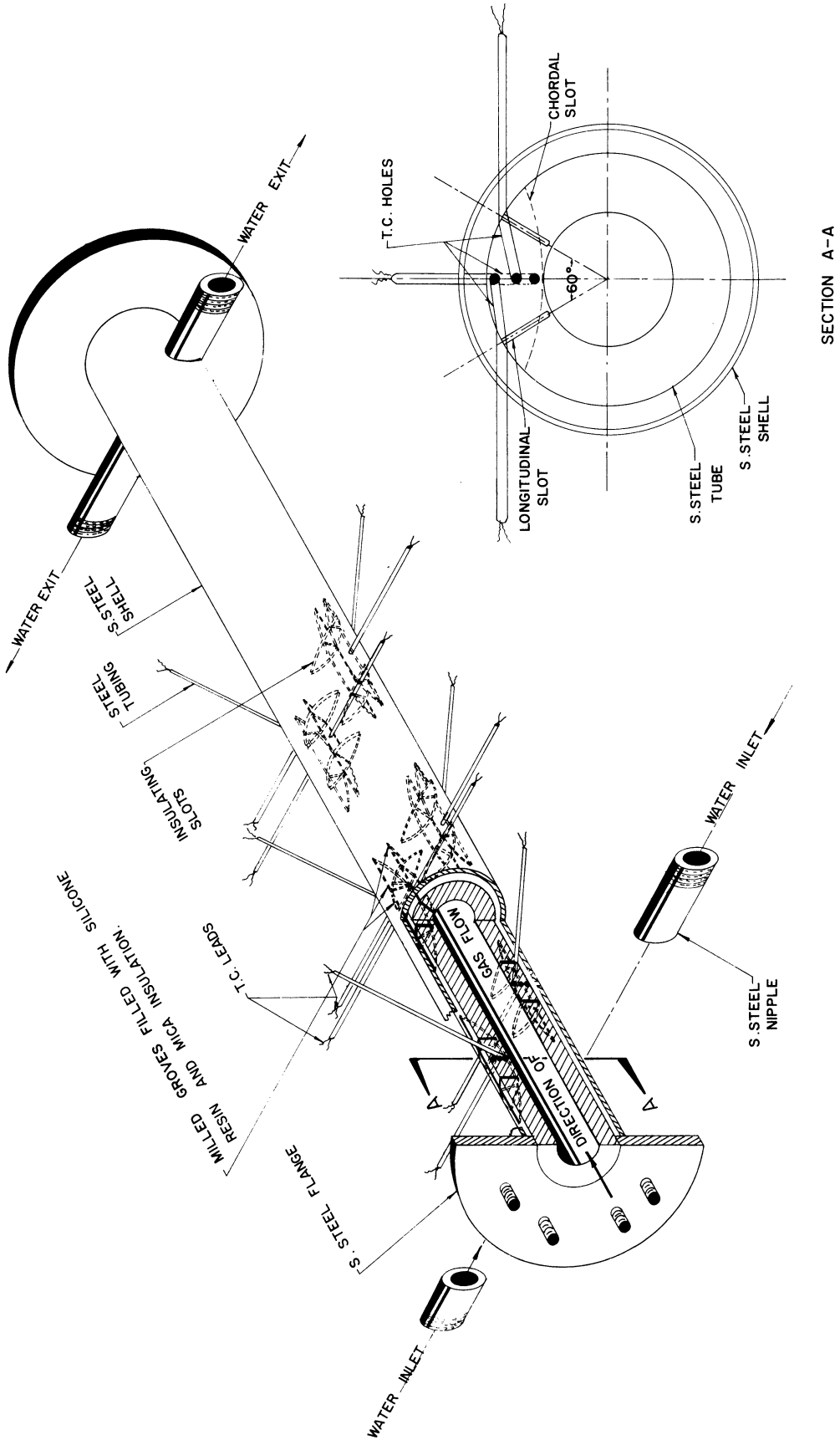

Figure 5. Detail of Heat Transfer Test Object

stations at 2, 6, and 10 inches were diametrically opposed to the stations at 4, 8, and 12 inches. The 20 inch tube could be turned around so that the stations would then be located at 2 inches intervals starting at 8 inches from the front of the tube. Three 42 mil holes were drilled in each sector to be on a radial line through the midpoint of the sector. The holes were drilled to radial positions of about 0.58, 0.75, and 0.92 inches. The holes to the top and middle started from opposite sides of the sector, while the bottom hole was drilled from the rear. The details can be best seen by examining Figure 5.

The thermocouples were made from 36 gage Chromel-Alumel wires enclosed in a stainless steel sheath of 40 mil outside diameter. Insulation of the wires from the sheath was provided by pure magnesium oxide, which is a good electrical insulator up to 3000°F. The wires were exposed at both ends of a 3 inch sheath length by removing about 1/4 inch of the sheath in a lathe. The thermocouple junctions were carefully made to approximate a point junction centralized at the end of the stainless steel sheath. The exposed wires at one end were twisted together close to the sheath so that lateral motion of the junction was minimized. After silver soldering the junction, the excess wire and solder was cut and filed away. The junction was examined under a microscope to see if a small centralized junction was present. If the junction was excessively large, or if the wires did not appear well connected, the junction was reconstructed. Each satisfactory junction was then checked against a calibrated thermometer in a steam bath.

To install the thermocouples, small silver solder chips were dropped into each hole in the test object. The solder was melted by careful heating with a torch, and the thermocouple pushed to the bottom of the hole, where it became fastened upon cooling.

After insertion of the thermocouples, the grooves were filled with thin strips of mica fastened together with a water resistant, high temperature insulating resin. The whole test object was baked at 300°F to cure the resin. The low thermal conductivity of the mica and resin effectively insulate each sector from the remainder of the unit.

Onto each end of the test unit was welded a stainless steel flange, 6 inches in diameter and 1/4 inch thick. A stainless steel annular tube, 2.5 inches in outside diameter and 1/8 inch thick was put on the test object in two halves. The ends of the annulus were welded to the flange pieces and the seam closed with silver solder. The holes where the steel thermocouple sheaths protruded through the annular shell were soldered tight. Water inlet and outlet nipples were welded on to diametrically opposite sides of the annulus at both ends. Two thermocouples wells were placed in the inlet water line and one in the outlet line, each thermocouple well containing a 26 gauge copper-constantan thermocouple. The outlet and one inlet thermocouple were connected to provide the differential change in water temperature.

Since the test section was designed to assume a horizontal position, provision was made for removal of gases from the annular shell. A hole was drilled into the top piece of the annular shell at both ends. A 1/4 inch pipe nipple and stop cock was attached. Gases were removed

from the annulus by allowing water to run through the stopcocks for a few moments.

The thermocouple leads from the steel sheaths were carefully soldered to insulated 16 gauge chromel and alumel leads. The junctions were insulated with a plastic resin. From the junctions the wires ran to a low-resistance rotary selector switch, from which one couple at a time could be routed on a single pair of insulated leads to a potentiometer. The cold junction temperature was measured by a thermometer with 0.1°F graduations, placed on the top of the potentiometer.

In determining the hot junction temperature, the emf corresponding to the cold junction thermometer reading is taken from standard tables. An arbitrary reference temperature of 32°F was selected for convenience in using the tables. The cold junction emf is added to the emf indicated on the potentiometer. The actual hot junction temperature corresponds to the total emf and is read from the tables. Since temperature differentials are used in calculated rates of heat transfer, any errors in the cold junction temperatures are reduced in significance.

During construction and installation of the test object, three thermocouples became inoperable. Two of them were located at the 12 inch station and one at the 10 inch station. Since two satisfactory thermocouples remained at the 10 inch position, the rate of heat transfer at this location could be obtained.

The fifteen operable thermocouples were tested after completion of the runs in a constant temperature water bath. No measurable difference was found between the different thermocouples. The standard cell of the potentiometer was checked against another standard cell recently calibrated by the National Bureau of Standards.

The galvanometer sensitivity of the potentiometer allowed readings within 2 microvolts. The reproducibility of thermocouple readings during runs varied from 2 to 20 microvolts and depended upon the flame-generated oscillations.

Extension Section

An extension piece for the test object was provided by a ten inch length of the stainless steel tubing used in constructing the test object. A 6 inch flange was attached to one end of the extension and a one inch pipe thread was cut on the other. Since the flanges on the extension section and the test object had identical hole geometries, the extension could be attached to either end of the test object. The extension piece also aided in developing the velocity profile of the mixture entering the test object. The inlet mixture temperature to the test object was measured by an asbestos insulated, 26 gauge copper-constantan thermocouple. The thermocouple extended into the gas stream through a 1/4 inch polyethylene seal, located in the extension section one inch from the flange.

The plenum chamber was connected to the threaded end of the extension section by a length of one inch pipe. The immediate exit of the plenum chamber consisted of a 3 inch length of 0.97 inch inside diameter stainless tubing.

Flame Holder Assembly

The flame propagated within the tube from a flame holder. Preliminary experiments indicated a central plate or cone was satisfactory.

The flame holder was welded to the end of a 1/4 inch diameter stainless steel rod which extended back through the inlet piping. To keep the rod and flame holder carefully centered in the heat transfer unit, annular rings were attached to the rod at two positions. The annular rings were constructed of 1/32 inch thick steel and were connected to the central rod by four 1/16 inch diameter steel struts. A close fit between the annular rings and the test unit wall aided in insuring a centralized flame holder. Movement of the flame holder in the tube was provided by a wire attached to the upstream end of the rod. The wire extended back toward the plenum chamber and protruded from the side of the tube through a polyethylene seal. By pulling on the wire, the flame holder was moved upstream into the tube. Final positioning was achieved by inserting a thin stainless steel rule from the open end of the test object. The flame holder was pushed to the desired position by the rule. The accuracy of this positioning method was about 0.03 inches.

The bluff body flame holders were constructed from stainless steel. Runs were made using three flame holders.

1) a flat plate with a diameter of 0.70 inches and a thickness of 1/4 inch.
2) a flat plate with a diameter of 0.53 inches and a thickness of 3/16 inch.
3) a cone with a diameter of 0.70 inches and a 45° apex angle.

Pressure Drop Measurement

The efficiency of combustion was calculated from the pressure drop across the test unit during combustion. A pressure tap was located 1/2 inch from the plenum chamber in the exit pipe. Since a pressure node existed at the plenum chamber exit, the pressure at this point was unaffected

by the presence of any flame-generated longitudinal oscillations. A 1/16 inch hole was drilled through the pipe and the inside surface carefully filed to remove any protrusions. A 1/4 inch inside diameter steel tube was welded over the hole, and rubber tubing extended to the manometers. Since expected pressure differentials ranged from 0.05 to 10 inches of water, two manometers were used. For measurements between 2 and 10 inches, a vertical water in glass manometer was employed. The pressure difference could be read within 0.06 inches, giving a minimum accuracy of 3 percent. For low pressure drops, a micromanometer was utilized. A sketch is shown in Figure 6. A water reservoir is connected by rubber tubing to a piece of glass tubing, inclined slightly from the horizontal. The glass tube is attached to a screw thread assembly. The water meniscus in the glass tube is maintained approximately vertical by surface tension. In operation, the water meniscus is first positioned at a zero mark. After applying the pressure differential, the water meniscus is returned to the zero mark by raising or lowering the glass tube. The screw thread has 48 turns per inch. Since the reading can usually be determined within 1/4 of a turn, the manometer is accurate to about 0.005 inches.

Exit Probe Measurements

A thermocouple and pitot-static tube traverse were performed at the exit of the tube for a few runs. The thermocouple was constructed of butt welded 16 gage chromel-alumel wires. A 30° angle was formed by the two wires at the junction. The large diameter wire was used in order to extend the life of the thermocouple in the high temperature gas stream.

SCALE: APPROX. 1/3 SIZE

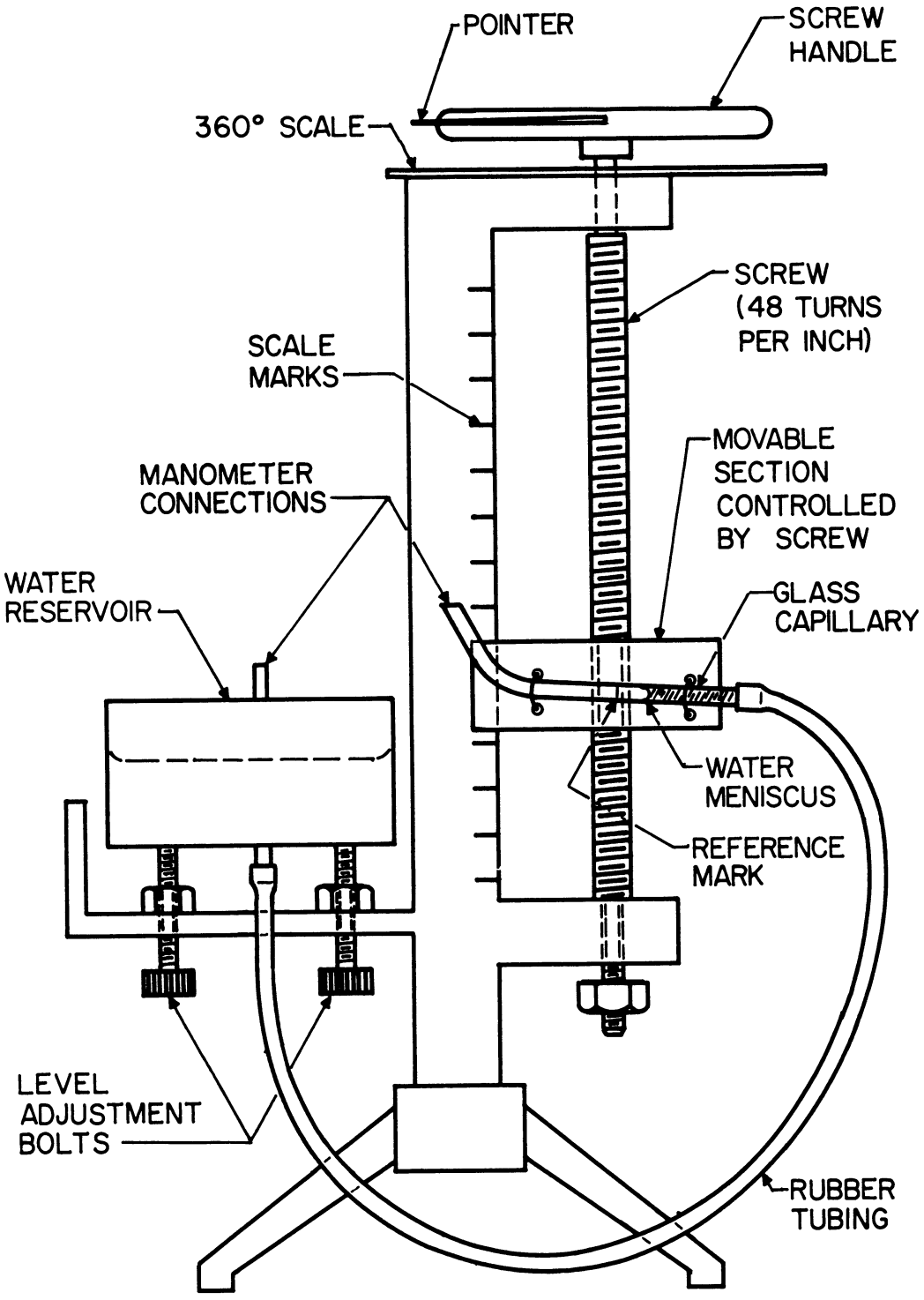

Figure 6. Detail of Micromanometer

No shielding was applied to the junction.

The total pressure probe consisted of a stainless steel tube with an outside diameter of 1/8 inch and an opening of 1/16 inch diameter. The tip was tapered slightly to reduce flow interference. The static pressure probe was also constructed from the 1/8 inch diameter tubing. Two 0.02 inch holes were drilled into the tube at a distance of 1/2 inch from a closed end to provide the static opening.

Ignition System

The wiring diagram of the ignition system appears in Figure 7. Functionally, the system was similar to an automotive ignition system. A repeating spark was produced by a 12 volt automotive coil connected to a vibrator tube and appropriate condensors. The spark plug fired about 100 times per second. Energy was supplied by a 12 volt storage battery.

Sound System

The relative amplitudes of the sonic frequencies generated by the combustion process were measured by a General Radio sound meter and sound analyzer. The diaphragm of the sound meter microphone was positioned four inches below the exit of the heat transfer test object. The sound analyzer was used to measure the amplitudes of the components of the frequency spectra relative to the overall sound amplitude. An absolute measurement of the intensity of sound within the tube was not attempted.

Acoustical Dampers

Organ pipe oscillations can be energetically damped by a quarter wave length tube placed in the region of a pressure antinode[51]. The

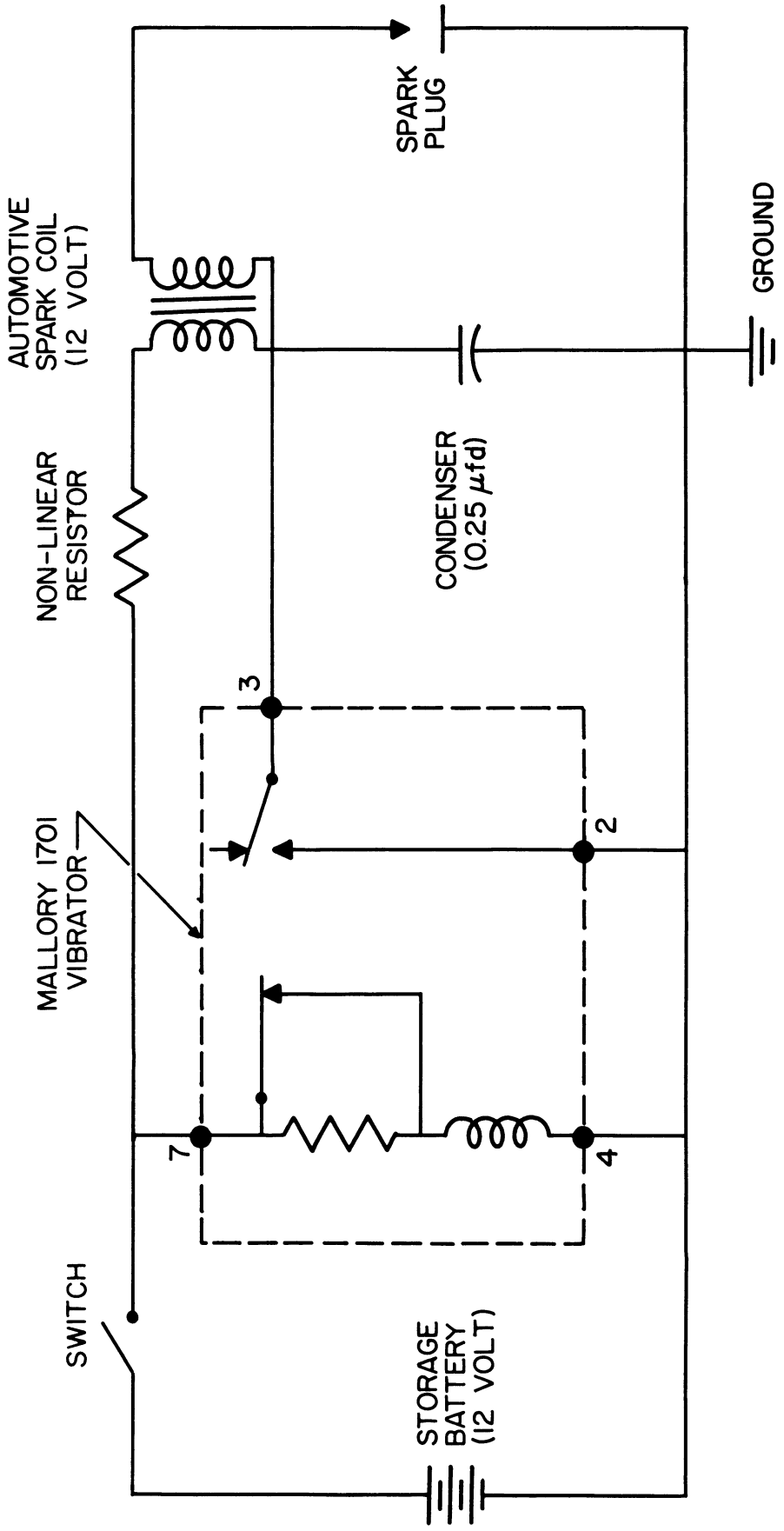

Figure 7. Wiring Diagram of Ignition System

theory of a quarter wave length tube has been outlined in the literature survey.

For a total tube length of 9 ft. between plenum chamber and test object exit, the major frequencies observed were around 210, 280, and 350 cycles per second, corresponding to pressure antinodes near 15, 12, and 9 inches from the plenum chamber, respectively. At each of these positions, a 1/4 inch hole was drilled through the pipe. A 1/2 inch length of a 1/4 inch pipe bushing was welded over each hole. A length of 1/4 inch pipe, capped at one end, could now be inserted in the bushing as a quarter wave length tube. The length of pipe required to damp an oscillation effectively depended on the frequency. Several lengths of 1/4 inch pipe were prepared as quarter wave length tubes.

When damping of the flame-generated oscillations was not desired, the 1/4 inch holes in the main pipe were sealed with polyethylene plugs.

Mixture Approach Conditions

At least two feet of one inch pipe was present between the plenum chamber and flame holder, allowing the inlet mixture to approach fully developed pipe flow. In order to determine whether the upstream velocity profile and turbulence level had any substantial effect on the rates of heat transfer, screens were installed upstream of the flame holder for a few runs.

Baines and Peterson[2] obtained correlations for the effect of screens on turbulence level and velocity profile over a wide range of variables. For screens of solidity ratios less than 0.5 and screen

Reynolds numbers greater than 100, they report a turbulence intensity less than 4 percent after 100 bar lengths. In order to obtain a relatively flat velocity profile, they recommend a few screens of moderate solidity placed in series.

Three 30 mesh brass screens with a bar width of 0.007 inches and a solidity ratio of 0.38 were used in the experiments. The screens were made to fit the inside diameter of the tube closely. The screens were placed at distances of 1, 1 1/2, and 2 inches upstream of the flame holder. They tend to produce an approach stream with a fairly flat velocity profile and a low turbulence level.

MATERIALS

The selection and source of some of the materials pertinent to the investigation are discussed below. A list of the major items used in the construction of the remainder of the equipment is listed in Appendix E.

Propane

Commercial propane was selected as a fuel due to its ready availability, reasonable cost, safe handling characteristics, and vapor pressure level for easy metering. The propane, containing about 97.5 percent propane, and the remainder propylene, was supplied by the Gallup-Silkworth Company.

Test Cylinder

Stainless steel was selected for the test cylinder because of its resistance to oxidation at high temperatures. The thermal conductivity of type 304 stainless steel is listed in Figure 45 of Appendix D. The tube was supplied by the Babcock-Wilcox Company.

Thermocouples

The 36 gauge chromel and alumel wires, insulated by magnesium oxide and enclosed in a stainless steel sheath, were supplied by the Aero Research Corporation.

VARIABLES OF THE PROCESS

A large number of process variables are involved in a study of heat transfer rates from bluff body stabilized flames within a cooled tube. The independent variables can be associated with the fuel, the inlet conditions, and the geometry of the system.

Fuel: nature of the fuel, such as reactivity and heat of combustion.

Inlet conditions: proportions of fuel and air, velocity, temperature, velocity distribution, scale and intensity of turbulence, homogeneity of the mixture, humidity.

Geometry: diameter of the tube, surface roughness, flame holder type and shape, flame holder blockage, total length of tube, length in which burning is conducted.

An important dependent variable, inside surface temperature, depends on the thermal resistance of the wall and external cooling condtions as well as the variables listed above.

Since a systematic study of all the independent variables is beyond the scope of a single investigation, a number of variables were held constant or nearly so. The remaining variables were examined with varying degrees of emphasis. A brief discussion of each variable follows. More detailed consideration of most of the variables is presented in other sections.

Fuel: Commercial propane was burned throughout the investigation.

Tube diameter: A single diameter of about 0.97 inches was used.

Tube roughness: Pressure drop measurements indicate that the roughness is approximately equivalent to commercial pipe.

Combustor pressure: Since the gases discharge to the open atmosphere and pressure losses in the combustor are small, the combustor operates at essentially atmospheric pressure.

Homogeneity of the inlet mixture: Unknown. Turbulence inducing screens in the plenum chamber and diffusion in the entrance piping promote mixing of the propane and air.

Inlet turbulence level: Unknown. A majority of the runs were conducted with developed pipe flow. A few runs were made with screens upstream of the flameholder, which produced a predicted turbulence intensity of about 5 percent at the flame holder.

Inlet velocity distribution: Unknown. The presence of turbulence promoting screens tends to flatten the velocity profile at the flame holder.

Inlet humidity: Maintained roughly constant at 0.001 lbs. water per lb. of dry air. Variations were due to lack of control on dehumidifier.

Inlet air temperature: Most runs were taken at about 70°F. A few measurements were made at 120°F.

Flame holder type and shape: The studies were conducted with centralized flat plates and cones.

Flame holder blockage: Extensive measurements were made on a flat plate of 52 percent blockage. More restricted studies were conducted using a flat plate of 30 percent blockage and a 45° cone of 52 percent blockage.

Total length of tube: Most data were taken with 9 feet between plenum chamber and discharge end of heat transfer unit. Some studies were

made on 3, 3.5, and 8 foot lengths.

Burning length: The flame holder was positioned at distances of 7, 9, and 11 inches from the exit of tube. In this manner, the first heat transfer station was always located 1 inch downstream of the flame holder.

Inlet mixture velocity: The approximate inlet values studied were 10, 20, and 30 feet per second, corresponding to inlet Reynolds' numbers of about 5,000, 10,000, and 20,000 respectively.

Inlet fuel-air ratio: Most runs were made with mixtures containing stoichiometric proportions, 10 percent excess propane (rich) and 10 percent excess air (lean). Some data were taken near the rich and lean blowoff limits.

EXPERIMENTAL PROCEDURE

Preliminary investigations, preparations for a run, operating procedures, and location of thermocouples are discussed in the following sections.

Preliminary Experimental Work

Prior to construction of the heat transfer test object, experiments were conducted to determine the feasibility of burning from a flame holder within a small diameter tube. In order to allow a wide range of mass flow rates within the capacity of the air supply (80 SCFM), a one inch diameter tube was selected for evaluation. The preliminary test object was a double pipe heat exchanger, 3 feet long, consisting of a one inch diameter pipe enclosed in a 2 inch pipe. Water was circulated through the annulus during tests. No provision was made for measurement of heat transfer rates. Experiments were conducted with a variety of flame holders to determine the length of tube in which combustion was possible. In general, there were two reasons for rejection of a flame holder (1) blowoff from the flame holder at low flow rates and (2) premature blowoff caused by flame generated oscillations. The oscillations were noted to become more severe as burning was conducted in longer lengths of tube. Both grid and low blockage bluff body type flame holders were rejected because of blowoff of the flame at low flow rates. An annular type flame holder gave apparent premature blowoff due to oscillatory combustion while burning in a 6 inch length of tube. Later experiments, however, indicated that cooling of the flame holder by the wall contributed to the

decreased stability. Centralized flat plate and cone type flame holders with blockage above 30 percent appeared to give satisfactory combustion in burning lengths up to 12 inches and over moderate flow ranges. The amplitude of the flame-generated oscillation was noted to increase with higher flow rates.

On the basis of the preliminary experiments, the heat transfer test object was constructed with six measuring stations spaced at two inch intervals along its length. Before taking any experimental data, the whole apparatus was checked for the proper operation of its component parts.

Preparations for a Run

To start operation, the desired water rate of about 5 gallons per minute was established through the annulus of the test object. The bleed ports at the top of the annulus were opened for a few moments to allow removal of any trapped air. The flow of air and propane vapor were adjusted to give the desired flow rate and fuel-to-air proportions. The thermostat on the electrical air heater was adjusted to provide the desired inlet mixture temperature to the heat transfer unit. Since maximum propane consumption rate was generally much lower than anticipated during design, it was found that use of the heating elements in the propane tank was unnecessary. The spark plug was placed immediately in front of the flame holder at the exit of the tube, and the fuel-air mixture ignited. The flame holder was then moved into the tube and carefully positioned at the desired depth.

When suppression of burner oscillations was wanted, a quarter wave tube was inserted into one of the locations provided in the main pipe. Since one frequency generally predominated, only one quarter wave tube was usually required to obtain adequate damping. Although theory was used as a guide, the length and position of the quarter wave tube was decided by trial and error.

Steady state conditions were generally reached within ten minutes.

Experimental Measurements

When the wall temperatures reached steady state, readings were obtained with the potentiometer for the fifteen operable chromel-alumel thermocouples imbedded in the wall of the test object. Two or more readings were obtained for the thermocouples at each of the five measuring stations to be certain that steady-state conditions had been attained.

At the beginning and end of each run, readings were recorded for propane and air flow rates, inlet rotameter pressures, inlet rotameter temperatures, pressure drop across the heat transfer unit, inlet gas temperature to the heat transfer unit, water flow rate, inlet water temperature, and differential water temperature across the annulus. If any significant variation in these variables was noted, the run was repeated. The overall noise level at the tube exit was read from the sound meter for each run. The frequencies and sound levels of any outstanding components in the overall noise level were obtained with the sound analyzer.

After a few runs, the fuel and air flow was stopped completely, and the temperature rise of the water in the annulus due to conduction from the room was recorded. This reading supplied a correction to the total temperature drop to give the net effect of heat transfer from the gas alone. In addition, the drag due to the flame holder and tube walls in the absence of combustion was determined for each run. The flow rate of air alone was adjusted to the total flow rate of air and propane used in each run and the pressure drop recorded.

The inside surface of the tube was inspected frequently. If any foreign matter appeared, the surface was cleaned with a mixture of methanol and acetone. Since the inside surface temperature did not exceed 400°F, there was no apparent oxidation of the stainless steel during the investigation.

Location of Thermocouples

Due to machining inaccuracies during drilling of the thermocouple holes in the test object, the locations of the bottom of the holes were not known with the desired precision. In addition, the presence of a small chip or burr in a hole could prevent the thermocouple junction from reaching the bottom of the hole. Each thermocouple junction was carefully formed so as to approximate a point junction at the end of the stainless steel sheath. The small junction also minimized the possibility of radial displacement of a junction toward the enclosing sheath. Thus, the thermocouple junction was located directly at the tip of the sheath and close to the center of the sheath. Preliminary tests indicated that the maximum possible displacement of

a junction was about 10 mils. By locating the tip of the sheath, then, the position of a junction can be estimated within 10 mils.

Following the conclusion of experimental runs, the test object was sliced transverse to the axis of the tube near each of the thermocouple stations. Each slice was cut down in a lathe until the centers of the ends of the sheaths were approached. Cuts were then removed 1 mil at a time and the region of a sheath tip inspected with a toolmakers microscope after each cut. In some cases the thermocouple junction could be seen with the toolmaker's microscope. A depth gauge was then used in conjunction with the microscope to measure the position of the junction. In other instances, however, the junction was destroyed in the grinding process. The location of the center of the sheath tip was then measured and used in evaluating the heat transfer data.

In cases when the junction was visible, the center of the junction could be measured within 5 mils. When the junction was destroyed, the location could be estimated within 15 mils.

For each thermally-isolated sector, Equation 6 indicates that a semi-log plot of measured temperature versus thermocouple position should be linear. The expected linear relation was observed for essentially all the data.

The maximum error in heat flux due to inaccuracy of thermocouple location is estimated to be 6 percent.

EXPERIMENTAL THEORY

In this section, a description of the theoretical considerations employed in evaluating the test results is presented. The theory is briefly outlined and important assumptions noted. Details of the derivations are found in Appendix C.

Measurement of Rate of Heat Transfer

For the conduction of heat in an isotropic solid, the following equation can be written

$$\rho\, C_p \frac{\partial T}{\partial t} = \text{div } (k \text{ grad } T) \tag{5}$$

By assuming

$$\frac{\partial T}{\partial t} = 0, \frac{\partial T}{\partial x} = 0, \frac{\partial T}{\partial \theta} = 0$$

and using an average thermal conductivity, k_{av}, the radial flux at the inside surface of a cylinder is

$$(q/A)_s = \frac{k_{av}}{r_s} \frac{T_s - T_o}{\ln \frac{r_o}{r_s}} \tag{6}$$

The inside and outside surface temperatures are obtained by extrapolation of the internally measured temperatures.

The total heat transfer in the test section can be obtained by an integration of heat fluxes and by the increase in enthalpy of the cooling water

$$q = W C_{pw} \Delta t_{w_{net}} = \int_o^A \left(q/A\right)_{s_{total}} dA \tag{7}$$

where Δt_w is the net increase in water temperature due to transfer of heat through the internal wall alone.

The assumptions of the analysis are not expected to cause a significant error. Since all experimental conditions were maintained as constant as possible during a run, the steady state assumption that $\partial T/\partial t = 0$ appears valid. The effect of longitudinal and angular gradients ($\partial T/\partial x$ and $\partial T/\partial \theta$) are made negligible by the installation of low thermal conductivity insulation in the longitudinal and chordal slots. The use of an average thermal conductivity has been examined by Churchill[9], who shows, for a similar case, that the heat transfer rate calculated with the assumption of a constant average thermal conductivity differs negligibly from the result obtained by a more involved rigorous procedure. The presence of thermocouple holes introduces an anisotropic region in the cylinder wall. By application of conformal mapping, the maximum error in flux measurement caused by the presence of these holes is estimated as less than 5 percent. The derivation and calculations are found in Appendix C.

A more thorough discussion of the above assumptions are presented by Churchill[9] and Zellnik[84].

Combustion Efficiency

For a thin discontinuity in flow, the general mass, momentum, and energy relations can be reduced to the following approximate one-dimensional equations

$$\text{Mass:} \quad \rho_1 u_1 A_1 = \rho_2 u_2 A_2 \tag{8}$$

$$\text{Momentum:} \quad \left(P_1 + \frac{\rho_1 u_1^2}{g_c}\right) A_1 = \left(P_2 + \frac{\rho_2 u_2^2}{g_c}\right) A_2 + F_D \tag{9}$$

$$\text{Energy: } \bar{C}_{p_1}(T_1-T_o) + \frac{u_1^2}{2g_c} + Q_r(T_o) - Q_t = \bar{C}_{p_2}(T_2-T_o) + \frac{u_2^2}{2g_c} \qquad (10)$$

If no steep gradients exist at stations 1 or 2, the equations can be applied to a deflagration with negligible error.

By combining the above equations with the ideal gas law and making suitable approximations based on experimental conditions, the following expression is obtained

$$Q_r(T_o) = \bar{C}_{p_2}(T_2-T_1) + Q_t = \bar{C}_{p_2}\left[\frac{P_2}{P_1}\frac{\bar{M}_2}{\bar{M}_1}\frac{A_2}{A_1}\frac{g_c T_1}{\rho_1 u_1^2}\left(P_1 - P_2\frac{A_2}{A_1} - P_D + \frac{\rho_1 u_1^2}{g_c}\right) - T_1\right] + Q_t \qquad (11)$$

where $Q_r(T_o)$ is the heat released due to chemical reactions at a temperature, $T_o = T_1$, and Q_t is the heat transferred through the wall. For any run, the inlet conditions denoted by subscript 1 are known. The average molecular weight of exit products, $\bar{M}_2$, depends on outlet concentration, but does not change significantly from $\bar{M}_1$. By measuring the mean static pressure at the outlet, P_2, and estimating the drag of the stabilizer and walls, P_D, the outlet temperature, T_2, can be computed. The mean heat capacity of the combustion products between T_o and T_2 can now be estimated. By integrating heat fluxes along the wall, Q_t is obtained. All terms in equation 11 are now known or closely approximated, and the heat released can be calculated.

Combustion efficiency is defined as the ratio of heat released due to chemical reaction to the heat which would be released if reaction were complete. The maximum chemical heat release is calculated from the inlet feed composition and is based on the limiting reactant, propane in

a lean mixture and oxygen in a rich mixture. From the combustion efficiency, the fraction of fuel burned and outlet composition can be calculated. The original estimates of composition used in evaluating $\overline{M}_2$ and $\overline{C}_{p_2}$ can then be improved and a better value of $Q_r(T_o)$ obtained.

The estimation of the P_D term is difficult. The drag of the stabilizer was assumed equal to the pressure drop measured without combustion at the same flow rate employed in the run. The drag of the walls during combustion was approximated from an average combustion chamber temperature. A more complete treatment of this problem is reported in the discussion section.

Resonant Frequency

The flame-generated oscillations produced in the combustion chamber were thought to be caused by resonance of the hot (burned)and cold (unburned)gases in the chamber. By solving the one-dimensional wave equation for fixed boundary conditions (both ends acoustically open), an expression relating the resonant frequency, f, to the length of column of burned gases, L_b, is obtained

$$\tan \frac{2 \pi f L_b}{a_1} = - \frac{a_1 \gamma_1}{a_2 \gamma_2} \tan \frac{2 \pi f (L_t - L_b)}{a_2} \qquad (12)$$

Subscripts 1 and 2 refer to unburned and burned gases, respectively. The derivation assumes a one dimensional sinusoidal wave with a normal interface between hot and cold gases.

The frequency can be determined either by trial and error or by plotting the tangent functions and noting the intersections. The first

intersection corresponds to the fundamental, the second to the first harmonic, and so forth.

EXPERIMENTAL RESULTS

The structure and stabilizing mechanism of turbulent flames propagating from a flame holder are inadequately understood. Thus, any theories postulated to explain the actual combustion process would be of limited validity. In addition, no measurements of local gas temperatures and local combustion efficiencies within the tube were made. The lack of adequate theory and local gas phase measurements combine to prevent generalization of the results.

The general features of the experimental data are best represented on plots of local heat transfer rates against distance downstream from the flame holder. In this manner, the effect of each variable studied can be shown graphically with all other variables held constant or nearly so. The theory of the heat transfer calculations has been discussed. A sample calculation is presented in Appendix B. The measured rates of heat transfer are local average values over the thermally isolated sectors of one-inch length. In the plots, then, the rates are designated by a horizontal line at each measuring station. Since more than one run is usually represented on a given figure, the ends of each line are keyed to distinguish the data for individual runs.

In drawing a smooth curve through the data, the curve should intersect each horizontal line so as to leave equal areas above and below the line. An illustrative graph is presented in Figure 8. For purposes of clarity, the shaded area under each horizontal line is omitted in subsequent figures.

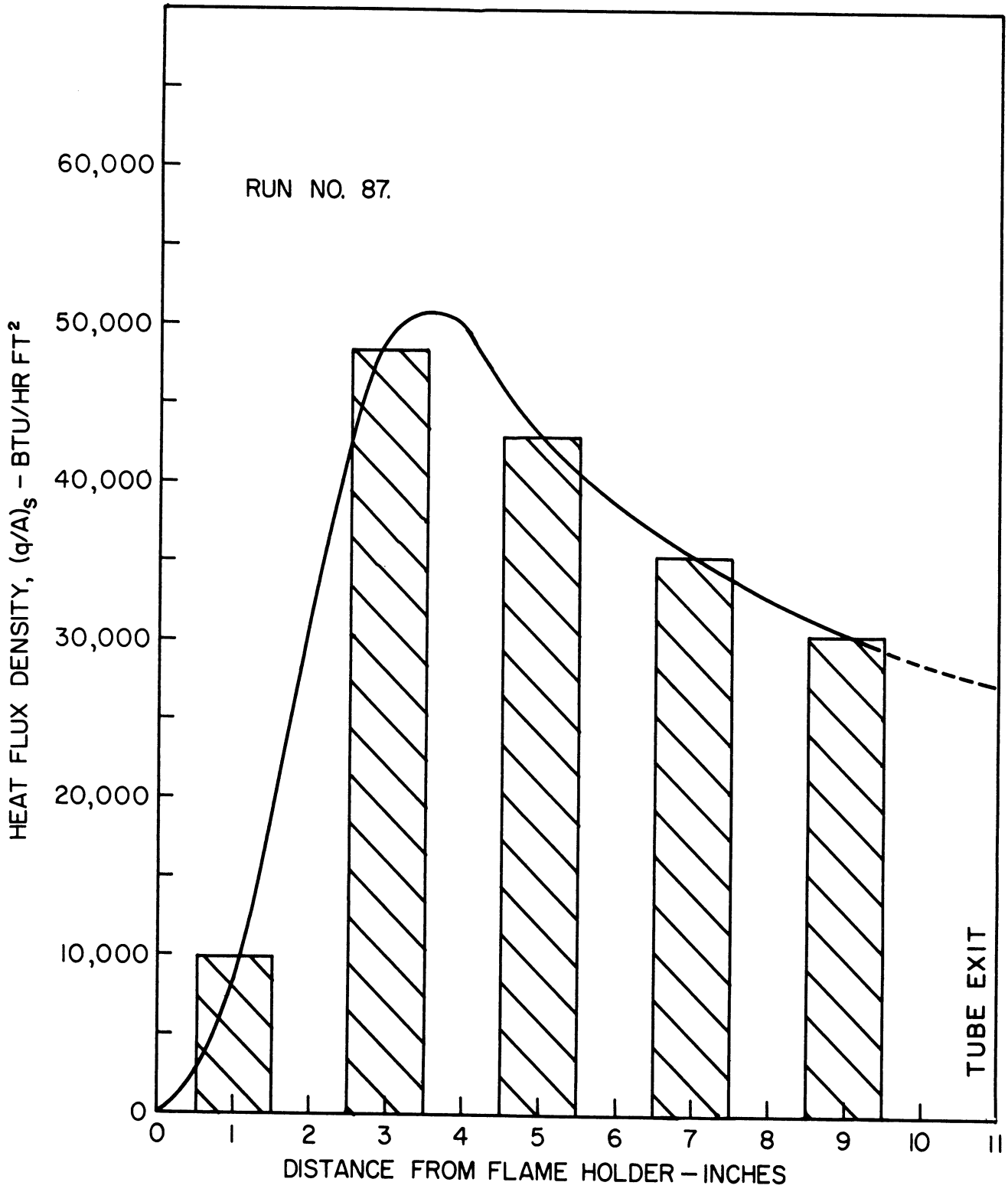

Figure 8. Illustrative Plot of Local Rates of Heat Transfer vs. Distance Downstream from Flame Holder.

Under many conditions of burning, flame-generated oscillations are produced by the combustion process. The amplitude and frequency of the oscillations influence the rates of heat transfer. Generally, one frequency was largely responsible for the observed sound level. In runs where flame-generated oscillations were present, the amplitude of the major frequency is noted on the plot. If the oscillations were effectively eliminated by a quarter wave tube, the term "oscillations damped" is placed on the plot.

Unless otherwise specified on the graphs, the data were taken on the flat plate flame holder of 52 percent blockage, with an inlet temperature of 70°F, and without screens upstream of the flame holder. Since plotting of all the runs would result in considerable duplication, only representative runs are plotted to illustrate the effect of the process variables. All significant features of the data are presented in the figures. The curves, in most cases, are extrapolated from the measuring station at 2 inches to the exit of the tube. A dotted line signifies the extrapolated portion of the curve. At the flame holder, there is a small but finite rate of heat transfer due to radiation and convection. The magnitude of this rate is unknown, but is normally insignificant on the scale of the figures. For convenience, then, the curves have been drawn to zero heat flux density at the flame holder.

A tabulation of all runs is given in Appendix A.

Flame-Generated Oscillations

The frequencies and relative amplitudes of the flame-generated oscillations were measured on a sound level meter and a sound analyzer.

The theoretical resonant frequency of a column composed of hot and cold gases is given by equation (12). This equation can be solved for the resonant frequency, f, either by plotting the two functions or by trial and error.

A plot of these functions for L_t = 9 ft., L_b = 9 in., a_1 = 1120 ft. per sec., and a_2 = 2660 ft. per sec. (T_2 = 3000°R) is shown in Figure 9. The first intersection of the curves gives the fundamental frequency, the second intersection yields the first harmonic, etc. Several strong harmonics were generated by the combustion process. For a given overtone, the frequency was observed to vary with fuel-to-air ratio. In the following table, the experimental frequencies for a Reynolds' number of 10,000 are compared with the theoretical frequencies from Figure 9.

Harmonic Number	Theoretical Frequency	Observed Frequency Range
2	200	212 - 214
3	267	282 - 291
4	334	346 - 350

The agreement between theory and measurement confirmed the assumption that the mode of oscillation was longitudinal.

The theoretical and observed frequencies also gave satisfactory agreement for other total tube lengths. For example, at a total tube length of 3.5 feet, the calculated fundamental frequency of 194 cycles per second is in reasonable accord with the observed frequency range of 192 to 210.

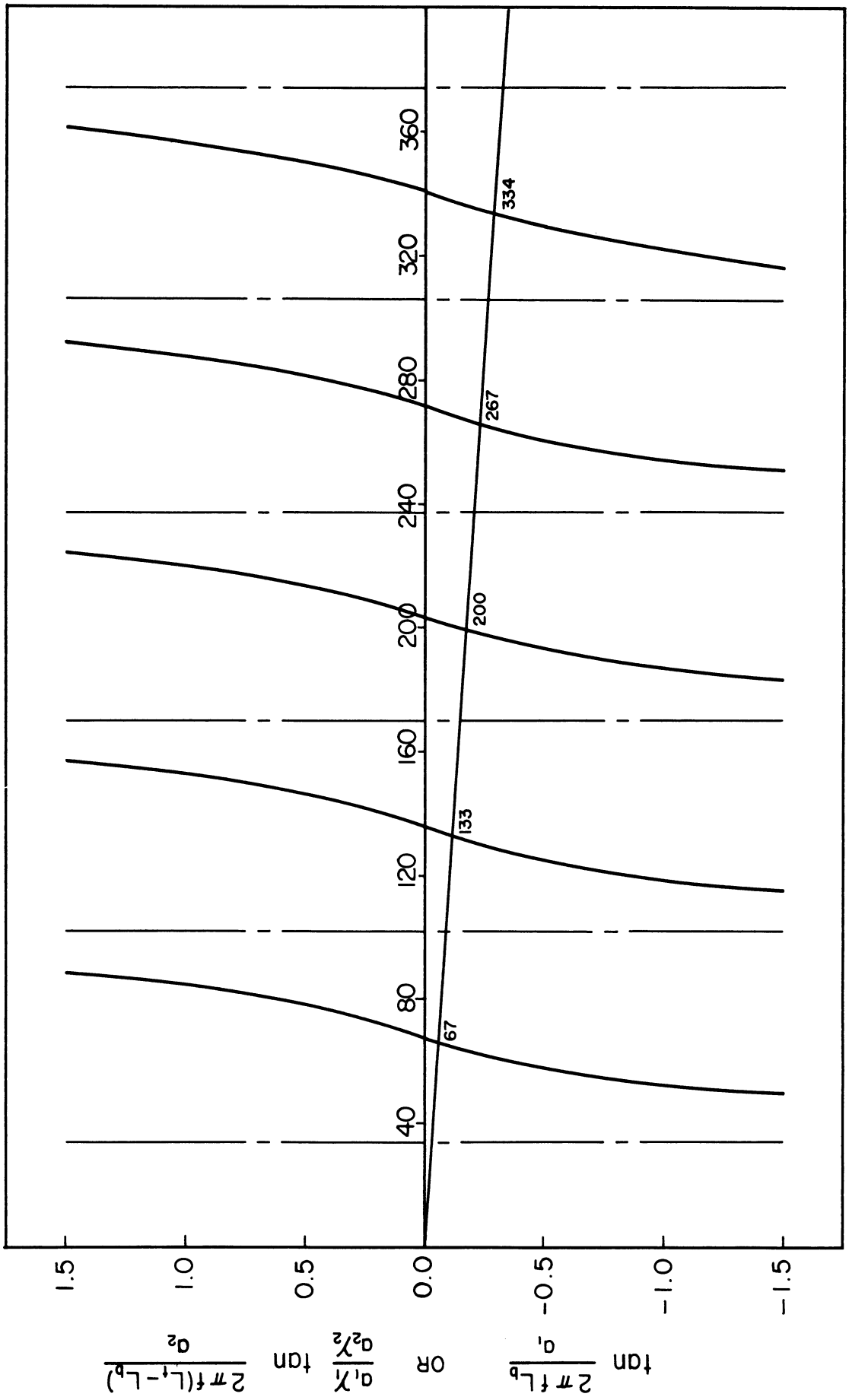

Figure 9. Theoretical Frequencies of Fundamental and Overtones for Longitudinal Oscillations.

Effect of Downstream Tube Length

The effect of tube length downstream of the flame holder is shown in Figures 10 to 13. The downstream tube lengths studied were 7, 9, and 11 inches. For lengths less than 7 inches, insufficient distance was present to indicate the characteristics of the heat transfer curve. At lengths greater than 11 inches, flame-generated pulsations frequently became severe enough to blow the flame off the stabilizer. Although pulsation of an undamped flame increased with increased burning length, no significant change in amplitude or frequency of oscillation was observed.

The effect of burning length on local rates of heat transfer does not appear to be important. The burning length is of more significance in its effect on stability.

Effect of Inlet Flow Rate

In Figures 14 and 15, the effect of inlet flow rate is presented. The Reynolds' number ranges from 5,000 to 20,000. The lower flow rate limit was selected to avoid the transition region between laminar and turbulent flames, and to maintain a level of flow in which flashback was unlikely. The upper flow rate limit was imposed in order to allow the flames to spread to the tube wall within the minimum burning length studied. At higher flow rates, negligible heat transfer to the tube walls was observed.

The effect of increased flow rate is to increase the peak in the heat transfer curve and to shift the peak downstream toward the tube exit.

The total heat transfer to the tube wall along the burning length was obtained by an integration of heat fluxes for each run in Figures 14 and 15. The results, presented in Figure 16, show an increase in total heat transfer with increasing Reynolds' number.

Each value of total heat transfer was then expressed as a fraction of the heat which would be released by complete combustion of the inlet mixture. In Figure 17, the fraction of entering chemical energy transferred to the wall is observed to decrease with an increase in Reynolds' number.

Over the range of Reynolds' numbers investigated, the total heat transfer to the wall is higher for oscillating combustion than it is for damped combustion.

Effect of Fuel-to-Air Ratio

The proportions of fuel and air were generally varied between 10 percent excess propane and 10 percent excess air. For this range of fuel-to-air ratios, typical heat transfer curves are shown in Figures 18 and 19.

For a Reynolds' number of about 10,000 and a burning length of 9 inches, the fuel-to-air ratio was varied between the rich and lean blowoff limits. Some of the results are presented in Figures 20 to 22. No strong longitudinal oscillations were detected in very lean mixtures. A high frequency oscillation was observed near the rich limit.

As expected from kinetic considerations, the maximum heat transfer is obtained near a stoichiometric mixture. When the equivalence ratio is changed to richer or leaner mixtures, the rates of heat transfer

are reduced and the peak is shifted toward the exit of the tube.

The total heat transfer to the tube wall and the fraction of chemical energy in the entering stream transferred to the tube wall are plotted against the dimensionless fuel to air ratio in Figures 23 and 24, respectively. A maximum in heat transfer occurs near a stoichiometric mixture on both figures. For all fuel to air ratios studied, oscillating combustion is observed to give higher total heat transfer rates than damped combustion.

Effect of Inlet Temperature

Due to limited capacity of the air heater, the effect of inlet mixture temperature was studied at only two levels, 70°F and 120°F. The results are shown in Figure 25. A slight increase in heat transfer is observed with increased temperature.

Effect of Flame-Generated Oscillations

The influence of flame-generated longitudinal oscillations on the rates of heat transfer is shown in Figures 26 to 28. In these figures, a base curve for damped oscillations is plotted to permit comparison. The longitudinal resonance flattens the peak of the damped curve and shifts the peak closer to the flame holder. The flattening of the heat transfer profile by the oscillations is more pronounced at higher flow rates. The net result of the change in the heat transfer distribution accompanying longitudinal resonance is a small increase in the total heat transfer to the tube wall.

For the series of runs made at a Reynolds' number of 10,000 and a burning length of 9 inches, the frequency of the predominant oscillation

shifted to higher harmonics as the fuel to air ratio was increased. The measured frequencies are plotted against fuel-to-air ratio in Figure 29. Due to a hysterisis effect, however, each frequency is not uniquely associated with a given fuel to air ratio. By increasing the fuel to air ratio at a frequency discontinuity, a higher harmonic is excited. If the fuel-to-air ratio is now decreased slightly into the region of the lower harmonic, the higher harmonic often remains. Under certain conditions, then, the hysterisis effect can be used to study two harmonics with all other variables unchanged. Examples of the hysterisis effect are given in Figure 30. The rates of heat transfer are slightly increased by the higher harmonic. A small error in resetting the fuel-air ratio to its original value could be responsible for some of the difference between the curves.

A hysterisis effect with respect to flame holder position presented another means of determining the influence of oscillations on heat transfer. Since a pressure node exists near the tube exit, oscillations are not excited in this region. If the flame holder is inserted until oscillations are produced and then withdrawn a small distance, the oscillations will persist a small distance into the original unexcited region. This technique was not utilized since damping presented a more versatile and controllable method of removing flame-generated oscillations.

Effect of Total Tube Length

By decreasing the length of tube between the plenum chamber and test object exit, the fundamental frequency of the system is increased. The effect of total tube lengths of 9, 8, and 3.5 feet on rates of heat

transfer is shown in Figure 31. The observed frequencies correspond to the third harmonic for the 9 and 8 foot lengths and to the fundamental for the 3.5 foot length. A small increase in peak heat transfer rates appears to occur with an increase in frequency.

For total tube lengths of 3 and 3.5 feet, an unusual effect was observed at the lowest flow rate studied (Re = 5,000). The intensity of oscillation was substantially increased over that observed at the same flow conditions in the longer tube lengths. In addition, the flame became highly luminous. The rates of heat transfer at a position one inch downstream of the flame holder were abnormally high as shown in Figure 32. A measurable rate of heat transfer was also noted one inch upstream of the flame holder. A possible explanation for the abnormal behavior is presented in the discussion section.

Effect of Flame Holder

The results thus far discussed were taken on the flat plate flame holder of 52 percent blockage. To determine the effect of flame holder blockage, some data were observed for a flat plate with a blockage of 30 percent. Typical results with damped oscillations are shown in Figure 33. In general, the lower blockage shifts the peak of the curve toward the exit. The maximum rate of heat transfer and the total heat transfer are approximately the same for both blockages.

When no damping was provided, the lower blockage flame holder was very susceptible to premature blowoff. Flame-generated pulsations were frequently of sufficient magnitude to extinguish the flame. For example, flames of fuel-air mixtures near stoichiometric consistently

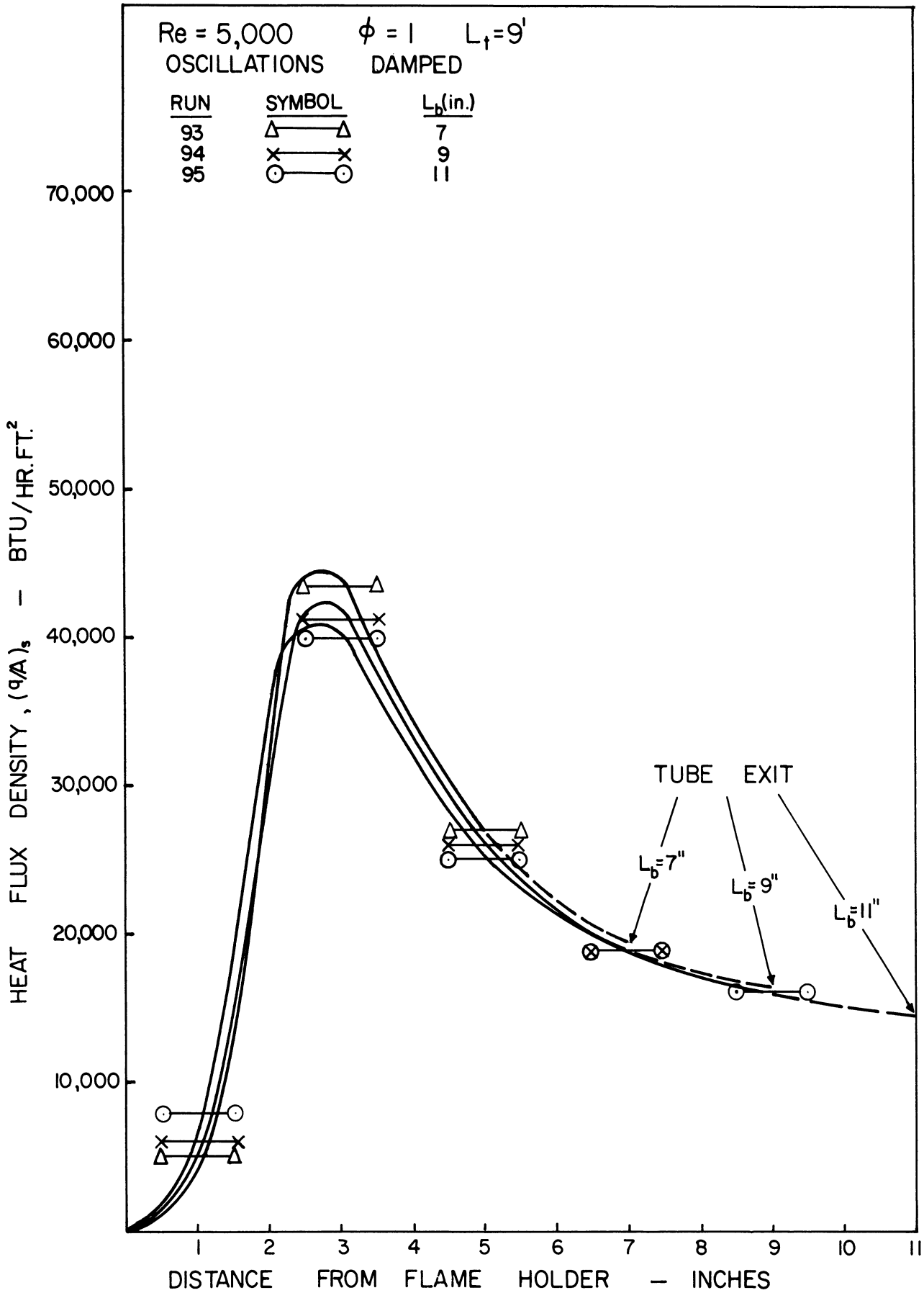

Figure 10. Effect of Burning Length on Local Rates of Heat Transfer.

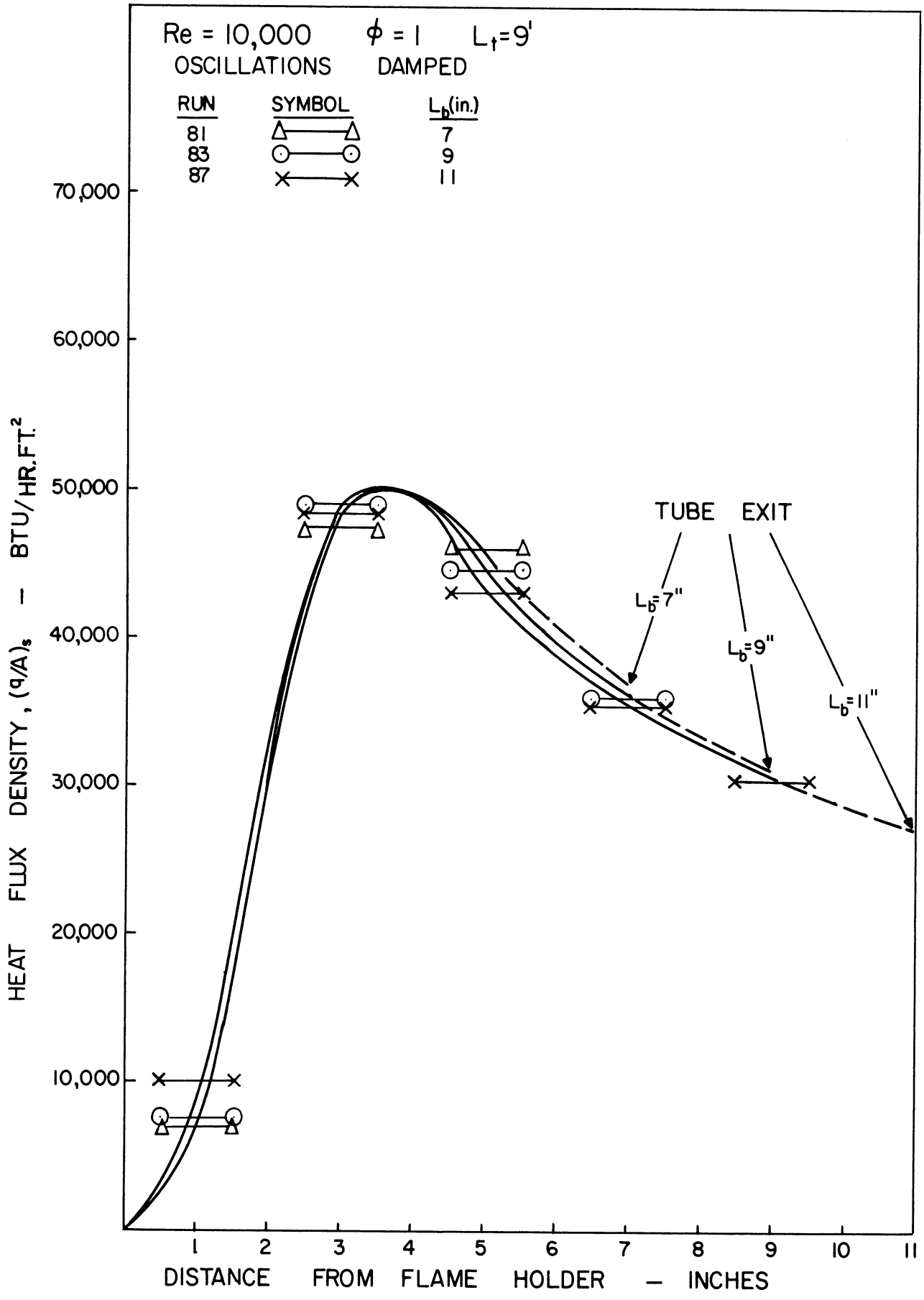

Figure 11. Effect of Burning Length on Local Rates of Heat Transfer.

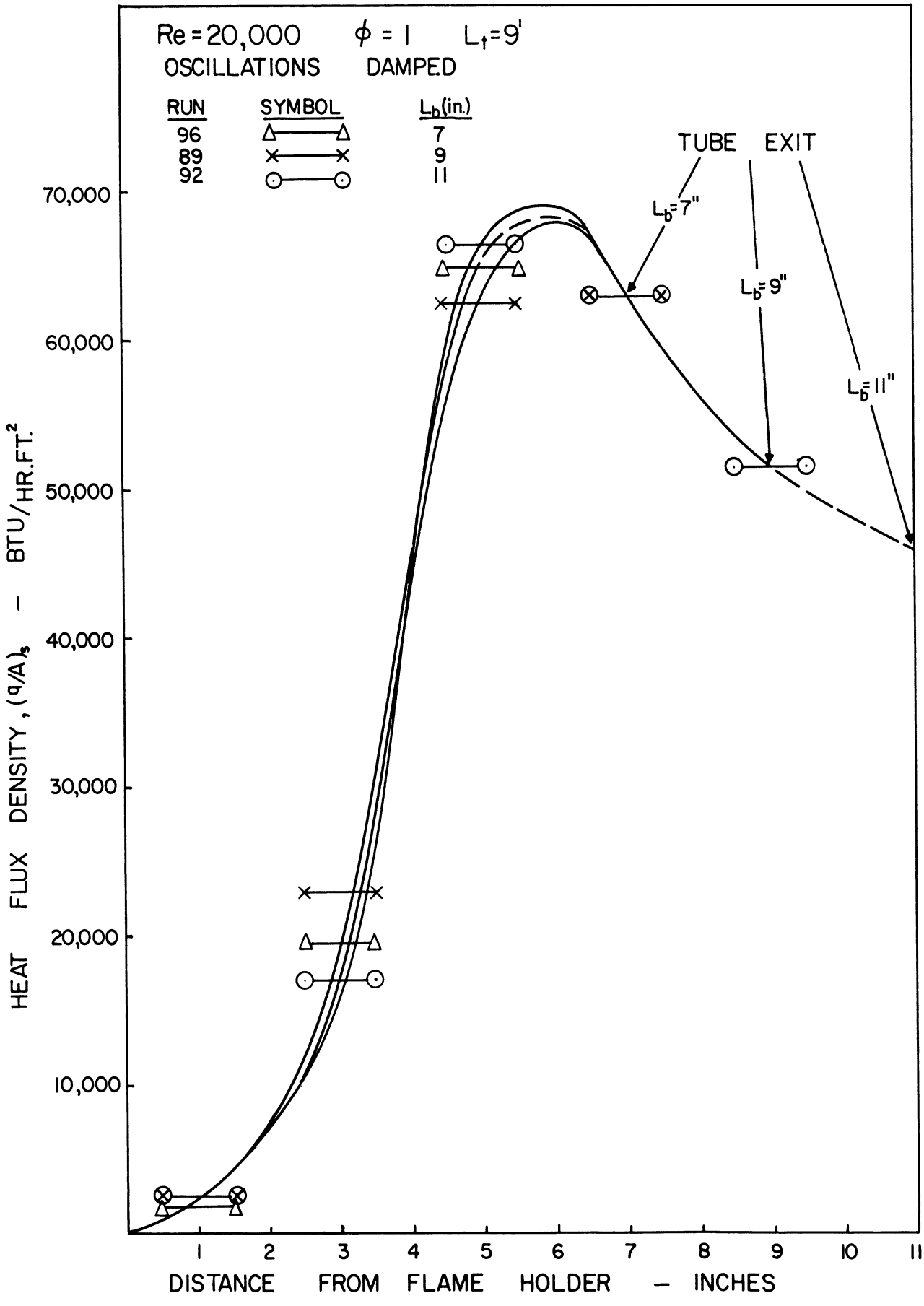

Figure 12. Effect of Burning Length on Local Rates of Heat Transfer.

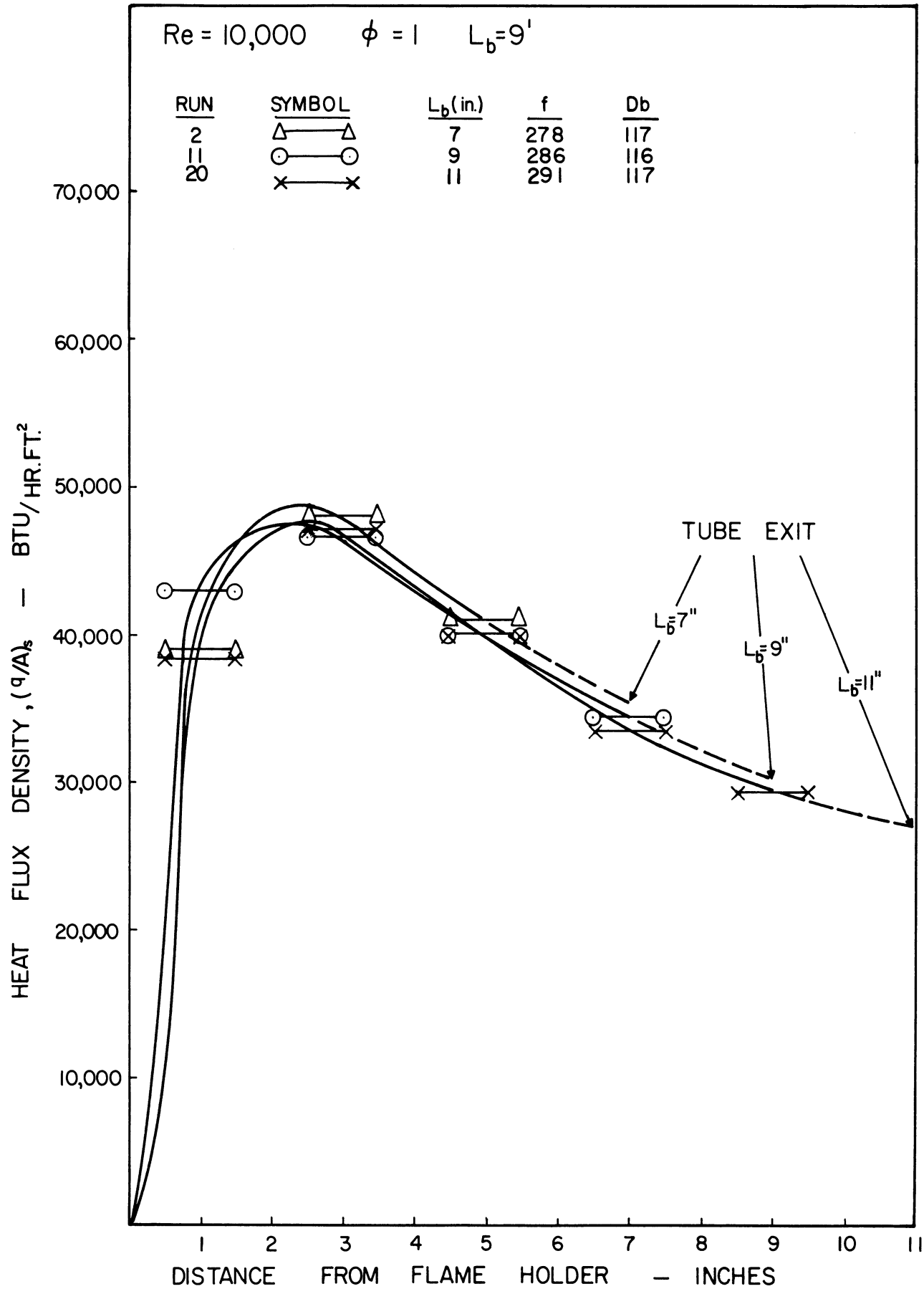

Figure 13. Effect of Burning Length on Local Rates of Heat Transfer.

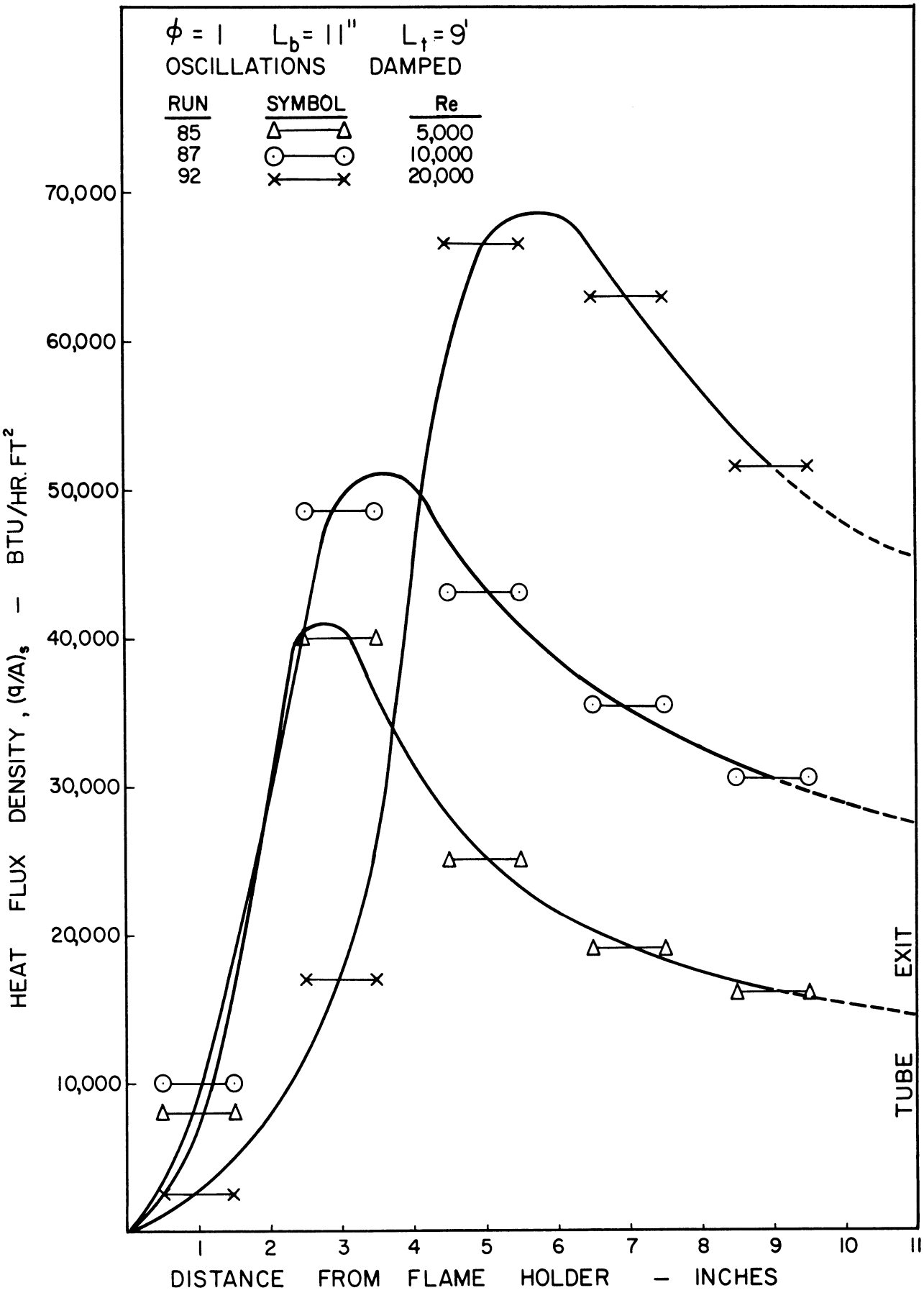

Figure 14. Effect of Flow Rate on Local Rates of Heat Transfer.

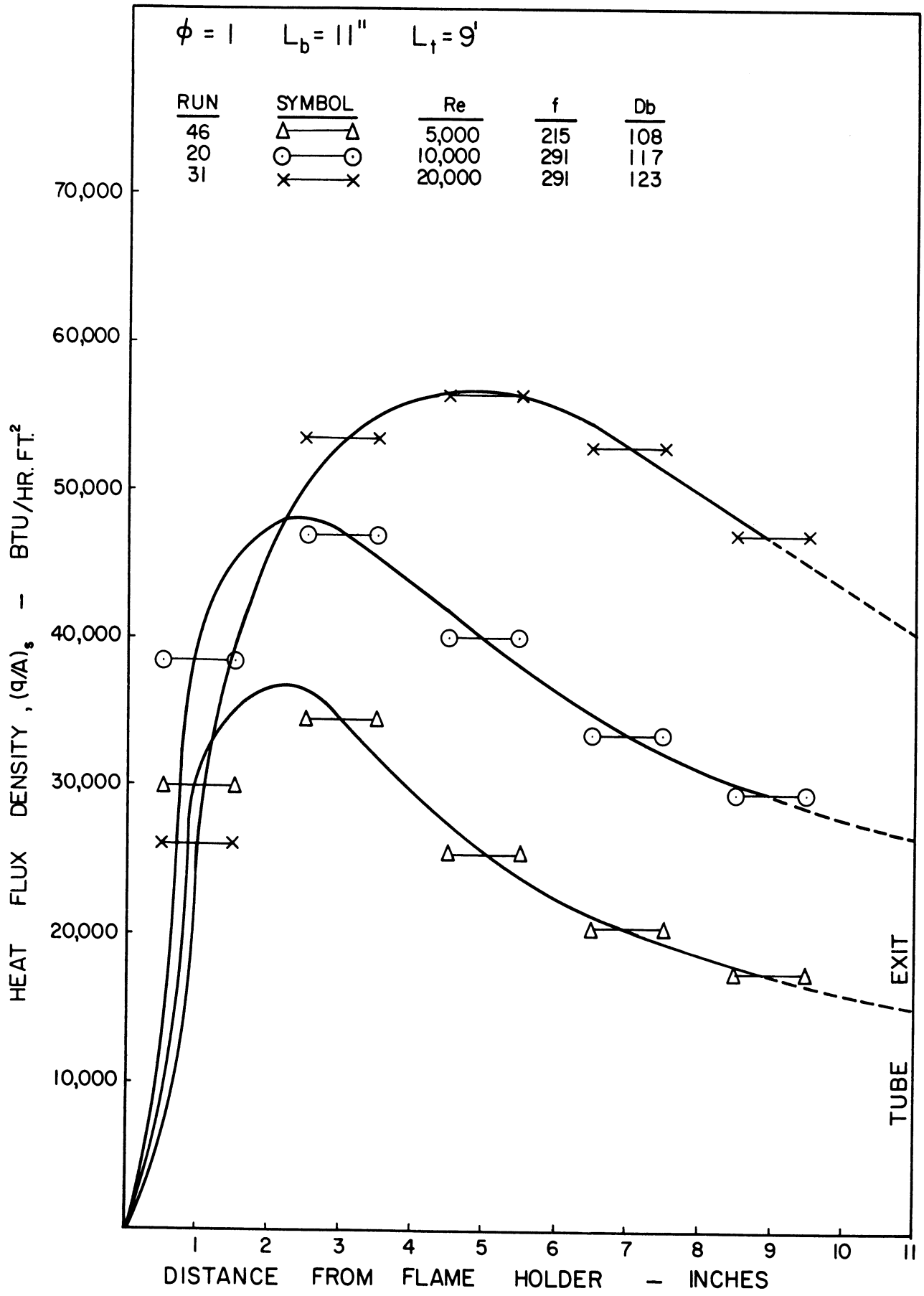

Figure 15. Effect of Flow Rate on Local Rates of Heat Transfer.

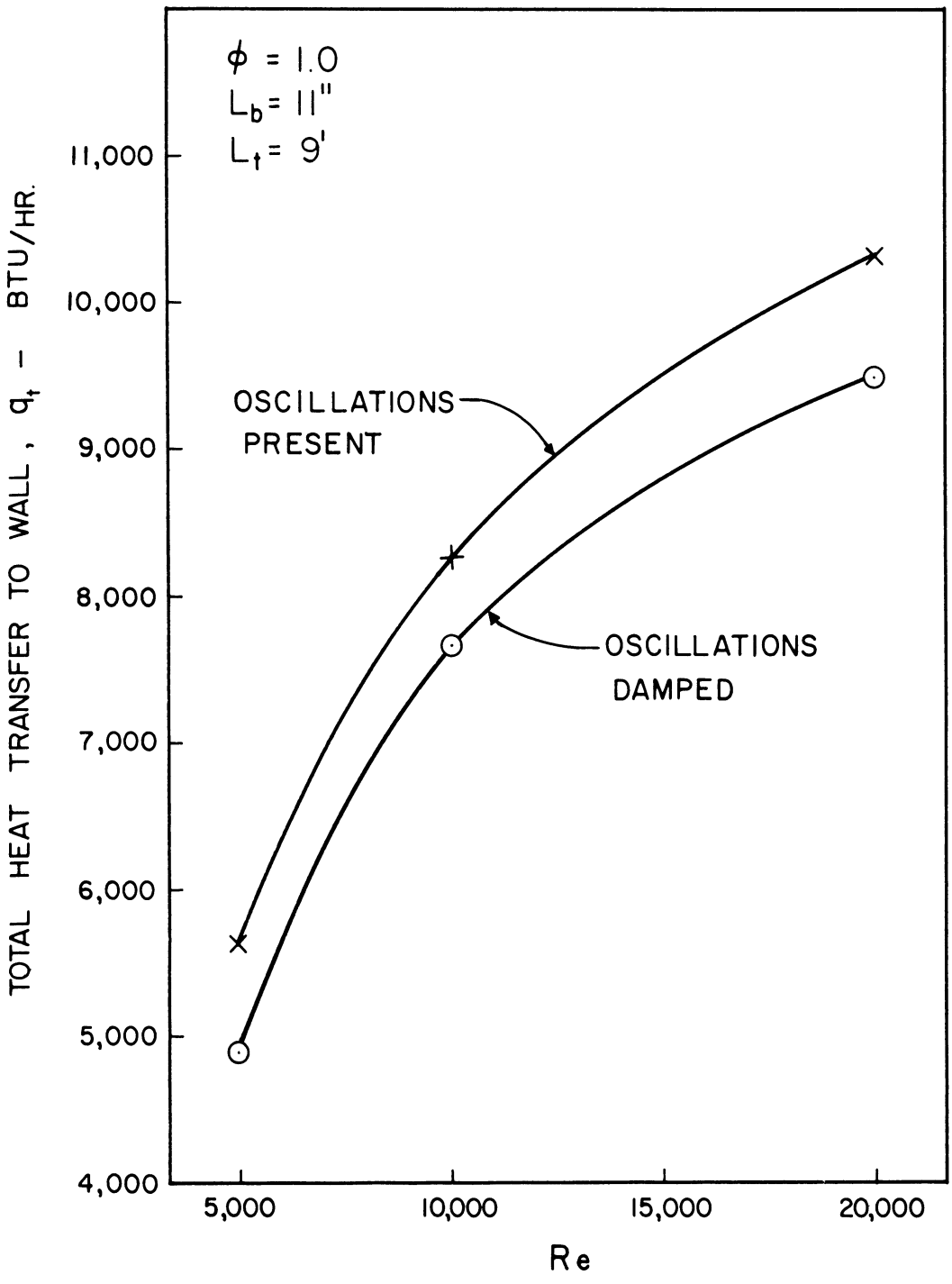

Figure 16. Effect of Reynolds' Number on Total Heat Transfer to Tube Wall.

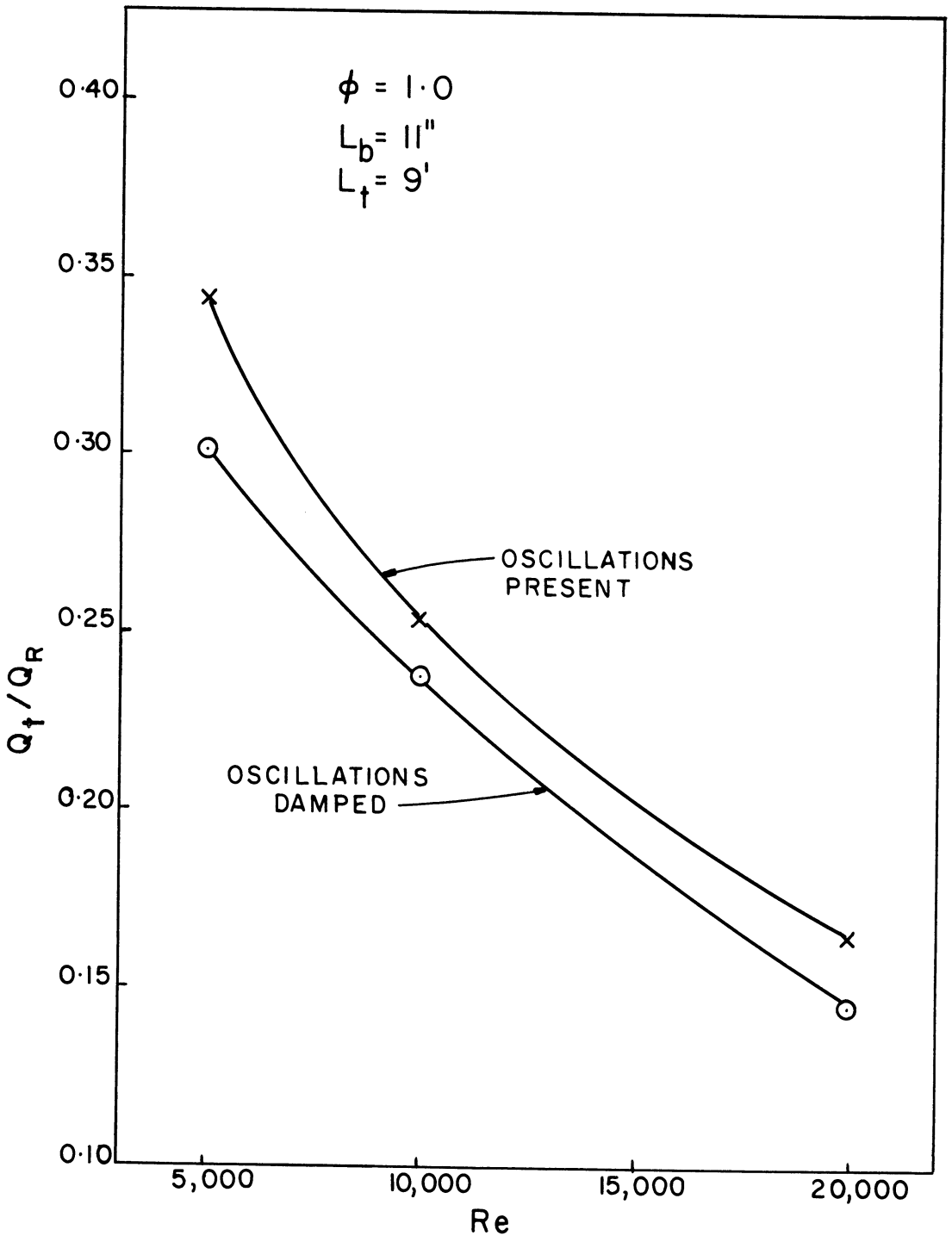

Figure 17. Effect of Reynolds Number on the Fraction of Entering Chemical Energy Transferred to the Tube Wall.

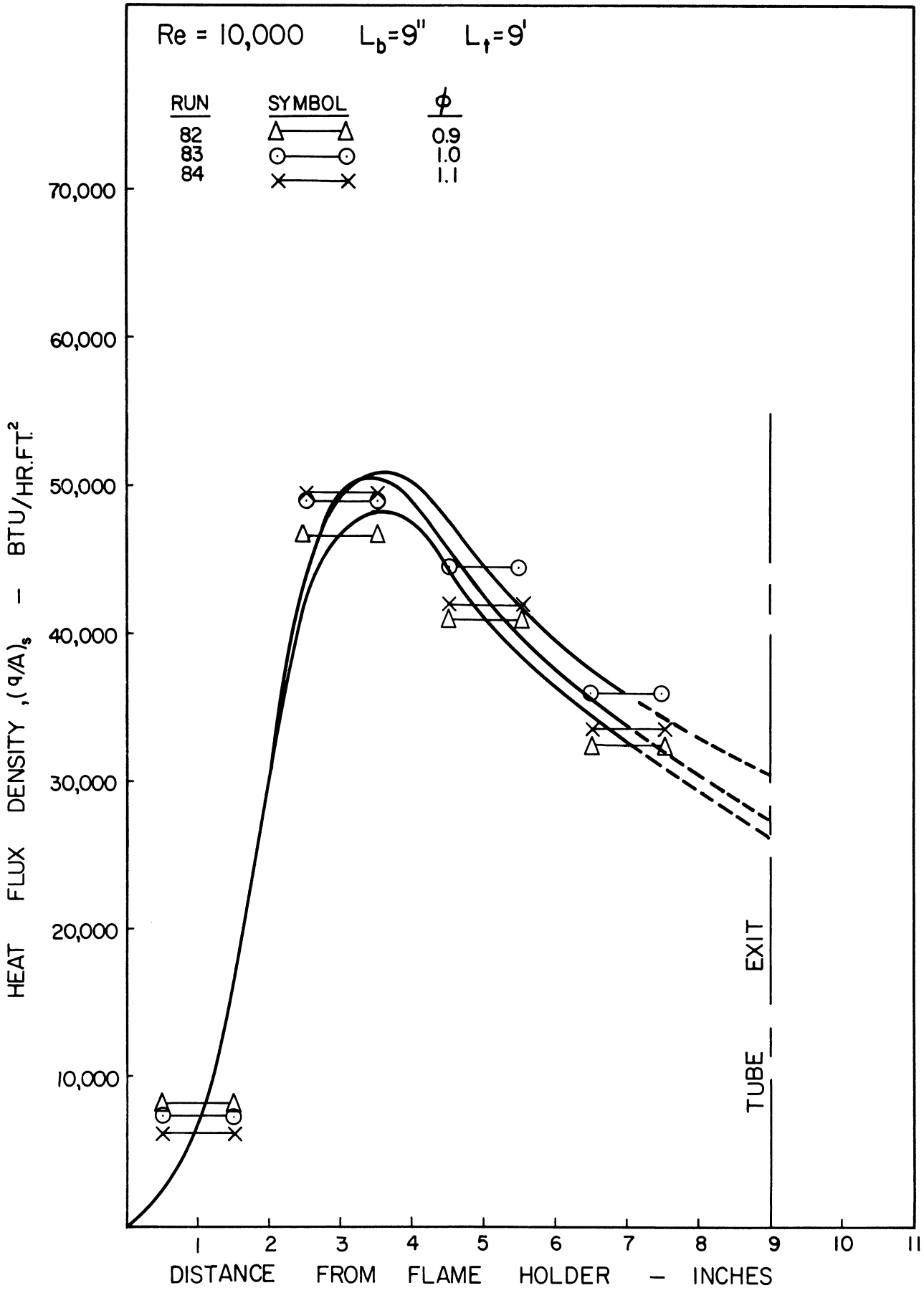

Figure 18. Effect of Fuel to Air Ratio on Local Rates of Heat Transfer.

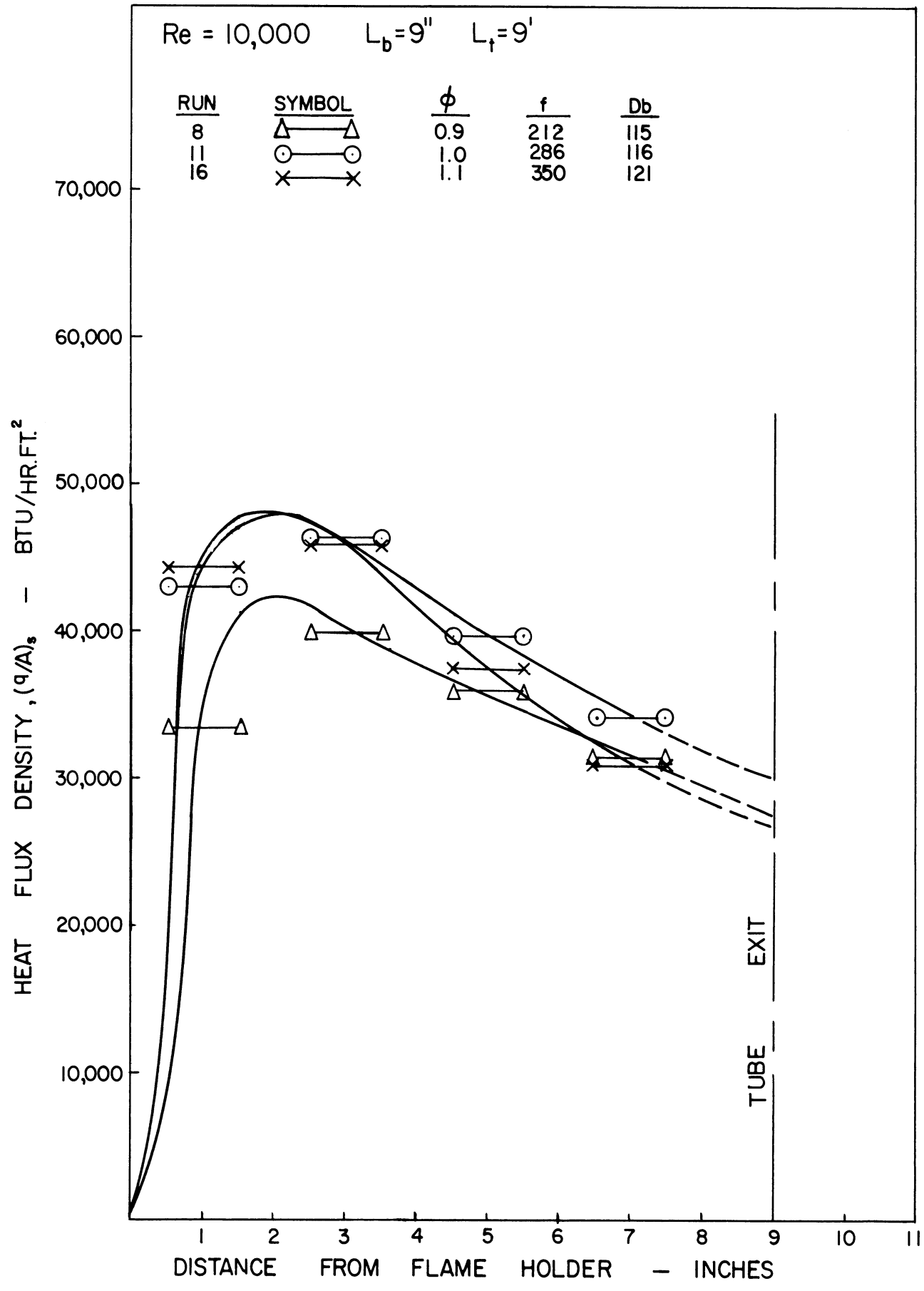

Figure 19. Effect of Fuel to Air Ratio on Local Rates of Heat Transfer.

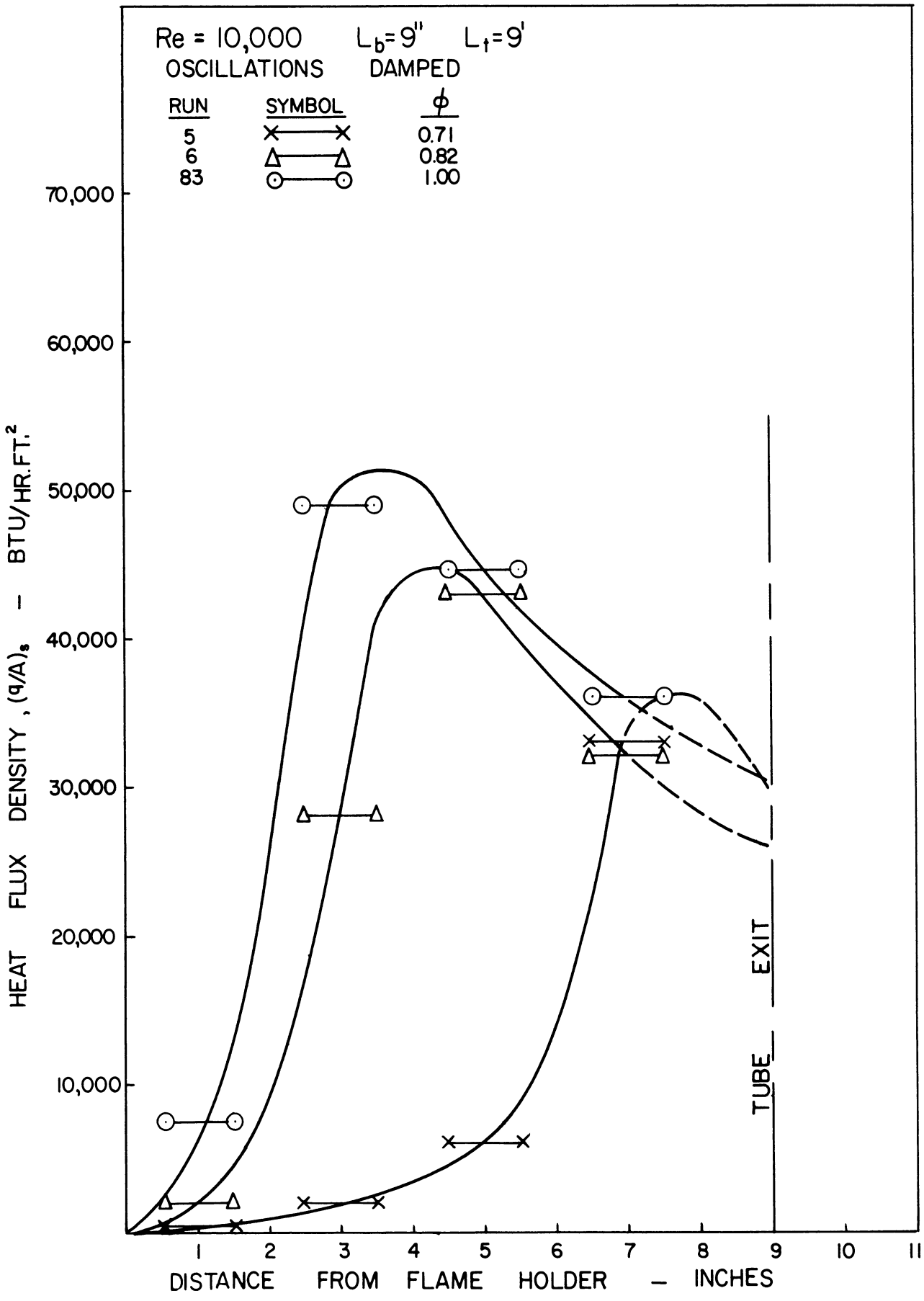

Figure 20. Effect of Fuel to Air Ratio on Local Rates of Heat Transfer.

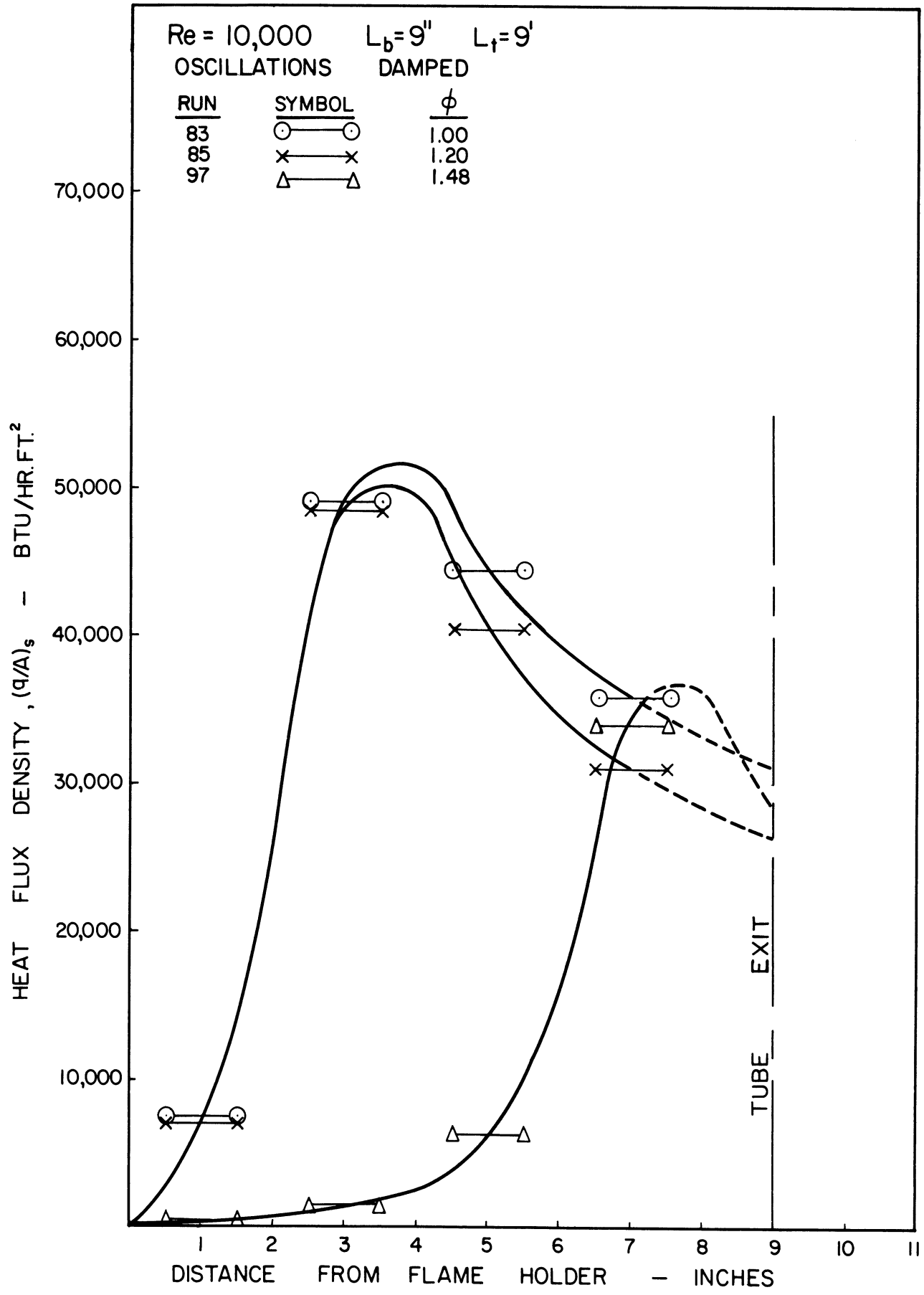

Figure 21. Effect of Fuel to Air Ratio on Local Rates of Heat Transfer.

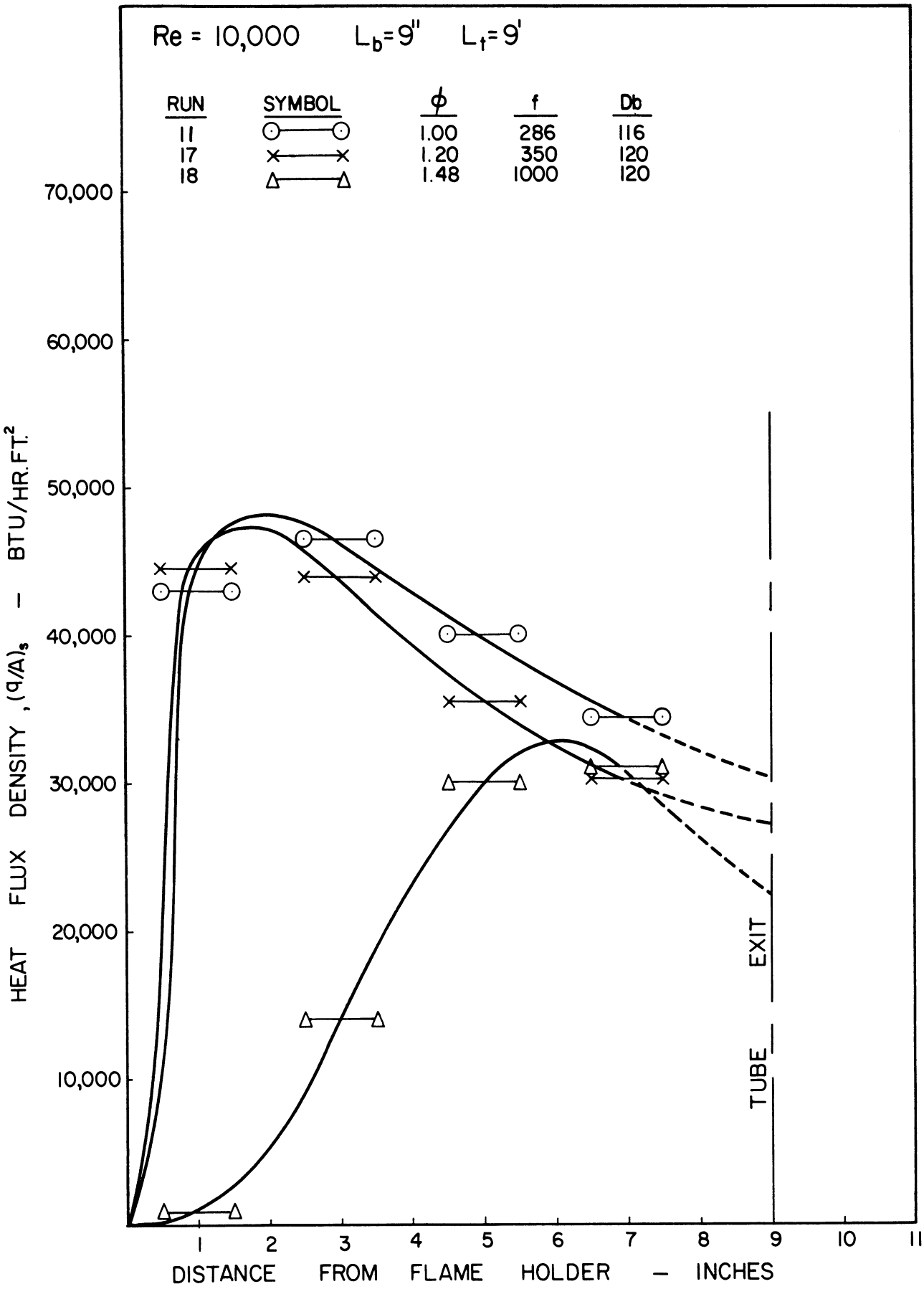

Figure 22. Effect of Fuel to Air Ratio on Local Rates of Heat Transfer.

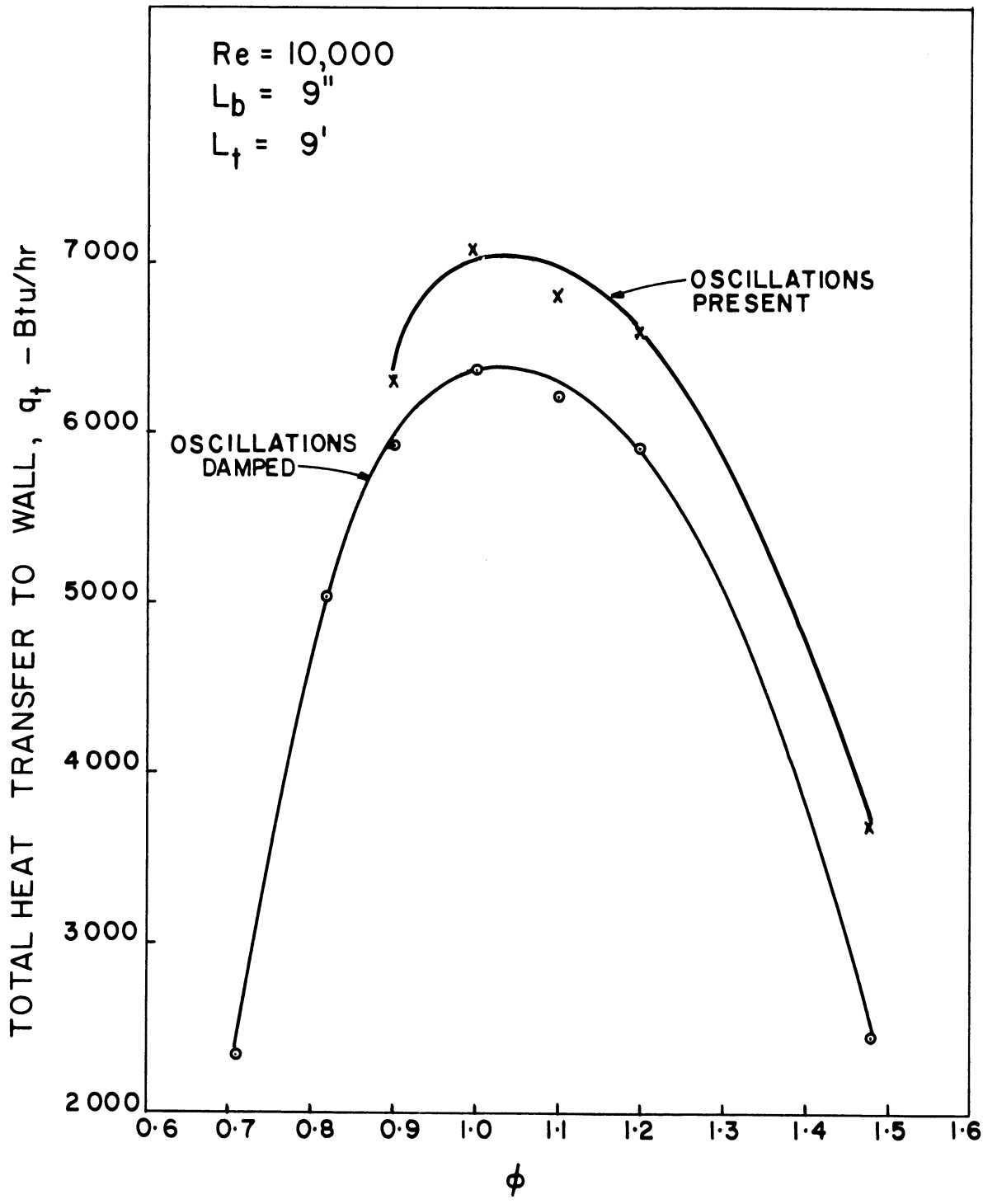

Figure 23. Effect of Fuel to Air Ratio on Total Heat Transfer to Tube Wall.

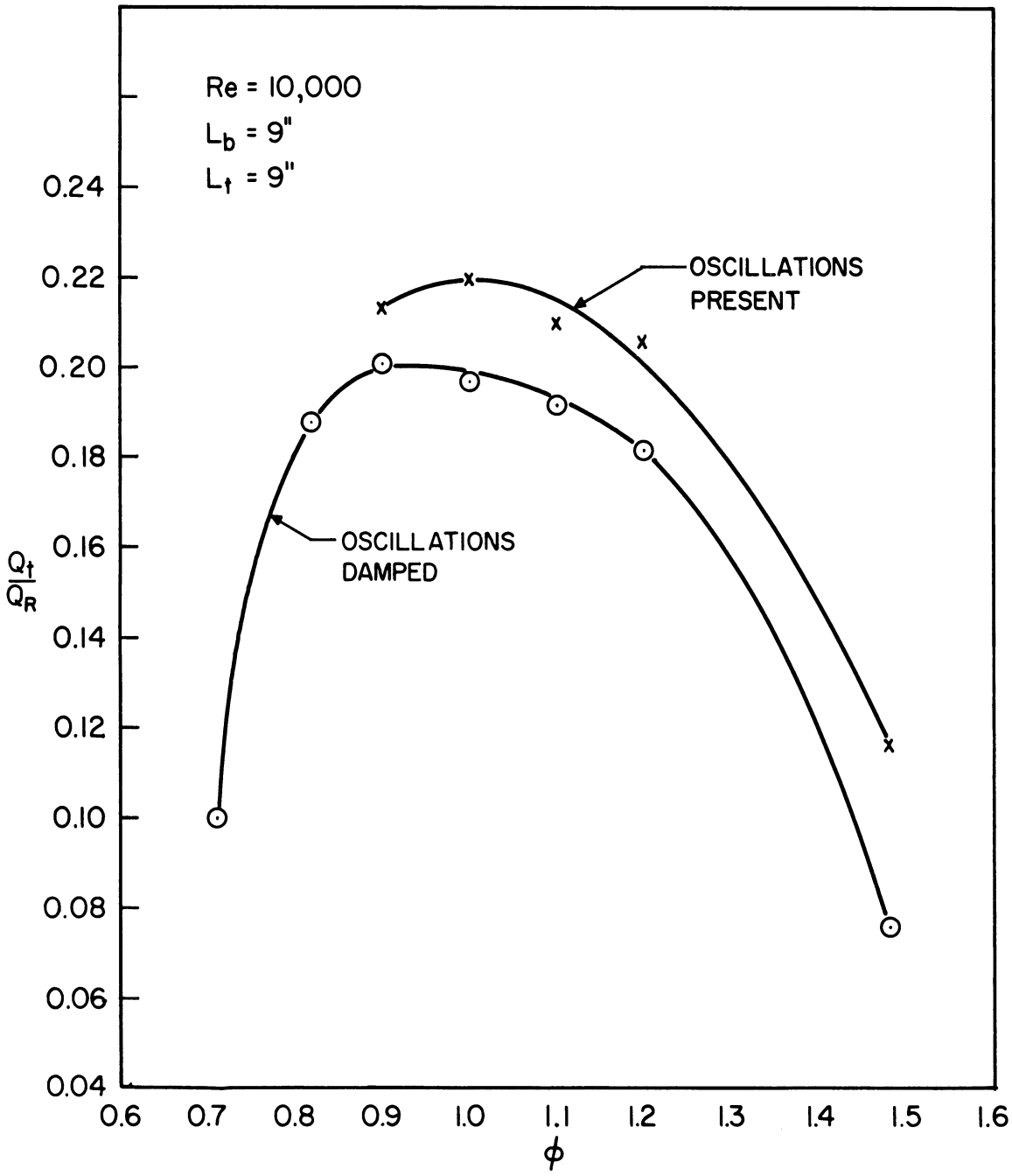

Figure 24. Effect of Fuel to Air Ratio on the Fraction of Entering Chemical Energy Transferred to the Tube Wall.

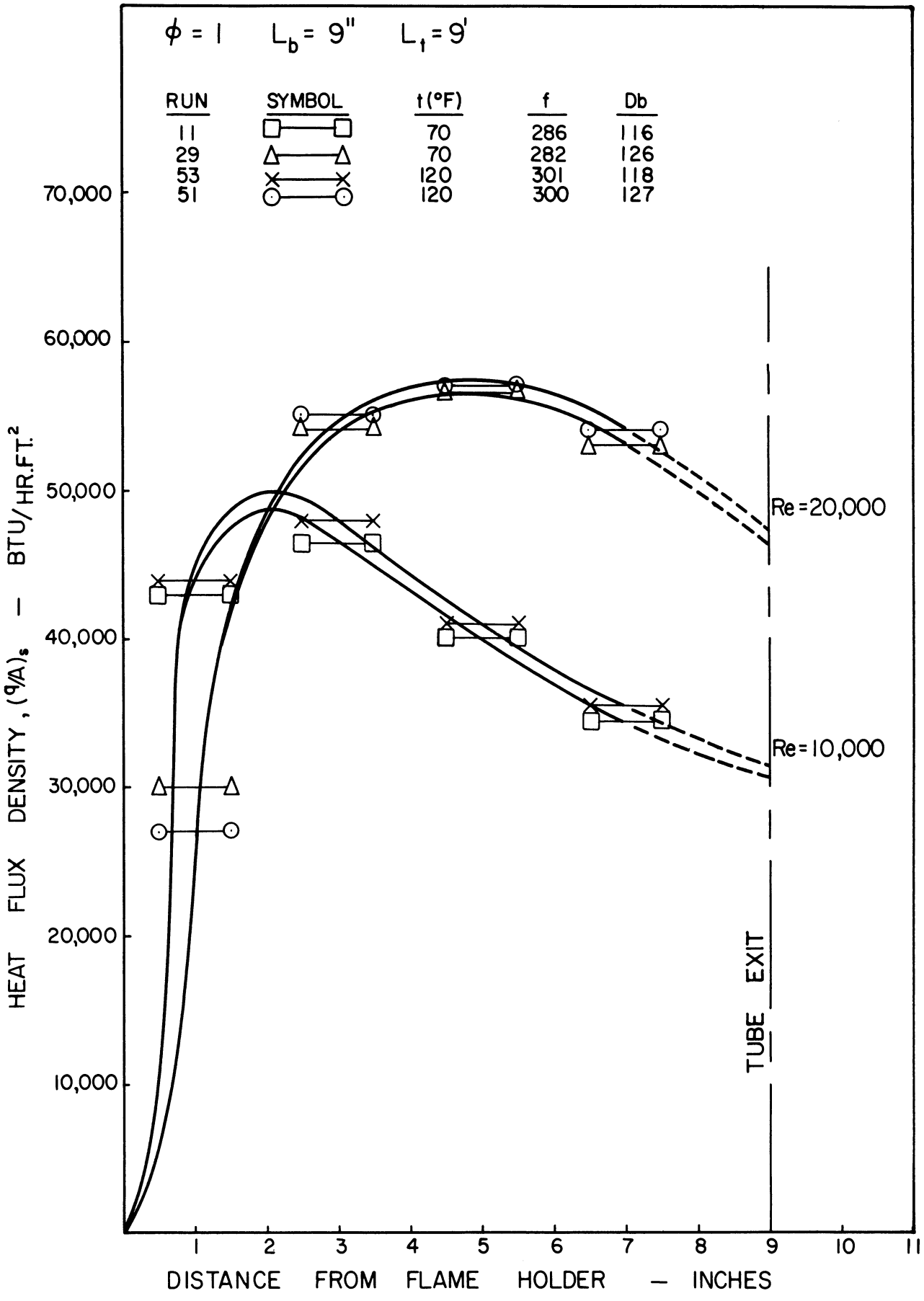

Figure 25. Effect of Inlet Temperature on Local Rates of Heat Transfer.

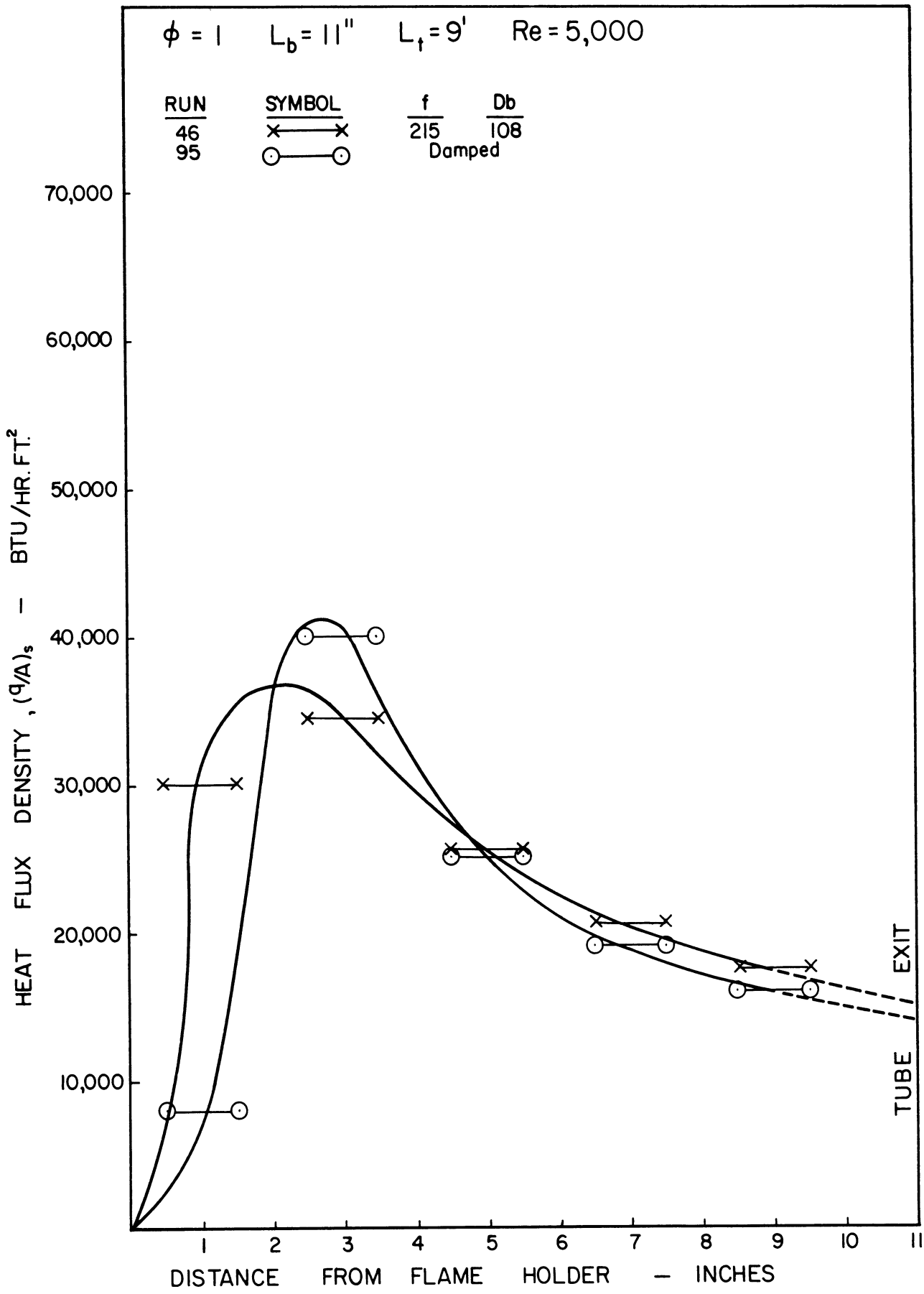

Figure 26. Effect of Resonance on Local Rates of Heat Transfer.

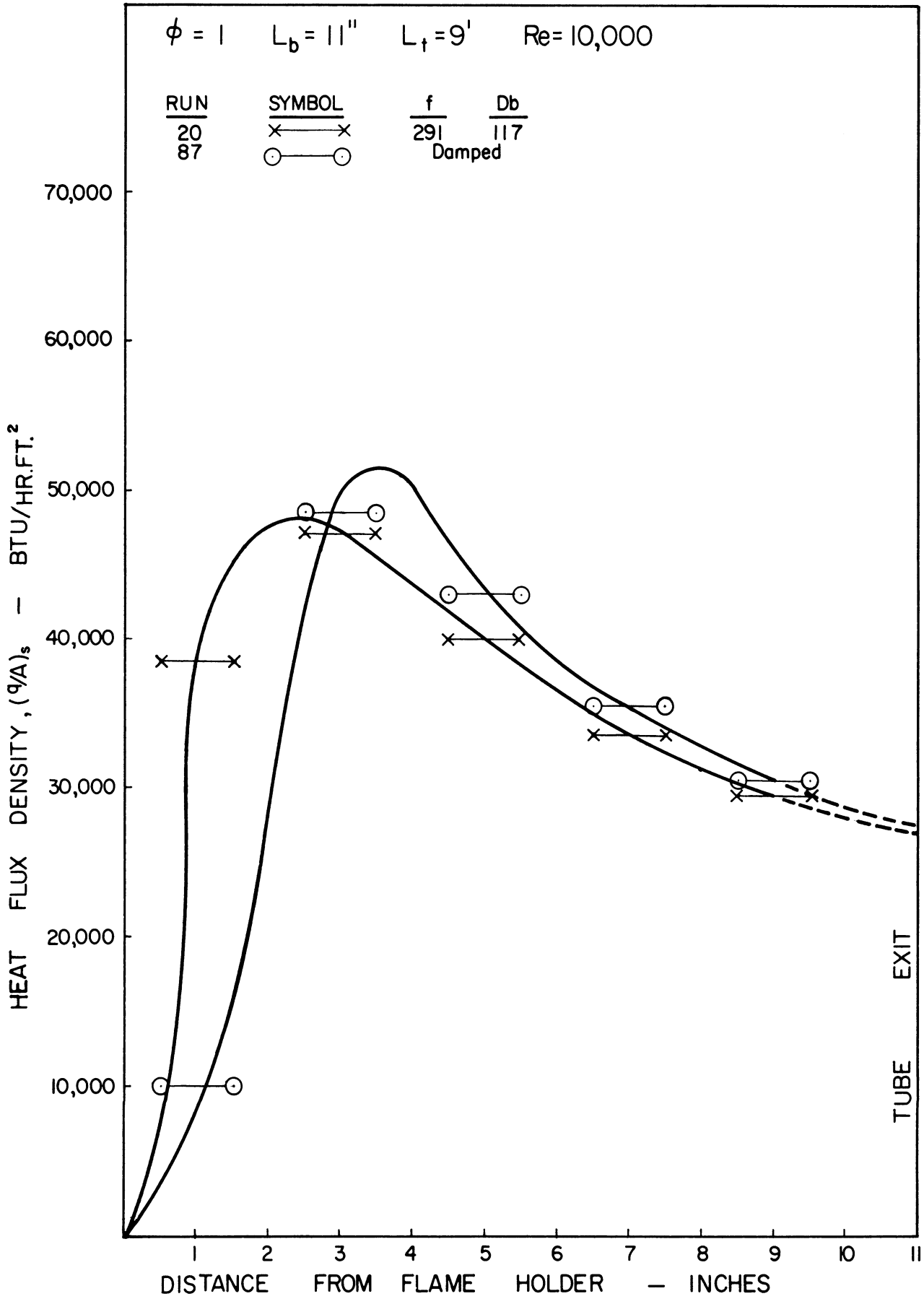

Figure 27. Effect of Resonance on Local Rates of Heat Transfer.

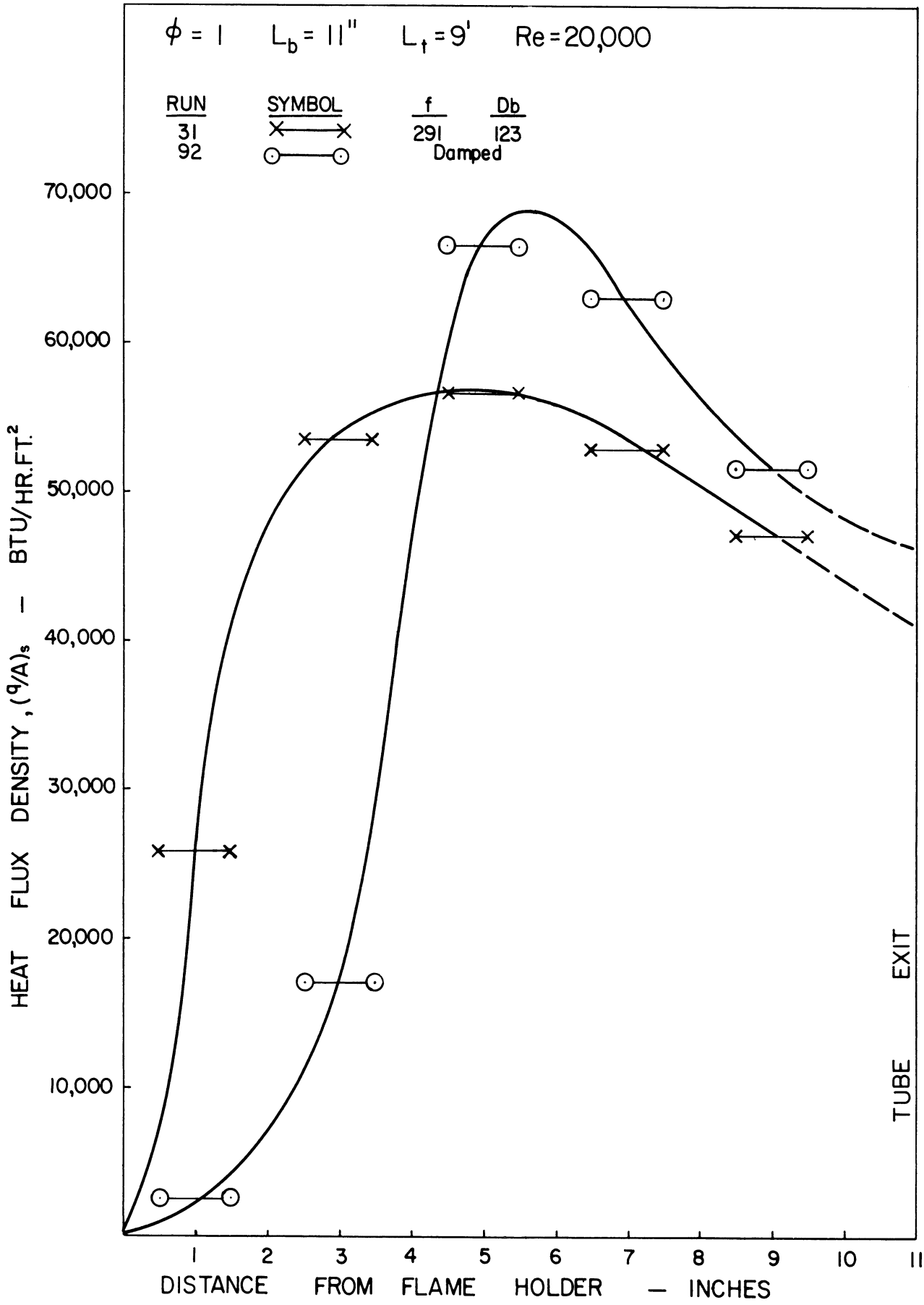

Figure 28. Effect of Resonance on Local Rates of Heat Transfer.

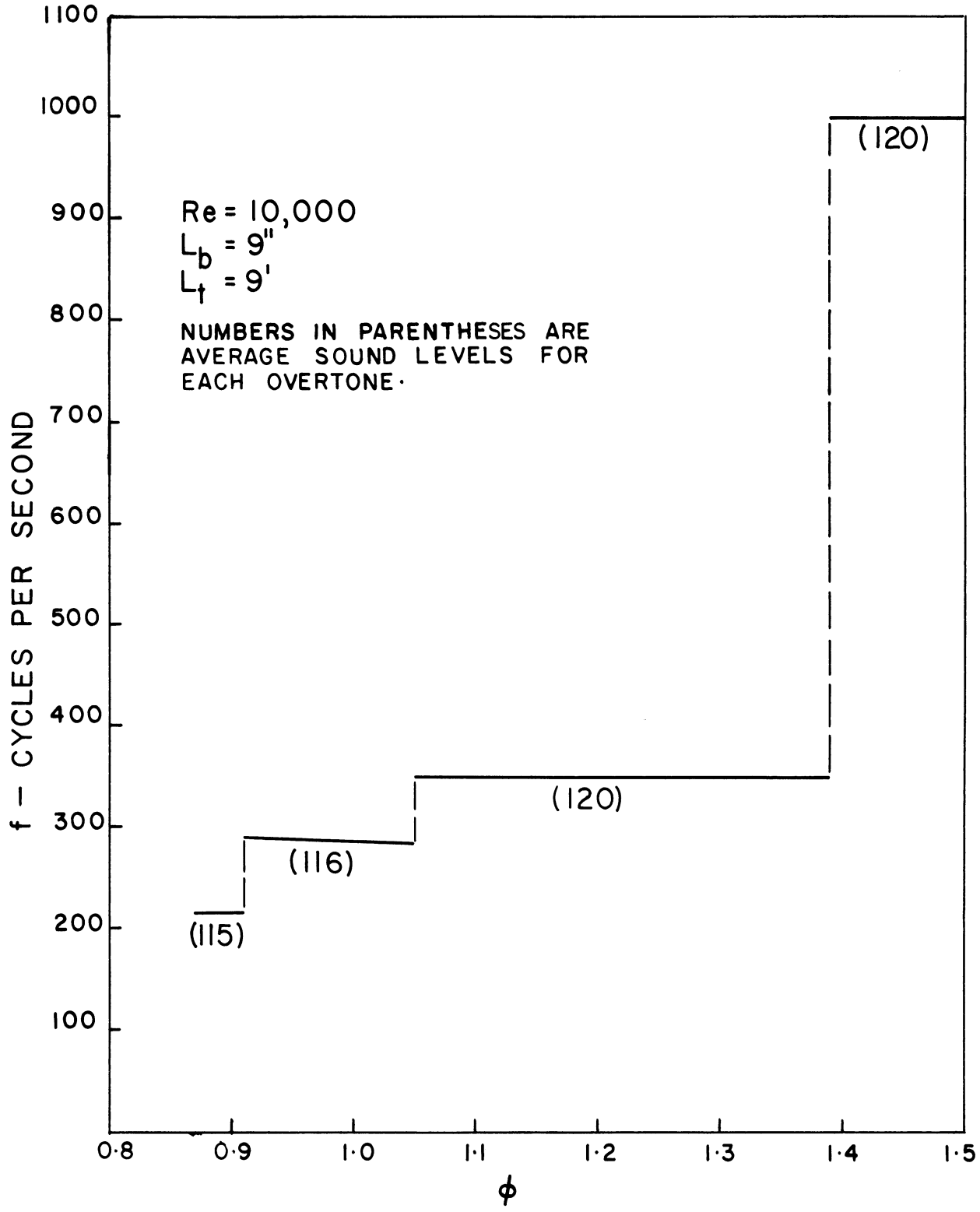

Figure 29. Effect of Increasing Fuel to Air Ratio on Measured Frequencies.

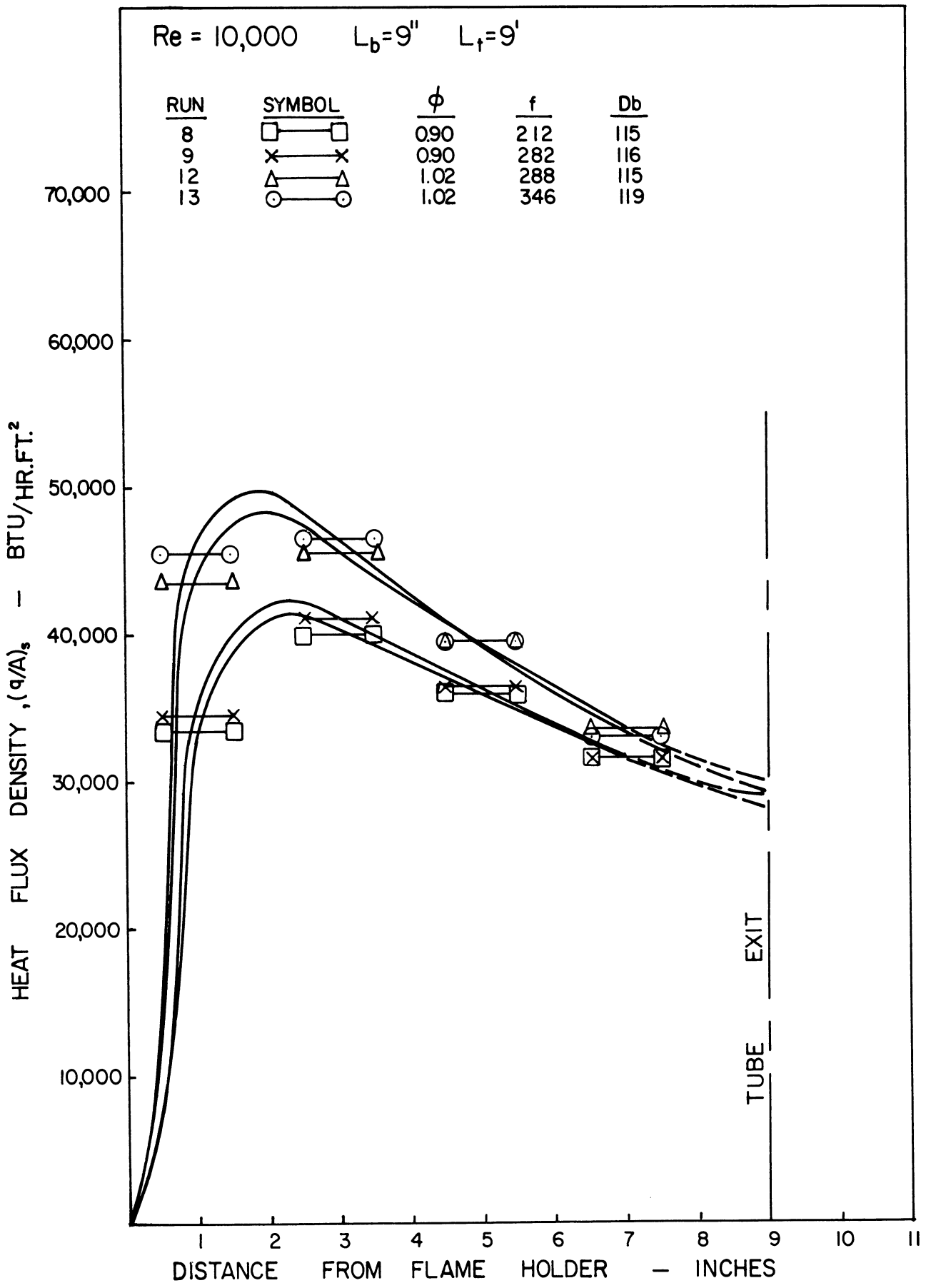

Figure 30. Effect of Hysterisis on Local Rates of Heat Transfer.

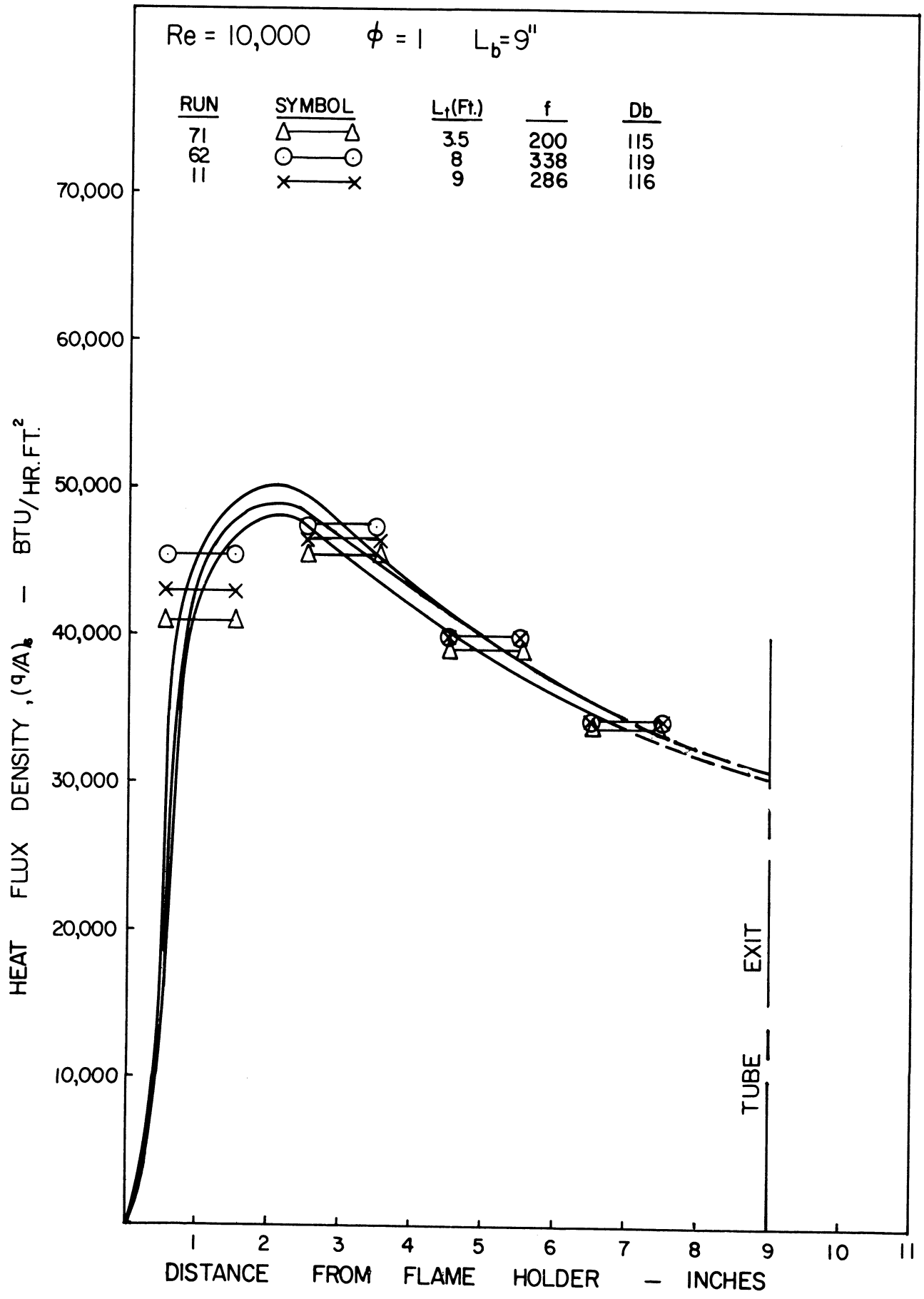

Figure 31. Effect of Total Tube Length on Local Rates of Heat Transfer.

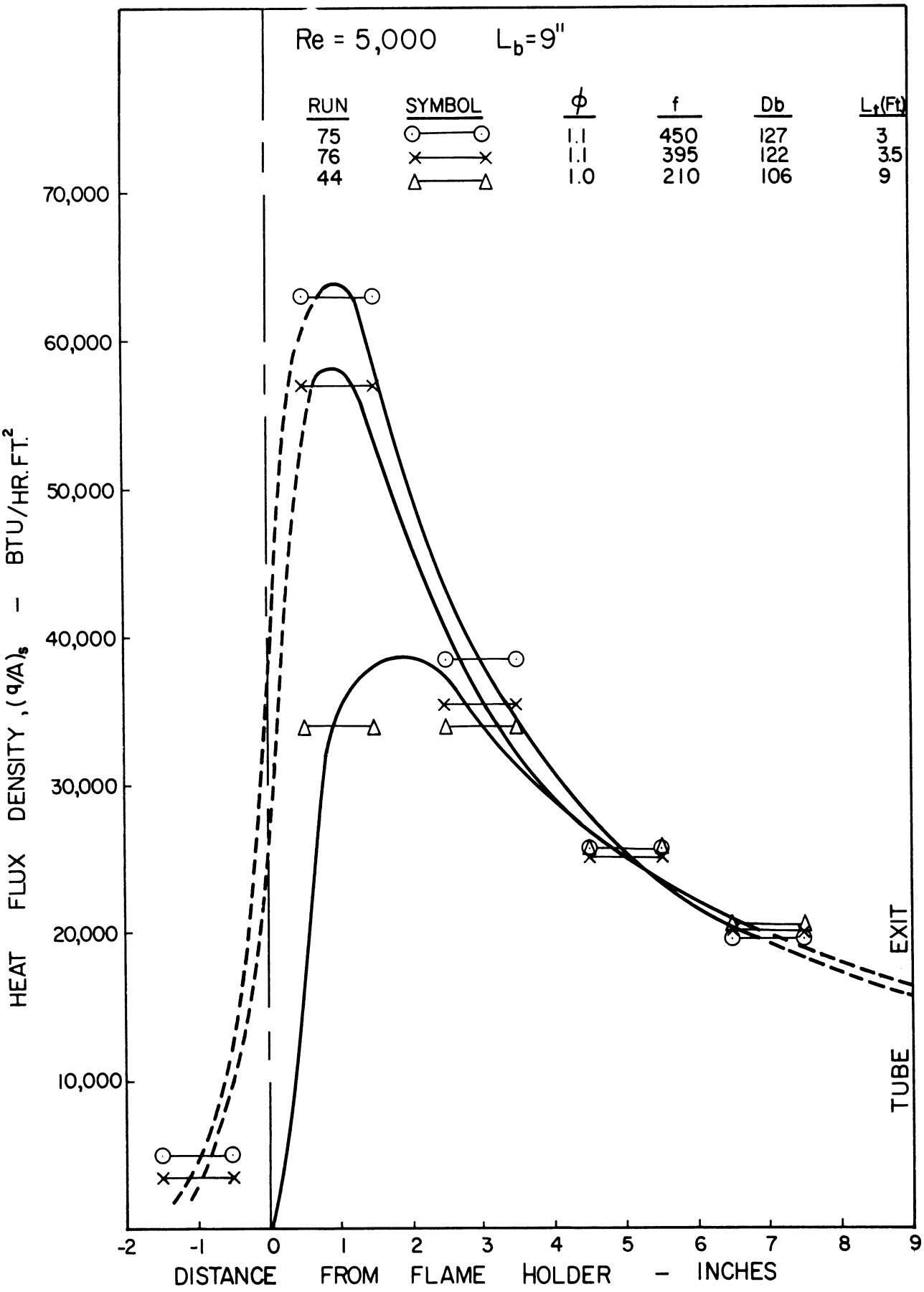

Figure 32. Effect of Total Tube Length on Local Rates of Heat Transfer.

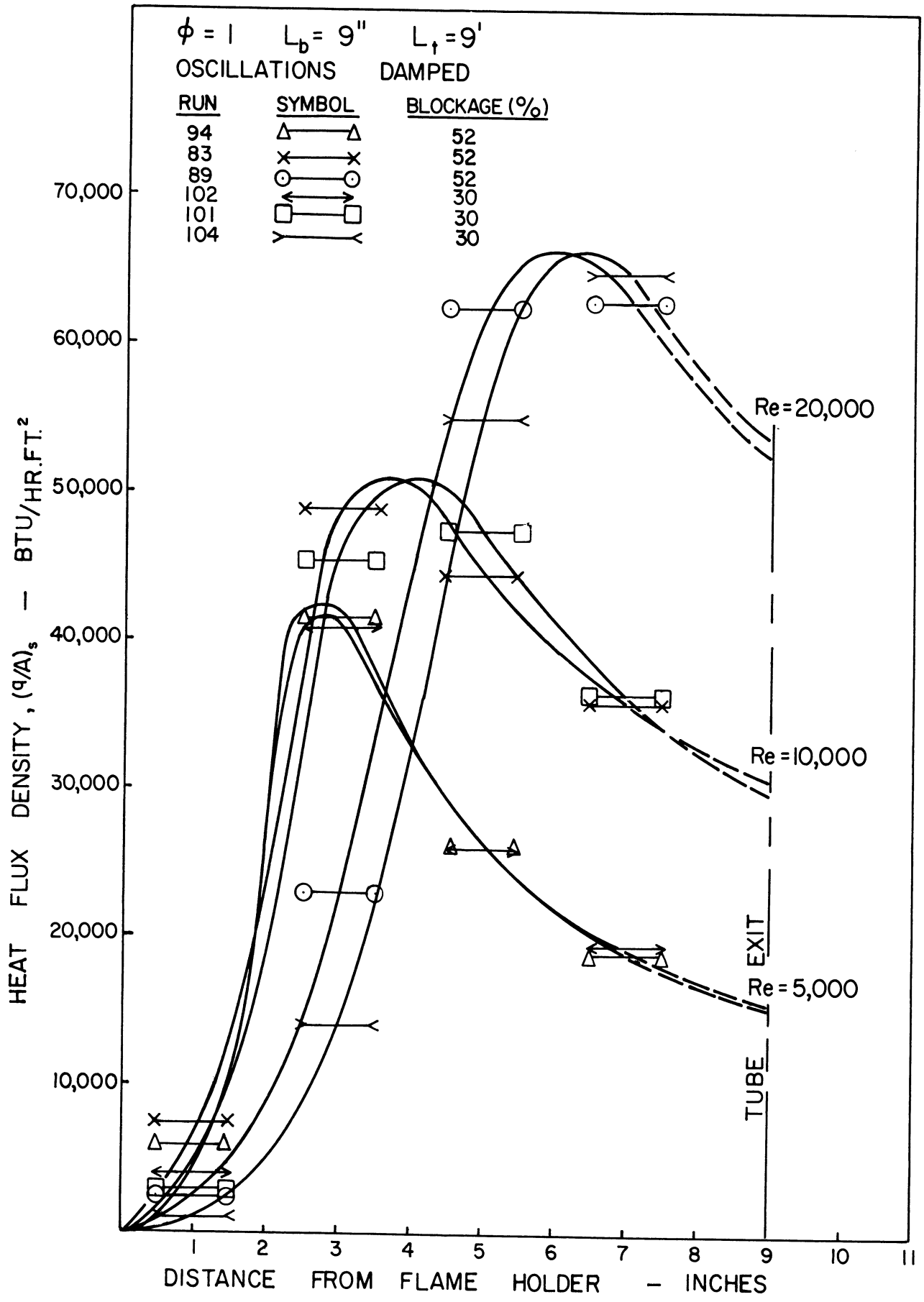

Figure 33. Effect of Flame Holder Blockage on Local Rates of Heat Transfer.

blew off at burning lengths greater than about 9 inches. The flame-generated oscillations caused the flame to pulsate considerably with subsequent extinction. Even in cases where the flame persisted, the pulsations often resulted in unsteady temperature readings. For these reasons, only data with damped oscillations were taken with the 30 percent blockage flame holder.

A few runs were made with a 45° conical flame holder of 52 percent blockage in order to determine the effect of flame holder shape. There was essentially no difference between the rates of heat transfer for the flat plate and conical flame holder of identical blockage.

Effect of Upstream Screens

All previous data were measured with no obstructions between plenum chamber and flame holder. Three 50 mesh screens were installed upstream of the flame holder to alter the velocity distribution and turbulence level. The screens tend to produce a flat velocity profile of low turbulence intensity at the flame holder. No effect of the screens on rates of heat transfer was observed. Turbulence generated by the combustion process probably overshadows the inlet turbulence level[62][83].

Total Heat Transfer

The total heat transferred to the wall along the burning length can be calculated by a water side heat balance and by integration of the local thermal fluxes. A comparison between the two methods is presented in Figure 34. The mean deviations of the water side values from those calculated by a rigorous integration of fluxes is about 4 percent. The

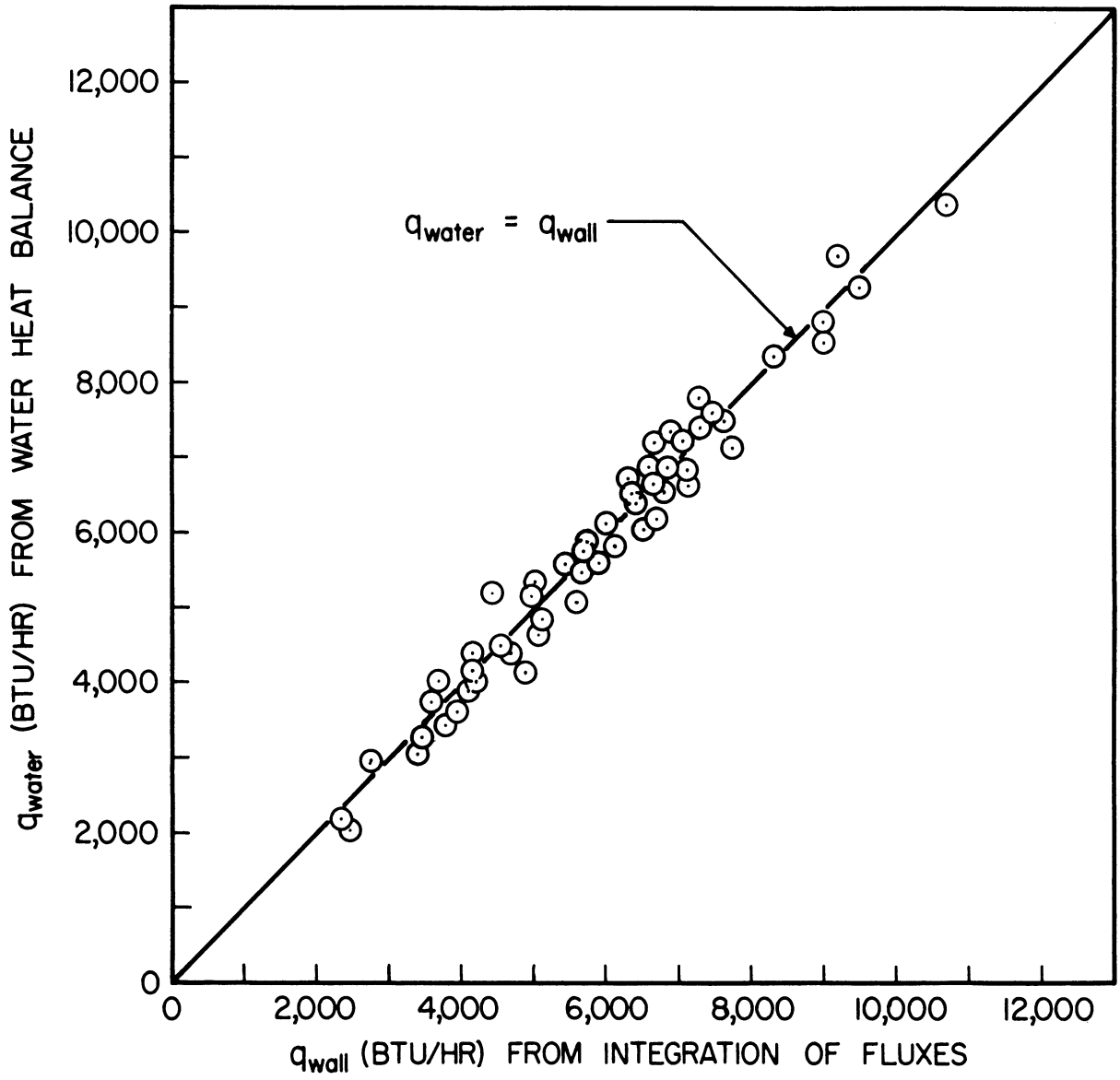

Figure 34. Summary of Heat Balances.

agreement is satisfactory considering the experimental error of the water side balance and the necessary extrapolation of the curve for local heat transfer rates.

Surface Temperature

No attempt was made to control the inside surface temperature at a constant level. Conditions in the annulus, however, were fairly steady during the investigation. The water flow rate was maintained at 5 gallons per minute for most runs, and the water temperature varied between 60 and 68°F. The rate of heat transfer between the inside surface of the tube and the water in the annulus can be expressed as

$$(q/A)_s = U_s \quad (t_s - t_w). \tag{13}$$

where U_s is the overall coefficient for the tube wall and the water film. Over the moderate temperature ranges encountered in the study, the resistance of the wall and the water films did not vary greatly. With both U_s and t_w reasonably constant, a plot of $(q/A)_s$ against t_s is expected to be almost linear.

The local rates of heat transfer are plotted versus local surface temperatures in Figure 35 and a straight line drawn through the data. The local surface temperatures are found to be predicted within 8°F by the equation

$$t_s = \frac{1}{275} \quad (q/A)_s + 65 \tag{14}$$

A theoretical evaluation of an average overall heat transfer coefficient for the wall and water film yielded a value of 279, thus confirming the experimental result. Since local surface temperatures are of little

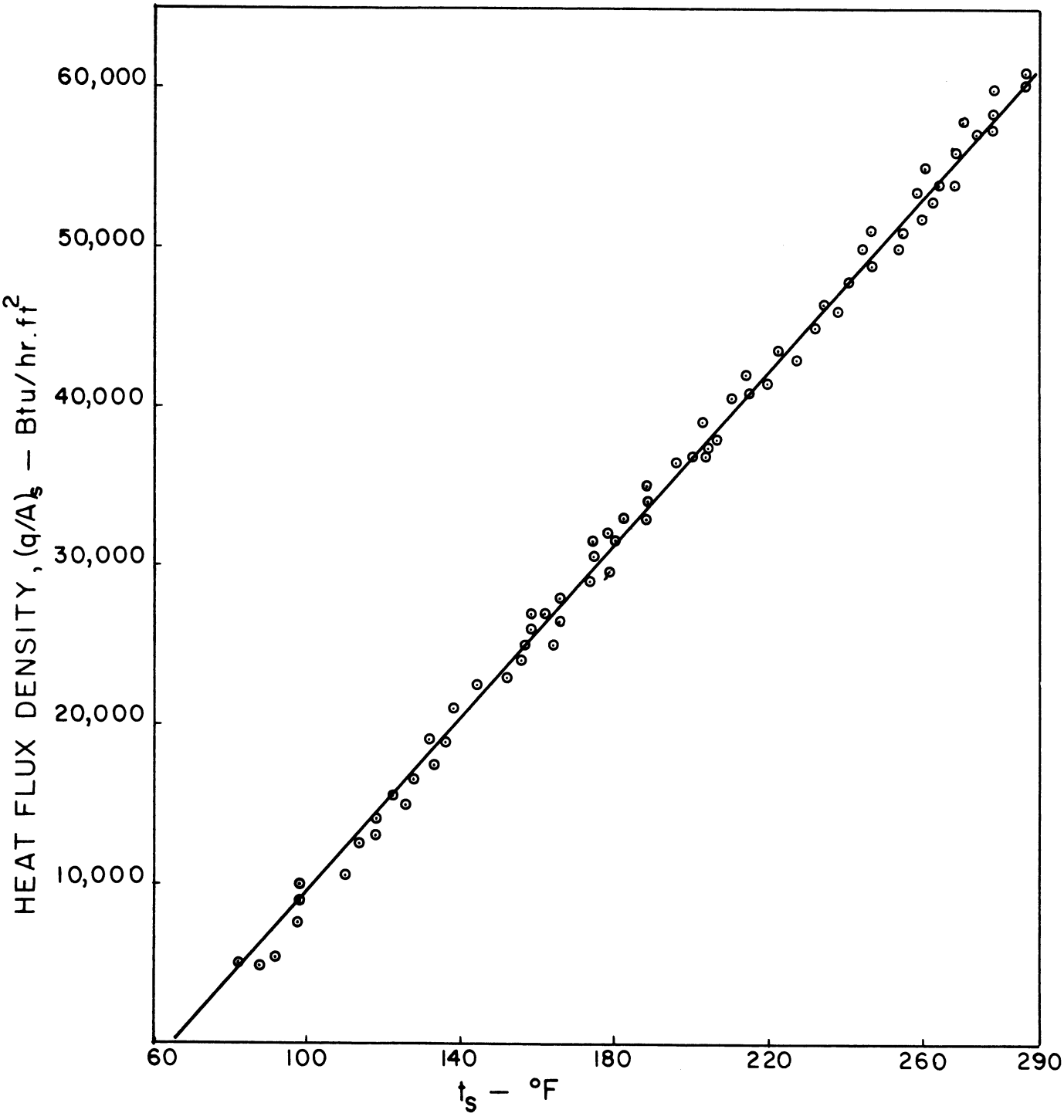

Figure 35. Relation of Local Surface Temperatures to Local Rates of Heat Transfer.

significance in the interpretation of the results of this study, they are not included in the detailed data of Appendix A.

Screech Combustion

Screech combustion is generally considered a high frequency transverse oscillation. Since it is usually accompanied by substantial increases in combustion efficiency and rates of heat transfer[71], an attempt was made to induce screech combustion. Rogers[56] suggested that screech is more likely to occur with high blockage flame holders, an insulated burning region, rich fuel-to-air mixtures, and with the flame holder near the exit of the tube.

A 2 1/2 inch length of ceramic tubing was inserted near the exit of the test object, and a flat plate flame holder of 75 percent blockage placed inside the liner. The ceramic liner had an outside diameter of 0.96 inches and a thickness of 0.10 inch. The liner served to insulate the flame zone near the stabilizer. To reduce heat extraction further, the cooling water flow rate in the annulus was reduced to 1 gpm. The fuel-to-air ratio of the burning mixture was varied over a wide range of values. To measure any high frequency oscillations, an Altec microphone was connected to an oscilloscope through a power source and band filter. No strong high frequency oscillations were observed. Since screech is generally observed in larger chambers, there may be some geometry effect which hinders a transverse oscillation in a tube of one inch diameter.

With the ceramic liner around the flat plate flame holder, an increase in the rate of heat transfer was frequently measured. A comparison between Figure 36 and Figure 11 indicates the improvement in heat flux with the ceramic liner. When viewed from the exit of the test object,

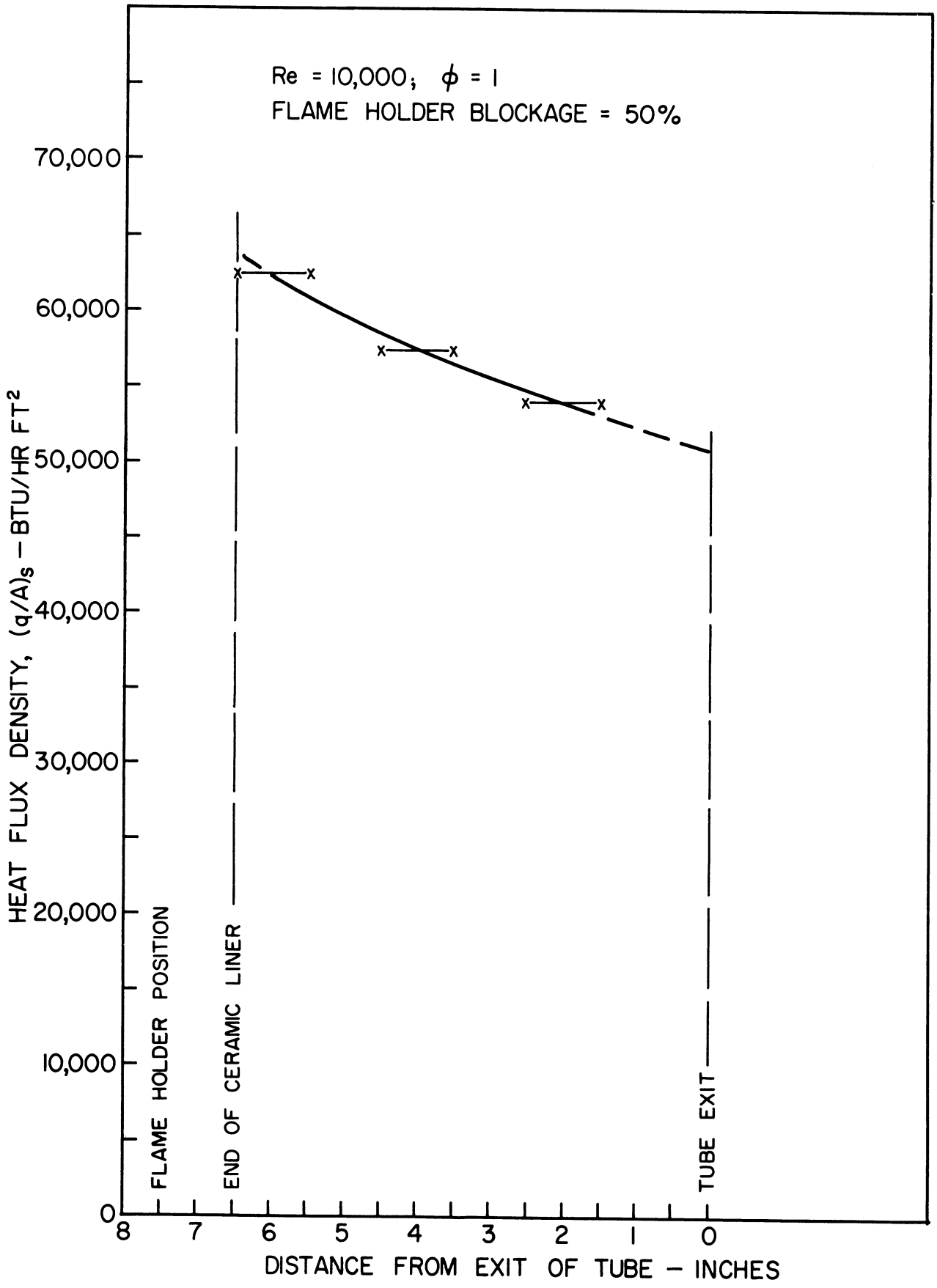

Figure 36. Local Rates of Heat Transfer with Ceramic Liner.

the downstream end of the ceramic liner was red. The increased heat transfer, then, appears to be caused by stabilization of the flame on both the ceramic liner and the central bluff body.

Heat Transfer Without Combustion

A brief study was made to determine the effect of a flat plate on heat transfer from a stream of heated air. The rates of heat transfer downstream from the flat plate of 52 percent blockage were measured for inlet Reynolds' numbers of 5,000, 10,000 and 20,000, and for inlet air temperatures of 100° and 130°F. From a knowledge of the local thermal flux and bulk gas temperatures, the local heat transfer coefficients were computed. The results obtained at 12 tube diameters from the flat plate were essentially the same as for fully developed flow. In an attempt to generalize the data, each local heat transfer coefficient was divided by the coefficient at 12 tube diameters downstream. The results correspond closely to the ratio c_x/c_{12}, where c_{12} has a value of 0.023. A plot of the ratio c_x/c_{12} against distance downstream of the flat plate, with Reynolds' number as a parameter, is presented in Figure 37. Since each curve is based on only two runs at low temperatures, the accuracy of the plot is limited.

Efficiency Measurements

The derivation of the one dimensional equation employed in calculating combustion efficiencies is presented in Appendix C. Except for the pressure drop due to the drag of the walls, the data required are known or can be closely approximated. The drag of the walls depends

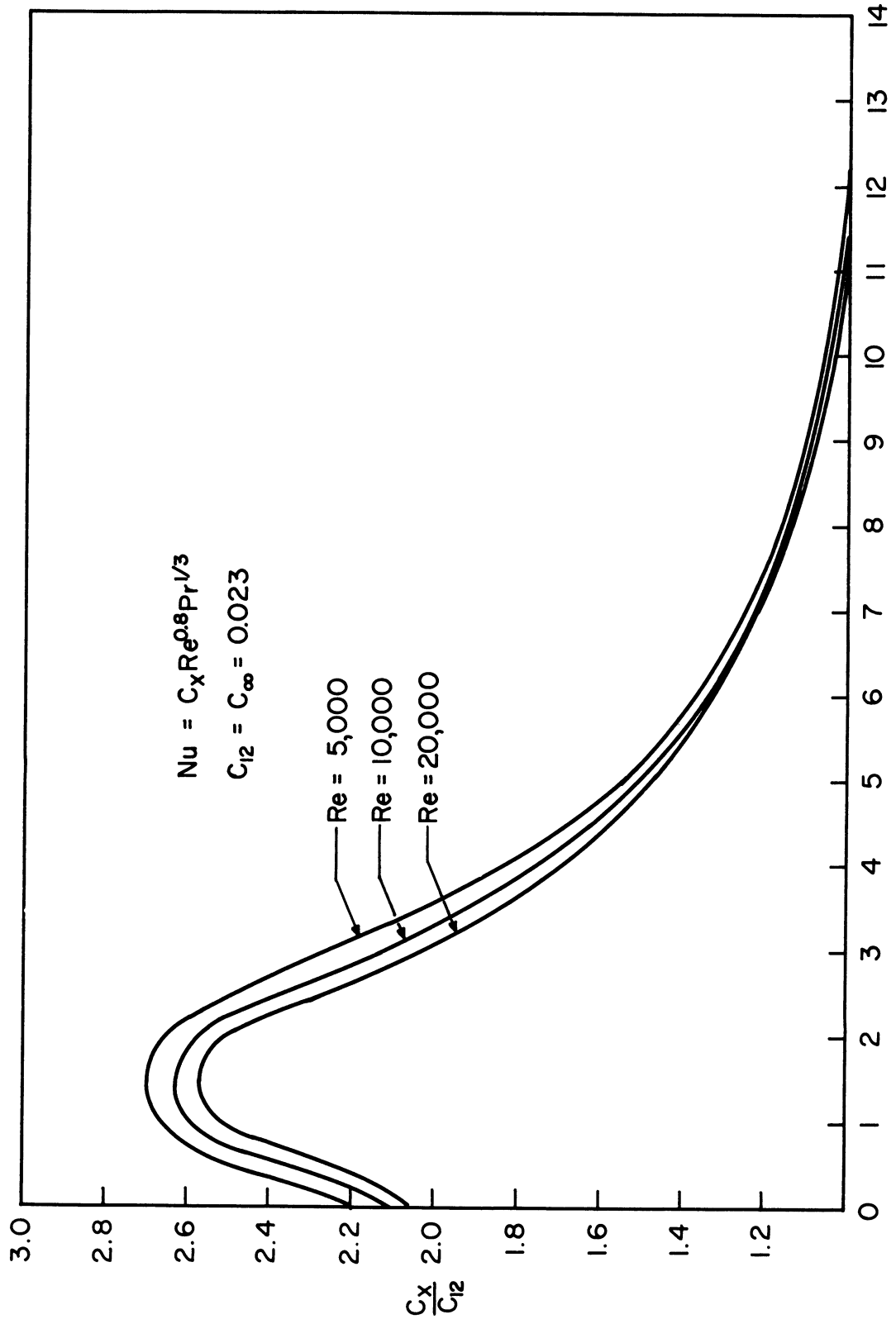

Figure 37. Effect of Flat Plate on Local Rates of Heat Transfer from Air.

upon the velocity and temperature distribution along the length of the tube, both of which are unknown.

An approximate procedure was used to estimate the drag of the walls during combustion. The heat transfer was assumed to be given by an expression of the form

$$Nu = c_x \, Re^{0.8} \, Pr^{1/3}$$

Using the values of c_x determined for low temperature air flow, the gas temperatures required to produce the observed heat fluxes were calculated. The ideal gas law was then applied to calculate the velocity profile from the temperature profile. From empirical cold flow data relating the drag of the walls to tube velocity, an average pressure drop due to wall friction was estimated. The many approximations are apparent. A critical review of the procedure is presented in the discussion.

In Figures 38A and 38B, typical data relating combustion efficiency to fuel-air ratio, flow rate, and tube length are plotted. Because of the scatter of the data, no attempt was made to separate the combustion efficiencies for damped and oscillating combustion.

The combustion efficiency decreases rapidly near the lean and rich blowoff limits. Between fuel to air ratios of 0.8 and 1.2, however, the fraction of limiting reactant burned remains fairly constant. At burning lengths of 11 inches, flow rate does not appear to have a significant effect on combustion efficiency. An increase in combustion efficiency occurs with increasing burning length. The increase is more pronounced at the higher flow rate where less reaction time is available.

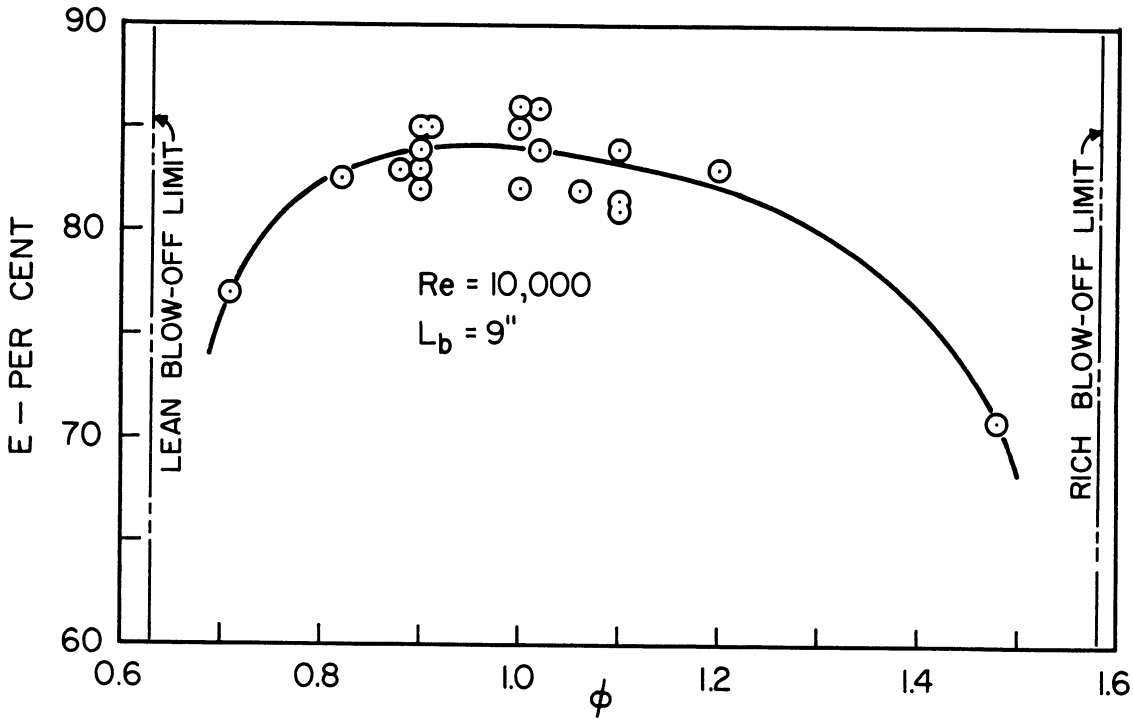

Figure 38A. Effect of Fuel to Air Ratio on Combustion Efficiency.

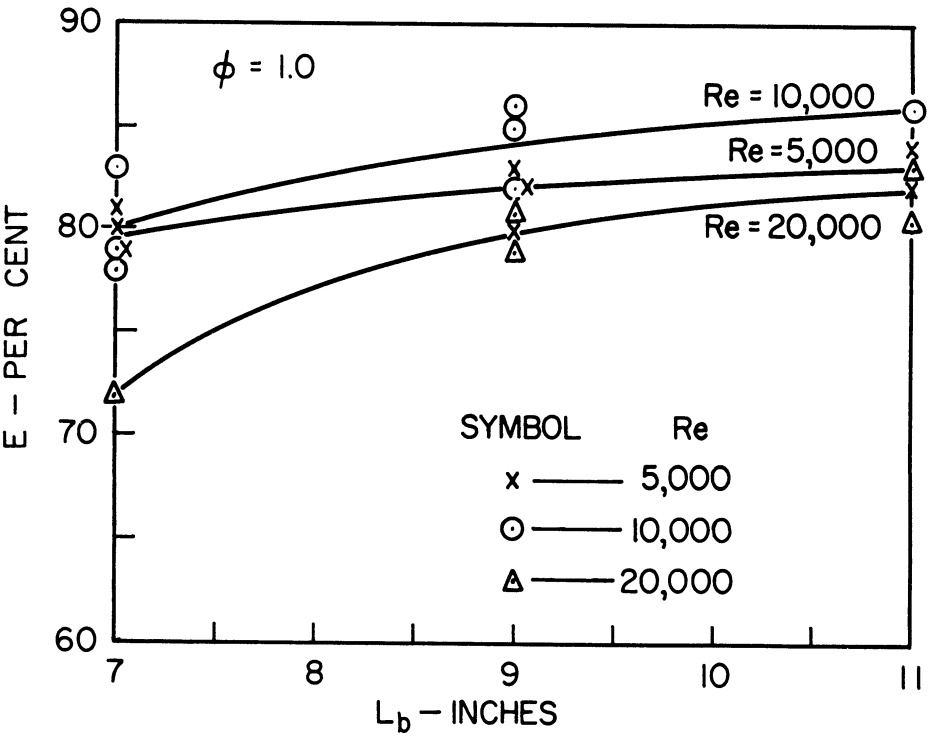

Figure 38B. Effect of Burning Length on Combustion Efficiency.

For a few runs, thermocouple and pitot-static tube traverses were made at the tube exit. The thermocouple readings were corrected for convection and radiation errors by the procedure outlined by Scadron and Warshawsky[60]. The average exit temperature, weighted according to mass flow, was used in a heat balance to compute the combustion efficiency. The efficiencies calculated from the thermocouple traverses average about 3 percent higher than the mean efficiency curves based on total pressure drop data.

The results of the traverse method indicate that flame-generated oscillations cause a small decrease in combustion efficiency. On the average, the efficiency for damped burning is about 2 percent higher than the efficiency when oscillations are present.

DISCUSSION

Effect of Process Variables

In the absence of flame-generated oscillations, changes in process variables produce no unexpected effects on the characteristics of the heat transfer profile curves.

An increase in inlet flow rate increases the peak rate in the heat transfer profile and shifts the peak toward the exit. The increase in peak heat flux mainly results from an increase in the heat transfer coefficient at the higher flow rate. The shift of the maximum toward the exit is probably a consequence of the higher flow rate transporting the burning particles further downstream before they spread to the wall.

The rates of heat transfer are expected to depend on chemical reaction rates, with greater heat transfer resulting from the higher heat release in faster burning mixtures. The reaction rate of propane-air flames is at a maximum near stoichiometric proportions. As expected from the kinetic considerations, the maximum rates of heat transfer are observed in the region of a stoichiometric mixture. As the inlet mixture is made rich or lean, the peak in the heat transfer curve decreases and shifts toward the exit. The decrease in the rate of flame spreading is caused by the lowering of the chemical reaction rate. The increase in the heat transfer curve at the higher inlet temperature can also be attributed to enhanced chemical kinetics.

Effect of Oscillations

The general effect of flame-generated longitudinal oscillations is to flatten the peak in the damped curve and to shift the peak of the damped curve toward the flame holder.

Ross[58] photographed flames propagating from an annular flame holder in a 1 inch diameter tube. With non-oscillating combustion, the central jet was sharply outlined. When flame-driven longitudinal oscillations were present, the recirculation zone was no longer definable. The central jet was now obscured, and the whole flame was pushed up against the face of the annular flame holder.

The shift of the experimental heat transfer peaks toward the flame holder for oscillating combustion, then, is in accord with the observations of Ross. The motion of the gas particles provides a possible explanation for the results. A longitudinal oscillation is a back-and-forth movement of gas particles at the frequency of the observed sound. The motion of the particles would be expected to create additional turbulence and to improve the mixing of the gases. Thus, hot burned gases are mixed with cold unburned gases, resulting in a lowering of the maximum temperature and a broadening of the temperature profile. Since the heat transfer curve depends on the temperature level, it likewise assumes a more flattened appearance. The particle motion would also promote back mixing of the gases, which tends to shift the position of peak heat transfer toward the flame holder. The observed results, then, are in accord with the hypothesized mixing model.

Although the heat transfer profiles are different during damped and oscillating combustion, the general magnitudes of the rates of heat

transfer do not differ appreciably. The maximum pressure amplitude of the oscillations encountered in this study is estimated as less than 0.5 psi. Berman and Cheney[4], studying instabilities in a 3 inch burner, noted no abnormal heat transfer effects resulting from longitudinal oscillations with amplitudes up to 100 psi. More definitive studies are required, however, in order to reach a general conclusion regarding the effect of flame-generated longitudinal oscillations on rates of heat transfer.

The cause of the premature blowoff from the low blockage flat plate stabilizer is not completely understood. Putnam and Dennis[53] found that stability limits of a flat plate flame holder were essentially unaffected by organ pipe oscillations. When the flame was able to spread to the walls before reaching the exit of the tube, however, they frequently noted premature blowoff due to a low frequency oscillation. The low frequency was directly associated with a large periodic variation in flame shape, which results from a periodic blowoff of the flame, and reignition from the central core behind the holder.

The observations of Putnam and Dennis regarding stability limits were confirmed in the present study. Near the rich blowoff limit there was a high frequency oscillation (above 1000 cps) which did not affect the stability limits of the low blockage flame holder. In the region of a stoichiometric mixture, however, organ pipe oscillations with frequencies around 200 cycles per second, frequently extinguished the flame. Considerable pulsation of the flame was observed prior to blowoff. In no instance

was a low frequency component detected. The low frequency oscillation described by Putnam and Dennis was not observed in this study.

The explanation for the premature blowoff may involve the dimensions of the flame holder. For a given flow velocity, there is a minimum flame holder size which will satisfactorily stabilize the flame. In the presence of certain flame-generated pulsations, a larger size flame holder might be required to maintain a stable flame. Thus, a flame holder giving satisfactory performance under damped conditions might be subject to premature blowoff with oscillating combustion.

Combustion Efficiency

The many approximations made in the evaluation of combustion efficiency from total pressure drop data limit the accuracy of the results. The majority of assumptions involved in the derivation of the simplified theoretical expression are reasonable. The most important errors in the theory are introduced with the assumptions of one-dimensional flow, and of no gradients at the exit end of the tube. A more rigorous derivation including the effect of gradients gave essentially the same results.

The most significant error in the application of the theory is probably incurred in estimating the drag of the flame holder and tube walls during combustion. The drag of the flame holder was taken directly from cold flow measurements. Barrere[3] indicates that the drag of a flat plate stabilizer is less with combustion. Lacking more precise measurements, the cold flow data was used. The complex procedure used to calculate the drag of the tube walls during combustion is of quite

limited accuracy. Since over 25 percent of the combustion chamber pressure loss was due to the drag of the walls, a significant error can result from the approximate method. For example, an error of 10 percent in the estimated drag of the walls can cause an average error of about 3 percent in the combustion efficiency. The scatter of the combustion efficiency data, then, is not surprising.

The combustion efficiencies based on the thermocouple, pitot tube traverses are also of limited accuracy. At the high temperatures measured, the thermocouple corrections are appreciable, ranging from 200° to 900°F. Although corrections were carefully applied, significant errors in temperature could result. The combustion efficiencies from the temperature traverse average about 3 percent higher than the efficiencies based on pressure drop data.

The trends of combustion efficiency with respect to process variables are generally expected. The rapid drop of efficiency in very lean and very rich mixtures follows from kinetic considerations. The increase in efficiency with increased burning length was expected, since flames were usually observed to fill the entire tube. For burning lengths greater than 9 inches, only a small difference existed between the combustion efficiencies at the three flow rates. The maximum at the intermediate flow rate was not anticipated and may be due to inaccuracies in the method of measuring efficiency. The cooling of the tube also provides a possible explanation. In an uncooled tube, combustion efficiency usually decreases with increased flow rate because of a decrease in residence time. With extraction of heat from the tube, however, the

rate of reaction is reduced. Since reaction rate depends exponentially on temperature, cooling of the tube can significantly lower the volumetric conversion rate. The measured heat extraction per unit mass of gas flow was found to increase with decreasing mass flow rate. The opposing effects of residence time and heat extraction, then, could conceivably result in a maximum combustion efficiency as flow rate was varied.

Resonant Frequencies

The agreement between observed and calculated frequencies indicate that the oscillations correspond to the longitudinal (organ pipe) mode of resonance. Several factors could contribute to the discrepancies between the experimental and theoretical values. The theoretical values are based on the assumption of an average burning temperature, from which the speed of sound, a_2, is estimated. The actual burning temperature depends upon the process variables, particularly upon the inlet fuel-to-air ratio. The derivation also assumed a normal interface between burned and unburned gases. Since the velocity around the baffle was large compared to the flame speed, the flame front was not normal to the walls of the burner. The effect of this error is difficult to evaluate. Another minor source of error results from the end effects of the doubly open pipe, which are not accounted for in the calculations.

At a Reynolds' number of 10,000 and a total tube length of 9 feet, a shift to higher overtones was observed with increasing fuel-to-air ratio. Each transition was also accompanied by an increase in the pressure amplitude. The jumps in frequency, shown in Figure 29, are incompletely understood. The explanation is probably related to the energy

of the system. As fuel-to-air ratio is increased up to the region of a stoichiometric mixture, the energy released by the burning process increases. It is possible that the additional available energy is capable of exciting a higher, more energetic overtone.

For all major frequencies except the highest (1000 cps) the pressure antinodes were well upstream of the flame holder. At the highest overtone, the calculated location of the pressure antinode was between the flame holder and the point of flame contact with the tube walls. According to Putnam and Dennis[50], oscillations are best promoted when the heat source is at the maximum pressure point. Since heat is released along the whole length of the flame from flame holder to point of wall contact, a hypothetical point of heat release can be postulated a slight distance upstream from the wall contact point. In this case, then, the point of heat release is near a pressure antinode. The strong 1000 cycle per second overtone was observed in a very rich mixture near the blowoff limits, where oscillations might be expected to be weak. The location of the pressure antinode near a heat source provides an explanation for the intense oscillation.

Sound Pressure Level

Unusual results were noted for rich mixtures burning at low velocity in total tube length of 3 and 3.5 feet. The flame was a luminescent yellow, as opposed to the usual pale blue. The heat transfer one inch downstream of the flameholder and the sound pressure level at the exit of the tube were considerably higher than with the longer burning lengths. Even more unusual was the transfer of heat at a rate

of about 5000 BTU per hr. per ft.^{2} one inch upstream of the flame holder.

While studying organ pipe oscillations, Dunlap[13] noted that the flame burned upstream of the flame holder for low velocity runs. In such cases, he showed that the velocity amplitude due to the standing wave exceeded the average mixture velocity at the flame holder. The experimental observations indicate that a similar situation exists for the runs described above. The minimum pressure amplitude required to produce a particle velocity exceeding the flow velocity at the flame holder can be calculated. The theory and calculations are presented in Appendix C. The calculated sound pressure level at the flame holder is compared to the measured external sound level in the following table.

Tube Length Ft.	Observed External Sound Level, db	Calculated Internal Sound Level, db
3.0	127	159
3.5	122.5	148

No measured internal sound levels are available for comparison. The calculated values, however, are of reasonable magnitude.

Theoretical Considerations

The difficulties involved in theoretically describing a confined combustion process have been described. The work of Longwell et al.[48], previously reviewed in the literature survey, deserves particular mention. They studied experimentally flame spreading from V-gutter baffles in a two dimensional duct. Local combustion efficiencies were determined by probe traverses at several downstream cross sections. They applied several theoretical models in an attempt to interpret their data. The results are summarized in the following paragraphs.

If flame spreading occurred as a laminar flame front, the pressure would have little effect on the flame velocity. With extremely turbulent flow and violent mixing, the pressure would have an important effect. For complete homogeneous combustion, the flame velocity has been found to vary with pressure raised to the 0.8 power. The pressure exponents observed by Longwell ranged from 0.1 to 0.6 and are intermediate between the extremes of laminar and homogeneous combustion.

Experimental flame velocities were also intermediate between the two limits. If burning occurred as a laminar flame front under the experimental conditions, the flame velocity would be 2 ft/sec., and if it occurred as optimum homogeneous combustion[1], the flame velocity would range up to 340 ft/sec. The actual data indicated flame speeds of 5 to 50 ft/sec.

By assuming homogeneous combustion in local regions across a profile, an average flame velocity at each station could be calculated. The overall flame velocities computed from local homogeneous reaction rates were much greater than experimental values. Starting with one efficiency profile, they then calculated how effective turbulent flame velocities and efficiency profiles changed while moving downstream. The calculated flame velocities decreased, whereas the observed flame velocities increased. The concept of local homogeneous burning thus failed to predict both the overall effective flame velocities and the general shape of the efficiency profiles.

They concluded that no satisfactory general mechanism for flame spreading has been suggested. In general, reaction rates and pressure dependence for experimental flame spreading may have any values between

the extremes predicted by laminar flame front theory and by homogeneous reaction theory.

For the present investigation, it would be desirable to have a theoretical combustion model which would predict the longitudinal variation of efficiency. On the basis of Longwell's study, however, the application of theoretical models to yield an efficiency profile does not seem justified.

Calculated Heat Transfer Profile

In the absence of oscillations, the combustion process is considered as a gradual spreading of the burning mixture from the wake of the baffle to the wall of the tube. Burning then continues throughout the mixture in the remaining length of tube. The peak in the heat transfer profile probably occurs near the point where flames first contact the tube wall. Until the rapid rise near the peak of the curve, the rate of heat transfer is small. The cold unburned gases flowing near the wall reduce convective heat transfer until hot gases are able to propagate from the central core to the wall. After the peak rate is reached, heat transfer decreases rapidly with downstream tube length. Sensible heat energy is apparently removed by cooling at a faster rate than it is supplied by additional chemical reaction.

The local rates of heat transfer depend upon fluid dynamic and chemical kinetic considerations, which are interrelated in a complex manner. Local conditions are a result of the combined effects of the complicated flow and reaction phenomena. Measurements of local conditions, however, provide valuable information for theoretical analysis. For example, if local combustion efficiencies were known along the length of the tube an average gas temperature could be assigned to each cross section. Radiant and convective heat transfer could then be estimated from existing empirical

expressions, and compared with experimental values.

Local gas phase measurements were considered beyond the scope of this study. The installation of static pressure taps along the length of the test object would have permitted an approximate measurement of average local efficiencies. The results would be subject to most of the limitations that applied to the calculation of overall efficiency.

Lacking average local efficiencies, only a crude theoretical estimate of the heat transfer profile was possible. The flames were considered to first touch the wall near the peak of the experimental heat transfer curve. In order to compute theoretical heat transfer curves, the combustion efficiency at the peak of the experimental profile was assumed equal to the efficiency at the exit of the tube. An average bulk temperature at the peak was then calculated from the efficiency. The convective heat transfer coefficient was evaluated from the correlation of Zellnik[84] and corrected for the effect of the flame holder from Figure 37. Knowing the bulk temperature, the convective coefficient, and the relation of surface temperature to heat transfer rate (from equation (12)), the local rate of convective heat transfer at the peak was calculated. Radiation was evaluated from the data of McAdams[42]. A stepwise procedure was now used to calculate the local rates of heat transfer downstream from the experimental peaks. The results of the calculations are presented in Figures 39 to 41. In each figure, the experimental curve for damped combustion is drawn for comparison.

At the peaks, the calculated values are slightly higher than the measured results. The calculated rates then decrease rapidly and

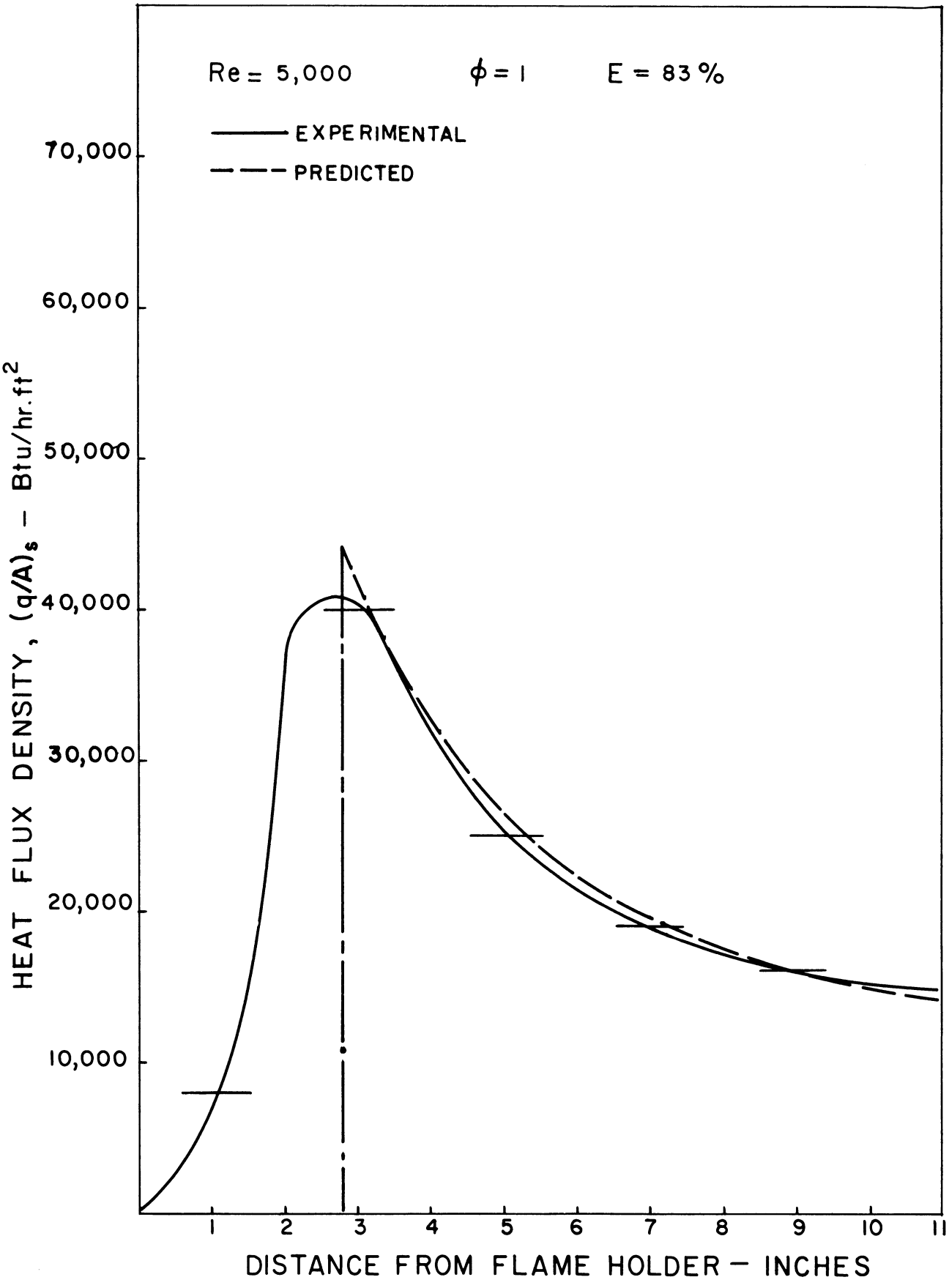

Figure 39. Comparison of Experimental and Predicted Profiles.

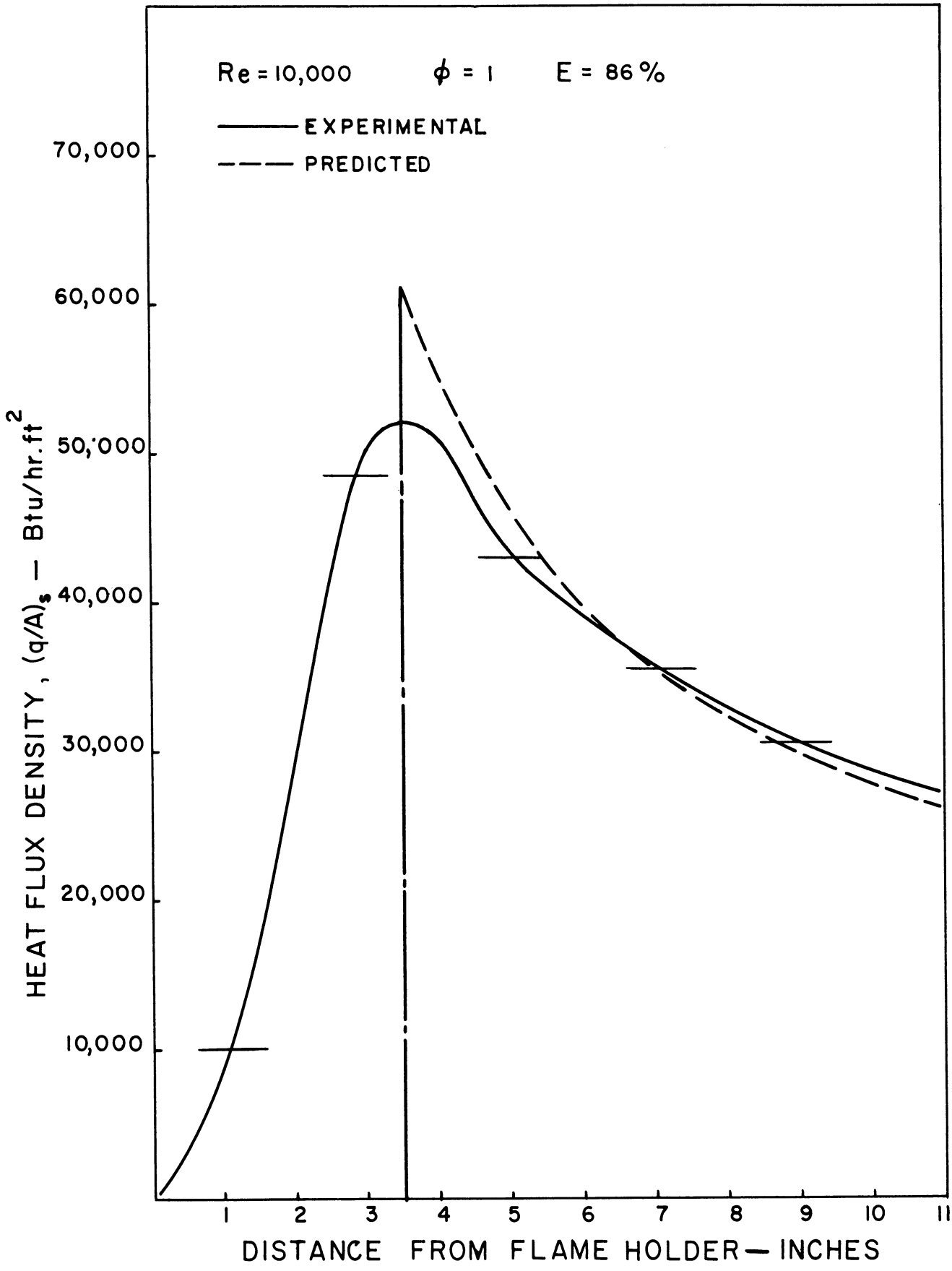

Figure 40. Comparison of Experimental and Predicted Profiles.

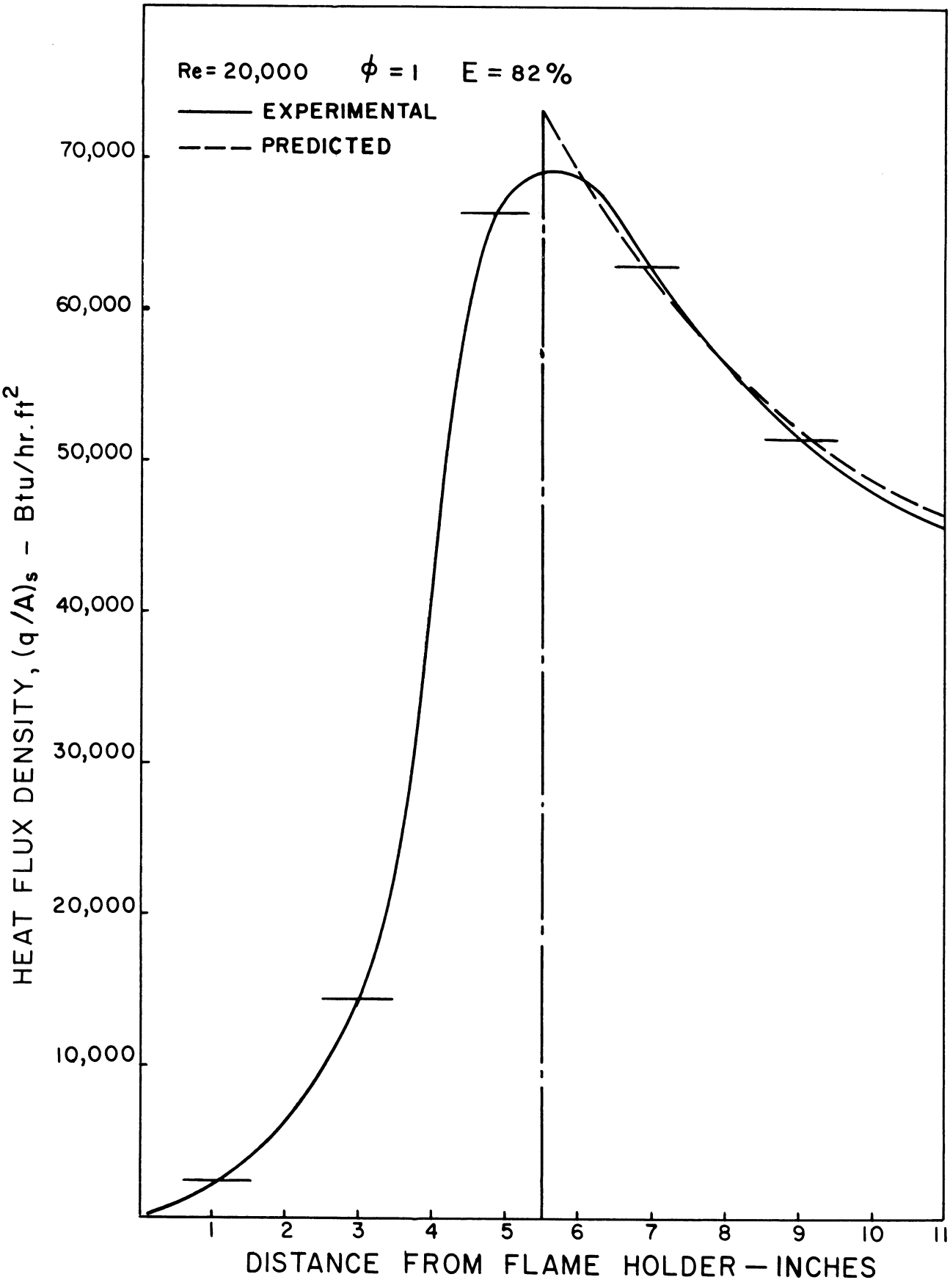

Figure 41. Comparison of Experimental and Predicted Profiles.

tend to follow the experimental curves. The apparent agreement of experimental and theoretical curves, however, is not entirely expected. Since flames were observed along the entire length of tube, combustion efficiency did not reach its final value at the peak of the experimental curve, as was assumed in the calculations. In particular, the data for a Reynolds' number of 20,000 indicate a large increase in efficiency downstream of the experimental peak. If the assumed efficiency at the peak is greater than the actual value, the calculated rate of heat transfer would be expected to be higher than the experimental rate. In addition, the extraction of heat upstream of the experimental peak lowers the temperature level at the peak. This would also tend to increase the predicted rate at the peak above the experimental. The differences between theoretical and experimental rates at the peak are considerably less than expected.

The heat released by the chemical reaction is the sum of the heat transferred to the walls and the sensible heat content of the exit gas above the datum temperature. Since the predicted and experimental sensible heat contents at the exit are about the same, total heat transferred should also be roughly equal in both cases. The total heat transfer area under the theoretical curve, however, is smaller. The difference is due largely to the heat transferred upstream of the peak in the experiments.

Several reasons can be postulated to explain the discrepancies between calculated and observed curves. The limited accuracy of combustion efficiencies has been discussed. Any error in efficiency is reflected in

the results. The effect of the combustion process on heat transfer coefficients is unknown. The variation of heat transfer coefficients downstream of the baffle was based on limited data using low temperature air. The burning process may alter the distribution and magnitude of this curve. Considering the many doubtful factors, extension of the calculated profiles to other runs did not appear warranted.

In the absence of flame-generated oscillations, both Timofeev[70] and Kilham[31] found that convective heat transfer from hot combustion products can be approximated from existing empirical expressionf for non-burning gases. In the present experiments, it is estimated that convective heat transfer contributed more than 90 percent of the total heat transfer. Although the predicted curves involve many approximations and are limited in accuracy, they give reasonable agreement with the observed data. The results, then, agree with the conclusions of Timofeev and Kilham that convective heat transfer from hot combustion products can be approximated from empirical data for non-burning gases.

The measured combustion efficiencies indicated that a large part of the burning occurred between the flame holder and the peaks in the heat transfer profiles. No satisfactory method could be devised to predict rates of heat transfer in this region of rapidly changing combustion efficiency. More definitive studies are required in order to determine the effect of a combustion process on heat transfer coefficients.

Future Work

Screech combustion is considered undesirable in rocket chambers due to the severe heat transfer effects. The emphasis in research has been

on methods and designs which will eliminate or minimize screech combustion. The control and application of screech combustion, however, has been largely neglected. Controlled screech combustion would have potential application in processes requiring a high heat flux. A study of the effect of screech combustion on rates of heat transfer would appear warranted. the investigation would include the design of a heat transfer unit in which a stable transverse oscillation could be maintained.

Blackshear[5] suggested another method for increasing rates of heat release through the application of acoustic disturbances. A flame is anchored on a V-gutter flame holder which is supported by a hollow blade that extends upstream to a lowdspeaker. Standing sound waves are excited in the hollow blade and the sound is permitted to issue through slots in the flame holder. The disturbances result in transverse velocity components in the flame zone. Both theory and experiment indicate that the rate of heat release in a duct can be improved by supplying acoustic disturbances that a flame zone can amplify. The sound level at the plane of the exhaust was considerably less with excitation at the flame holder than with excitation of the flame by duct resonance. Blackshear's study suggests the possibility of increasing rates of heat transfer with low amplitude sound waves.

In the present investigation the effect of longitudinal oscillations on rates of heat transfer was attributed to improved mixing through particle motion. In any extension of the study, photographs of the flame zone would be helpful in clarifying the effect of longitudinal oscillations on the degree of mixing.[58] It is also recommended that further

studies be conducted in a larger diameter tube. In addition to aiding in defining the effect of diameter, the larger diameter would permit the use of more effective flame holders such as the perforated can type. The possibility of increasing heat transfer by means of an annular ceramic flame holder was suggested in the present study.

CONCLUSIONS

The inadequacy of turbulent flame theories and the lack of local gas phase measurements prevented generalization of the results.

The effect of process variables and flame-generated longitudinal oscillations on the rates of heat transfer are summarized below:

1) An increase in the inlet flow rate increased the peak in the heat transfer profile and shifted the peak toward the exit of the tube.
2) The maximum rates of heat transfer were observed near stoichiometric inlet mixtures. When the inlet mixture was richer or leaner in fuel, the peak rate of heat transfer was reduced and the peak shifted toward the exit of the tube. The changes with fuel to air ratio are due to both chemical kinetic and available energy considerations.
3) Local rates of heat transfer increased slightly at the higher inlet temperature.
4) The flame holder blockage, the downstream burning length, and the total tube length did not, in general, exert a significant influence on local rates of heat transfer.
5) Flame-generated longitudinal oscillations tended to flatten the peak in the heat transfer curve for damped combustion, and to shift the peak of the damped curve toward the flame holder. Oscillating

combustion resulted in slightly higher values of total heat transfer to the wall than damped combustion.

For comparison with experimental data, heat transfer profiles were calculated using three major assumptions: (1) that the measured combustion efficiency at the tube exit was equal to the combustion efficiency at the peak of the experimental curve. (2) That the variation of heat transfer coefficient downstream from the flat plate flame holder, measured for air at low temperatures, was valid at high temperatures during combustion and (3) that the heat transfer equation of Zellnik[84] was applicable. Downstream from the experimental peaks, the predicted and experimental rates gave reasonable agreement. The results, then, agree with the conclusions of other investigators[51][70] that convective heat transfer from high temperature combustion products can be approximated from empirical data for non-burning gases.

The data of this investigation are specific to a single fuel and geometry. The reliability of the results for the prediction of heat transfer for other fuels and geometries is uncertain.

APPENDIX A

ORIGINAL AND PROCESSED DATA

Runs 1 through 97 were made with the flat plate flame holder of 52% blockage.

Runs 100 through 103 were made with the flat plate flame holder of 30% blockage.

Runs 110 through 112 were made with the conical flame holder of 52% blockage.

The inlet mixture temperature was 120°F for runs 50 through 53. The inlet mixture temperature was 70 $\pm$ 2°F for all other runs.

f major is the predominant frequency in the overall sound level. D_b major is the sound level in decibels for the predominant frequency.

The subscripts on the (q/A) data represent the distances downstream from the flame holder at which the measurements were taken. Units are Btu/hr.ft.^{2}

A + sign after a φ value indicates that the specified fuel-to-air ratio was approached from a richer mixture. A - sign after a φ value signifies an approach from a leaner mixture.

RUN NO.	1	2	3	4	5	6	7	8	9	10	11	12	13	14
G lbs/sec.ft^2	1.46	1.46	1.46	1.46	1.46	1.46	1.46	1.46	1.46	1.46	1.46	1.46	1.46	1.46
φ	0.90	1.00	1.10^-	1.10^+	0.71	0.82	0.88	0.90^-	0.90^+	0.91	1.00	1.02^-	1.02^+	1.06
L_t ft	9	9	9	9	9	9	9	9	9	9	9	9	9	9
L_b in	7	7	7	7	9	9	9	9	9	9	9	9	9	9
f major cps	210	278	283	342	-	-	214	212	282	291	286	288	346	350
Db major	115	117	117	120	-	-	113.5	115	116	116	116	115	119.5	120
Db overall	116	117	117.5	121	97	105	114	115	116.5	117	117	117	120.5	121
q water Btu/hr.	5180	4820	5450	5870	2210	4630	5820	6750	6550	6840	6810	6630	6380	7220
E %	78	79	80	81	77	82	83	83	85	85	82	84	86	82
$(q/A)_{1\text{ in.}}$	26,100	39,100	40,600	41,900	1,300	1,500	31,200	33,500	34,400	36,100	43,100	43,500	45,300	46,300
$(q/A)_{3\text{ in.}}$	42,500	47,800	46,100	47,000	2,100	28,100	38,000	40,000	40,900	42,700	46,400	45,600	46,400	45,700
$(q/A)_{5\text{ in.}}$	37,500	40,900	39,000	39,200	6,300	43,000	34,800	36,000	36,600	37,500	39,800	39,400	39,600	37,500
$(q/A)_{7\text{ in.}}$	-	-	-	-	33,200	31,900	31,100	31,600	31,500	32,600	34,300	33,400	33,100	32,200
$(q/A)_{9\text{ in.}}$	-	-	-	-	-	-	-	-	-	-	-	-	-	-

RUN NO.	15	16	17	18	19	20	21	25	26	27	28	29	30
G lb/sec.ft^2	1.46	1.46	1.46	1.46	1.46	1.46	1.46	2.92	2.92	2.92	2.92	2.92	2.92
φ	1.10	1.10	1.20	1.48	0.90	1.00	1.10	0.90	1.0	1.10	0.90	1.0	1.10
L_t ft.	9	9	9	9	9	9	9	9	9	9	9	9	9
L_b in.	9$^-$	9$^+$	9	9	11	11	11	7	7	7	9	9	9
f major cps	288	350	350	1000	215	291	356	-	340	280	-	283	280
Db major	116	121	120	120.5	114.5	117	120	-	125	127	-	126	128
Db overall	117	121	121	121	115	118.5	122	110	125.5	127	112	127	129
q water Btu/hr.	6570	6830	6210	4030	7340	8360	7140	3620	6630	7200	6030	8550	8810
E %	84	82	83	71	84	86	86	65	72	71	79	79	80
$(q/A)_{1\text{ in.}}$	39,700	44,300	44,500	1,200	28,200	38,600	39,000	500	26,100	24,800	1,200	30,200	32,400
$(q/A)_{3\text{ in.}}$	46,600	46,200	43,800	13,800	41,300	47,100	46,100	10,900	54,900	53,300	14,100	53,800	53,100
$(q/A)_{5\text{ in.}}$	37,400	37,500	35,400	30,200	35,500	40,200	37,200	47,800	55,000	56,600	44,800	56,600	55,900
$(q/A)_{7\text{ in.}}$	31,500	31,000	30,200	31,100	31,200	33,600	29,900	-	-	-	60,900	53,100	53,500
$(q/A)_{9\text{ in.}}$	-	-	-	-	27,800	29,400	26,600	-	-	-	-	-	-

RUN NO.	31	35	36	37	38	39	40	41	42	43	44	45	46	48
G lb/sec.ft^2	2.92	0.73	0.73	0.73	0.73	0.73	0.73	0.73	0.73	0.73	0.73	0.73	0.73	5.84
φ	1.0	0.90^-	0.90^+	0.96	1.0	1.10	0.84	0.90^-	0.90^+	0.97	1.0	0.90	1.0	1.0
L_t ft.	9	9	9	9	9	9	9	9	9	9	9	9	9	9
L_b in.	11	7	7	7	7	7	9	9	9	9	9	11	11	9
f major	291	210	132	133	208	278	-	-	133	138	210	133	215	-
Db major	124	95	105.5	104	108	109	-	-	104	105	106.5	103	108	-
Db overall	125	96	106	105	108	110	95	97	105	105.5	107.5	105	110	118
q water Btu/hr.	10380	3260	3740	3410	4190	3950	2980	3050	4400	4560	5320	4380	5060	5750
E %	81	78	79	78	81	79	80	80	82	81	80	82	82	75
$(q/A)_{1\text{ in.}}$	25,800	3,300	22,400	18,800	32,100	36,000	700	2,300	20,900	13,800	33,900	23,200	30,200	600
$(q/A)_{3\text{ in.}}$	53,600	37,700	31,200	36,900	35,900	33,100	5,200	38,700	31,600	36,700	34,100	30.400	34,600	7,200
$(q/A)_{5\text{ in.}}$	56,400	25,600	23,500	25,700	26,000	23,400	30,100	24,800	22,900	25,600	25,700	22,000	25,700	31,100
$(q/A)_{7\text{ in.}}$	53,000	-	-	-	-	-	20,200	18,100	18,000	20,100	20,600	16,900	20,500	56,400
$(q/A)_{9\text{ in.}}$	47,100	-	-	-	-	-	-	-	-	-	-	14,500	17,300	-

RUN NO.	50	51	52	53	60	61	62	63	64	70	71	72	73	74	75
G lb/sec.ft^2	2.92	2.92	1.46	1.46	1.46	1.46	1.46	0.73	0.73	1.46	1.46	1.46	1.46	1.46	0.73
φ	1.0	1.0	1.0	1.0	1.0	0.90	1.0	1.0	1.0	0.90	1.0	1.10	0.71	0.71	1.10
L_t ft.	9	9	9	9	8	8	8	8	8	3.5	3.5	3.5	3.5	3.5	3.5
L_b in.	7	9	7	9	7	9	9	7	9	9	9	9	11	11	9
f major cps	-	300	295	301	325	171	338	165	133	192	200	210	720	Damped	395
Db major	-	127	119	118.5	117	113	119	107	103	112	115	113	116	Damped	122
Db overall	113	127.5	119	118.5	118	114	120	108	105	113	116	115	116.5	94	124
q water Btu/hr.	5200	9670	5610	7620	6130	6450	7790	4020	4140	6450	6740	6230	4610	3760	7140
E %	74	82	82	86	83	82	85	80	83	84	86	81	80	80	83
$(q/A)_{1\ in.}$	2,900	27,200	40,100	43,800	42,100	29,800	45,500	34,000	32,800	33,800	41,100	37,300	1,000	600	57,100
$(q/A)_{3\ in.}$	13,800	55,100	47,900	48,100	48,000	41,600	47,300	34,300	34,500	40,900	45,300	43,400	5,200	2,300	35,400
$(q/A)_{5\ in.}$	55,600	56,900	42,000	41,200	41,400	36,700	39,900	26,100	25,200	36,100	39,200	36,600	32,600	13,900	25,200
$(q/A)_{7\ in.}$	-	54,000	-	35,600	-	32,600	34,100	-	20,600	31,400	33,800	31,500	29,100	35,200	19,600
$(q/A)_{9\ in.}$	-	-	-	-	-	-	-	-	-	-	-	-	23,400	28,600	

RUN NO.	76	80	81	82	83	84	85	86	87	88	89	90	91	92	93
G lb/sec.ft^2	0.73	1.46	1.46	1.46	1.46	1.46	1.46	1.46	1.46	1.46	2.92	2.92	2.92	2.92	0.73
φ	1.10	0.90	1.0	0.90	1.0	1.10	1.20	0.90	1.0	1.10	1.0	0.90	0.90	1.0	1.0
L_t ft.	3.0	9	9	9	9	9	9	9	9	9	9	9	9	9	9
L_b in.	9	7	7	9	9	9	9	11	11	11	9	9	11	11	7
f major cps	450	Damped	Damped	Damped	Damped	Damped	Damped	Damped	Damped	Damped	Damped	Damped	Damped	Damped	Damped
Db major	127.5	Damped	Damped	Damped	Damped	Damped	Damped	Damped	Damped	Damped	Damped	Damped	Damped	Damped	Damped
Db overall	128	105	104	104	103	104	105	104	105	106	109	111	109	109	91
q water Btu/hr.	6970	4570	4670	6110	6430	6410	5640	7220	7480	6950	7650	6590	8210	9300	3840
E %	82	80	78	85	85	84	85	87	86	84	81	77	80	83	79
$(q/A)_{1\ in.}$	63,000	4,700	6,800	8,200	7,400	6,200	6,700	3,300	9,700	10,300	2,300	1,700	1,600	2,400	4,700
$(q/A)_{3\ in.}$	38,500	43,300	47,300	46,600	48,800	49,400	48,300	42,700	48,600	47,700	23,200	12,300	11,200	17,000	43,400
$(q/A)_{5\ in.}$	25,700	44,000	46,100	41,100	44,500	42,000	40,700	43,300	43,000	40,200	62,700	44,900	61,100	66,500	27,200
$(q/A)_{7\ in.}$	19,900	-	-	32,700	36,100	33,600	30,900	30,200	35,400	30,800	63,000	62,200	55,800	62,900	-
$(q/A)_{9\ in.}$	-	-	-	-	-	-	-	25,400	30,500	27,100	-	-	48,400	51,600	-

RUN NO.	94	95	97	100	101	102	103	104	110	111	112
G lb/sec.ft^2	0.73	0.73	1.46	1.46	1.46	0.73	0.73	2.92	0.73	1.46	2.92
φ	1.0	1.0	1.48	0.90	1.0	1.0	1.0	1.0	1.0	1.0	1.0
L_t ft.	9	9	9	9	9	9	9	9	9	9	9
L_b in.	9	11	9	9	9	9	11	9	9	9	9
f major cps	Damped	Damped	Damped	Damped	Damped	Damped	Damped	Damped	Damped	Damped	Damped
Db major	Damped	Damped	Damped	Damped	Damped	Damped	Damped	Damped	Damped	Damped	Damped
Db overall	92	94	105	104	105	91	92	110	91	103	111
q water Btu/hr.	4300	5110	2040	5590	6360	4140	5000	7500	4400	6500	7500
E %	82	84	70	81	83	81	82	80	81	84	80
$(q/A)_{1\ in.}$	5,600	8,300	1,500	1,300	2,700	3,800	2,000	1,300	4,300	6,200	1,900
$(q/A)_{3\ in.}$	41,500	40,000	1,700	28,700	45,400	40,900	44,100	16,600	40,800	49,300	21,900
$(q/A)_{5\ in.}$	25,900	25,200	6,200	47,500	47,600	26,200	25,700	55,400	26,400	43,500	63,100
$(q/A)_{7\ in.}$	19,100	18,800	32,300	35,400	36,500	19,600	19,200	65,000	18,500	36,400	62,800
$(q/A)_{9\ in.}$	-	15,900	-	-	-	-	15,000	-	-	-	-

APPENDIX B

DATA PROCESSING

The calculations for Run 11 are outlined below to illustrate the procedures used in processing the data. Original data for run 11:

Air flow rate = 5.66 SCFM

Propane flow rate = 0.238 SCFM

Inlet temperature = 70°F

Water flow rate = 5GPM

Inlet water temperature = 63.3°F

Net water temperature rise = 2.8°F

Pressure drop with combustion = 1.64 in. water

Pressure drop due to inlet tube and flame holder = 0.49 in. water

Burning length = 9 inches

Total tube length = 9 ft.

Flame holder blockage = 52 percent

Major frequency = 286 cycles/second

Sound level of major frequency = 116 decibels

Overall sound level = 117 decibels

For the measuring station 3 inches downstream from the flame holder the temperatures and thermocouple locations were as follows:

Temperature, °F	Radius, mils
196.0	587
149.5	741
105.5	917

Local Rates of Heat Transfer

Since the method of calculation is identical for all measuring stations, only the station at 3 inches downstream from the flame holder is treated in detail.

The surface temperatures are determined by extrapolating a straight line plot of temperature versus log r. From the graph in Figure 42A, the outside surface temperature t_o is 95.5°F and the inside surface temperature t_s is 236.0°F. Thus the average temperature of the wall is 165.7°F, at which temperature the thermal conductivity of 304 stainless steel is 9.23 BTU/hr. ft. °F.

The heat flux is calculated from equation (6).

$$(q/A)_s = \frac{k_{av}}{r_s} \frac{(t_s - t_o)}{\ln \frac{r_o}{r_s}} = \frac{9.23\ (236.0 - 95.5)}{\frac{0.485}{12} \times 2.303 \log \frac{0.968}{0.485}}$$

$$= 46{,}400 \text{ BTU/hr. ft.}^2$$

By a similar procedure, the rates of heat transfer are calculated at the other measuring stations. The results of the calculations are

L_b, in.	Flux, BTU/hr. ft.^{2}
1	43,100
3	46,400
5	39,900
7	34,300

These heat flux are plotted against length in Figure 42B. Since the heat flux represents the average rate over a one inch length of tube,

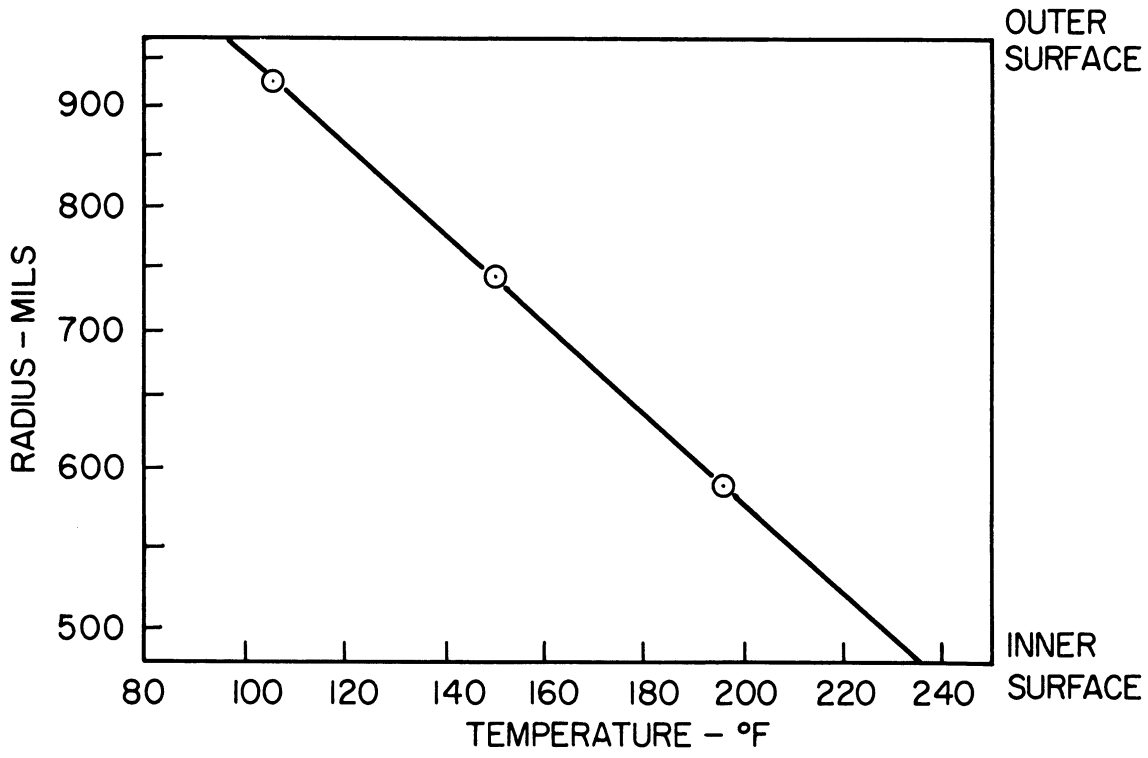

A) Temperature Profile in Tube Wall

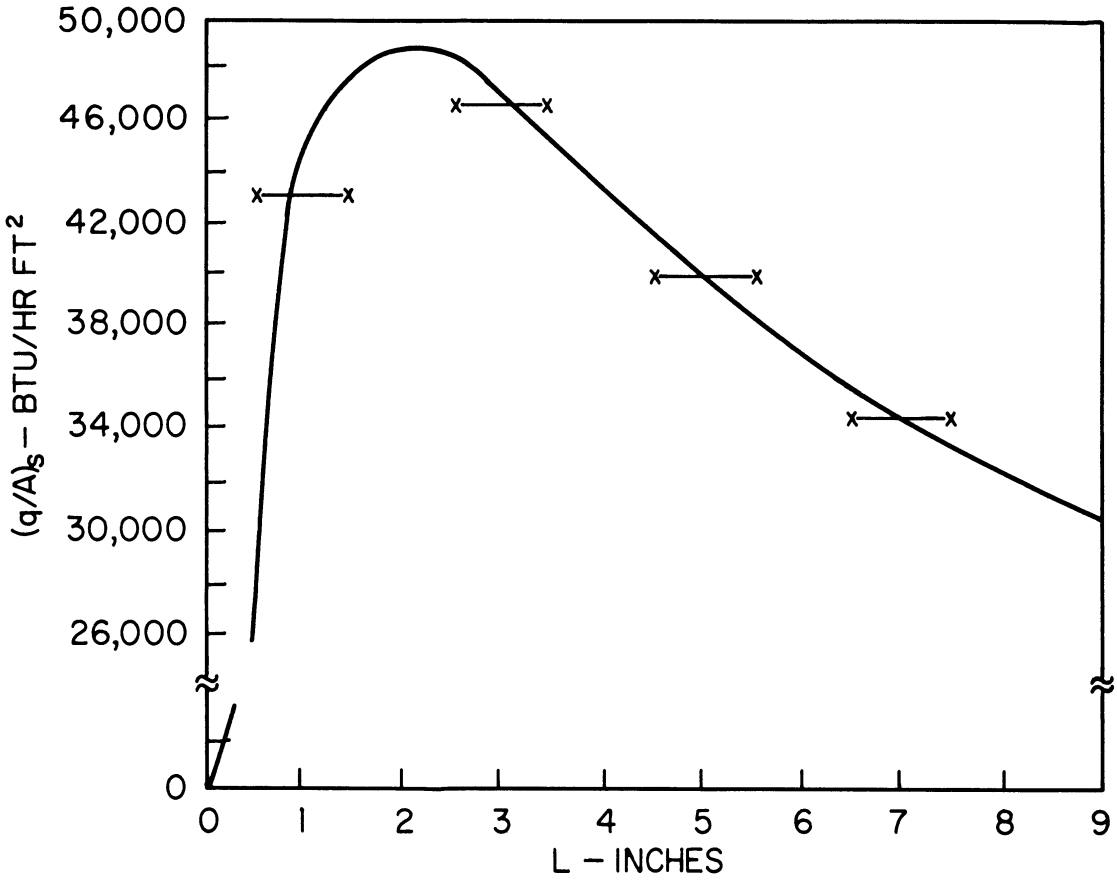

B) Heat Transfer Profile

Figure 42. Graphical Data for Run No. 11

the curve through the data intersects each flux line so as to leave equal areas above and below the line.

Total Heat Transfer

The total heat transferred through the wall can be determined from a water side heat balance and from graphical integration of the heat fluxes.

Graphical integration of Figures 42B gives:

$$q_t = \pi D_s \int_0^9 (q/A)_s \, dL = 7240 \text{ BTU/hr.}$$

The increase in the temperature of water flowing through the annulus is 2.9°F. Since 0.1°F is due to conduction from the room, the net rise in water temperature is 2.8°F. The flow rate of water is 300 gallons/hr. Applying a heat balance to the water side results in $q_t = W C_p \Delta t = 300 \times 8.34 \times 1.0 \times 2.8 = 7010$ BTU/hr.

The difference between the two methods is about 3.3 percent.

Fuel to Air Ratio

For a stoichiometric mixture of 97 percent propane and 3 percent propylene burning to completion, 23.74 mols of air are required for each mole of fuel. The theoretical fuel to air ratio for a stoichiometric mixture is

$$\frac{\text{Fuel}}{\text{Air}} = \frac{1.0}{23.74} = 0.0421$$

The actual fuel to air ratio for this run is

$$\frac{\text{Fuel}}{\text{Air}} = \frac{0.238}{5.66} = 0.0421$$

Dividing the actual fuel to air ratio by the fuel to air ratio for complete combustion of a stoichiometric mixture gives

$$\varphi = \frac{0.0421}{0.0421} = 1.0$$

Inlet Reynolds' Number

The total inlet flow rate is 5.90 SCFM, which is equivalent to W = 27.0 lbs/hr. The mass velocity is

$$G = \frac{W}{A} = \frac{27.0}{0.00513} = 5260 \text{ lbs/hr. ft.}^2$$

The bulk viscosity for the inlet mixture is 0.0425 lb/ft. hr., and the tube diameter is 0.97/12 foot. Subsituting into the expression for Reynolds' number gives

$$Re = \frac{DG}{\mu} = \frac{(0.97/12)(5260)}{0.0425} = 10{,}000$$

Combustion Efficiency

The combustion efficiency (percent of limiting reactant consumed) is calculated from equations (44) and (48).

$$E = \frac{Q_r^{(T_1)}}{Q_R^{(T_1)}} \times 100 = \frac{\overline{C}_{p2}\,(T_2 - T_1) + Q_t}{Q_R^{(T_1)}}$$

$$\frac{T_2}{T_1} = \frac{P_2}{P_1}\,\frac{\overline{M_2}}{\overline{M}_1}\,\frac{A_2}{A_1}\,\frac{g_c}{\rho_1 u_1^2}\left[P_1 - P_2\frac{A_2}{A_1} - P_D + \frac{\rho_1 u_1^2}{g_c}\right]$$

where subscripts 1 and 2 refer to conditions at the inlet and outlet, respectively.

The tube areas at the inlet and outlet measuring stations were essentially equal.

For the propane-propylene fuel, the heat of combustion is 879,000 BTU.lb. mol. at 70°F. The weight ratio of mixture to fuel in the inlet stream is 729.1 lbs. mixture/lb. mol. fuel. Hence, the maximum heat release due to chemical reaction is

$$Q_R^{(70°F)} = \frac{879000}{729.1} = 1205 \text{ BTU/lb. mixture}$$

By integration of heat fluxes, $q_t = 7240$ BTU/hr.

Thus

$$Q_t = \frac{q_t}{W} = \frac{7240}{27.0} = 266 \text{ BTU/lb.}$$

For the evaluation of T_2, the conditions at station 1 are readily calculated.

$$\bar{M}_1 = 29.5$$

$$\rho_1 u_1 = 1.475 \text{ lb}_m/\text{sec. ft.}^2$$

$$u_1 = 19.3 \text{ ft./sec.}$$

$$\frac{\rho_1 u_1^2}{g_c} = 0.884 \text{ lb}_f/\text{ft.}^2$$

In order to determine $\bar{M}_2$ and $\bar{C}_2$, the outlet composition is required. As a first trial, the efficiency is assumed to be 80 percent. Assuming oxidation is complete, the products of combustion are CO_2 and H_2O. The following table illustrates the calculation of $\bar{M}_2$ and $\bar{C}_{p2}$.

Basis: 1 lb. mol propane fuel

Products	N	x	$\bar{M}$	$\bar{M}X$	C_p(60-2540°F) BTU/ft^3 °F	C_p x
CO_2	2.4	0.094	44	4.14	0.0318	0.0030
H_2O	3.2	0.125	18	2.25	0.0260	0.0032
N_2	18.75	0.734	28	20.55	0.0199	0.0146
O_2	1.0	0.039	32	1.25	0.0199	0.0008
C_3H_8	0.20	0.008	44.1	0.35	0.080	0.0006
	25.55	1.000		28.54		0.0222

The heat capacity data from Perry[47] represent the average values between 60°F and an assumed outlet temperature of 2540°F. The units are BTU/ft^3 °F, with volume measured at 60°F. Converting to mass units, the mean heat capacity of the mixture is 0.295 BTU/lb. °F.

The total pressure drop between plenum chamber and tube exit during combustion is 1.64 in. water. From cold flow measurement with air, the drag of the flame holder and inlet piping is found to be 0.49 in. water. The drag due to the burning length during combustion, however, is unknown. To estimate this term the following procedure is used. From the heat transfer profile curve, the rates of heat transfer are read at each one inch increment. The non-luminous radiant contributions to total rates of heat transfer are estimated from the procedures and data presented in McAdams[42].

$$(q/A)_r = 0.173\ \epsilon_s' \left[\epsilon_G \left(\frac{T_G}{100}\right)^4 - \alpha_G \left(\frac{T_S}{100}\right)^4 \right]$$

Since gas temperature is required to evaluate radiation, a temperature distribution is assumed.

The convective rate of heat transfer is found by subtracting the radiant heat transfer from the total rate. By dividing the convective rates by the appropriate c_x/c_{12} from Figure 37, the effect of the baffle on heat transfer is eliminated. The results correspond to the convective rates for fully developed pipe flow. The equation of Zellnik[84] for heat transfer from high temperature gases can now be applied

$$Nu = \frac{hD}{k} = \frac{(q/A)_C\ D}{(T_G - T_S)k} = 0.023\ Re^{0.8}\ Pr^{1/3} \left(\frac{T_G}{T_S}\right)^{0.33}$$

where properties are evaluated at the surface temperature. The local surface temperatures are read from Figure 35, using the actual experimental rates of heat transfer. The above equation can now be solved for local gas temperatures. If the assumed temperature distribution for radiant heat transfer is in error, the procedure is repeated.

An approximate temperature profile is now available. Application of the continuity and ideal gas equations permits calculation of the velocity profile from the temperature distribution. An average velocity is assigned to each one inch increment. The pressure drop corresponding to each average velocity is read from the cold flow data of Figure 43. The sum of the pressure drops over the increments gives the total drag of the walls due to burning.

As an illustration of the procedure, the calculations are outlined for the measuring station 5 inches from the flame holder.

To determine radiant contribution, assume E = 80 percent and $T_{(5\ in.)} = 2980°R$. Since the tube approximates an infinite cylinder the mean beam length $L' = 0.9\ D = 0.0728$ ft. The partial pressures are 0.094 atm for CO_2 ahd 0.125 atm for H_2O. Using Figures 4-13 through 4-17 in McAdams[42], $\epsilon_G = 0.016$ and $\alpha_G = 0.03$. The surface emissivity is estimated as 0.80 from Perry[47]. The surface temperature corresponding to the total heat transfer rate of 39,900 BTU/hr. ft.^{2} is read as 210°F from Figure 35. Hence, the radiant heat transfer is

$$(q/A)_r = 0.173\ \frac{0.80 + 1.0}{2}\left[0.016\left(\frac{2940}{100}\right)^4 - 0.03\left(\frac{670}{100}\right)^4\right]$$

$$= 1900\ \text{BTU/hr ft.}^2$$

The convective heat transfer, then, is 39,900 - 1900 = 38,000 BTU/hr. ft.^{2}.

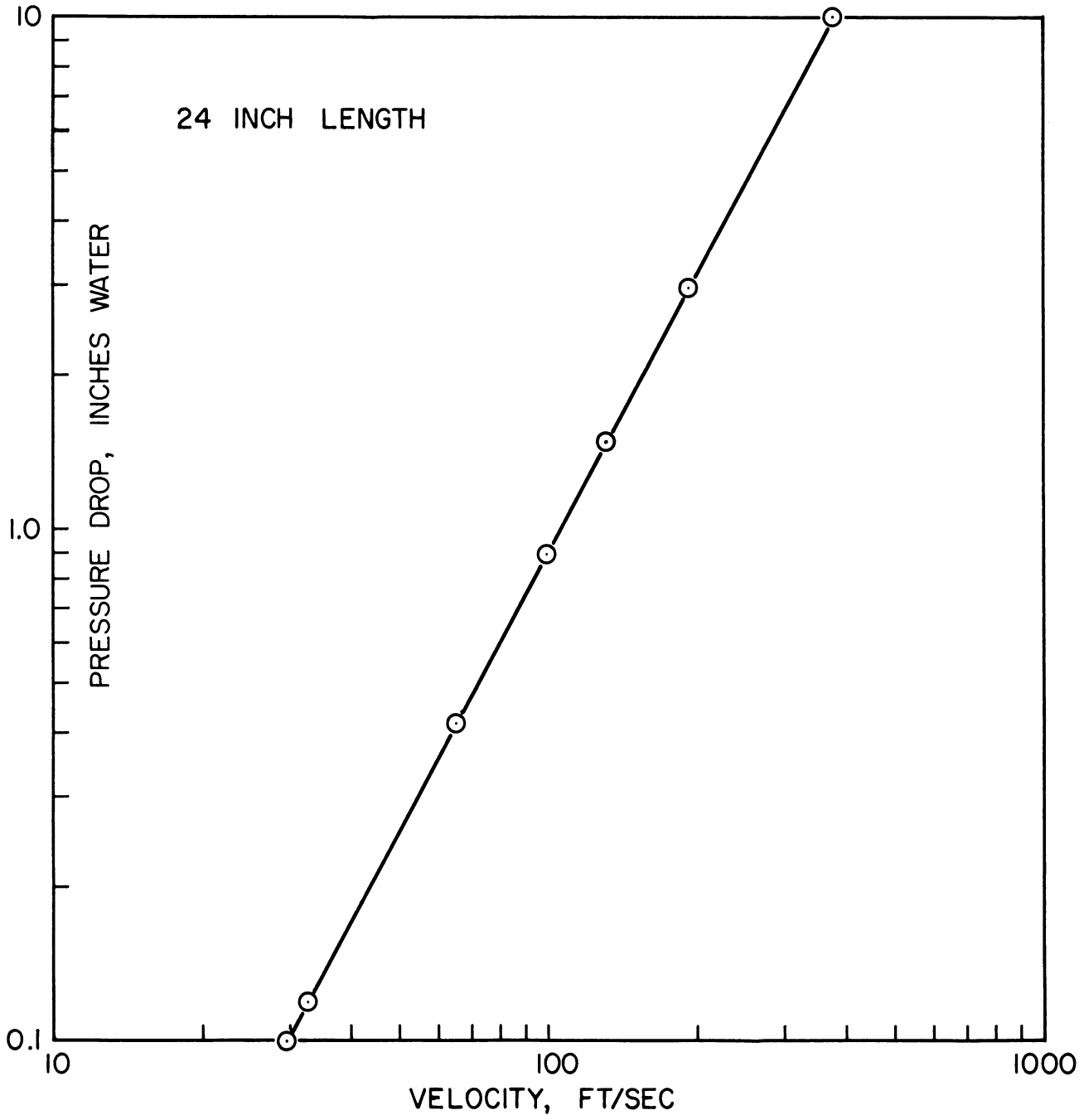

Figure 43. Pressure Drop Due to Drag of Test Object Walls.

From Figure 37, the value of c_x/c_{12} at 5 inches is 1.50. The convective heat transfer for fully developed pipe flow then, is 38,000/1.50 = 25,300 BTU/hr. ft.^{2}. The properties of the mixture at the local surface temperature are estimated from reference (21). The results are:

$\mu_s = 1.30 \times 10^{-5}$ lb/ft.sec., $k_s = 1.74 \times 10^{-2}$ BTU/hr. ft. °F, and Pr = 0.705. Substituting in equation (1)

$$\frac{25{,}300\ (0.0809)}{(T_G - 670)(0.0174)} = 0.023\left(\frac{0.0809 \times 1.475}{1.30 \times 10^{-5}}\right)^{0.8} (0.705)^{1/3} \left(\frac{T_G}{670}\right)^{0.33}$$

Solving by trial and error, $T_G = 2980°R$. The velocity is given by

$$u_2 = u_1 \frac{\rho_1}{\rho_2} = 19.3 \times \frac{T_2}{T_1} = 19.3 \times \frac{2980}{530} = 108.7 \text{ ft./sec.}$$

The average velocity between 4 and 5 inches is 105.8 ft/sec. Referring to Figure 43, the pressure drop due to wall drag over this increment is 0.042 in. H_2O.

The above procedure is applied to one inch increments over the burning length of 9 inches. The sum of the pressure drop increments is found to be 0.33 in. H_2O. The total pressure drop due to drag of flame holder and tube walls is 0.33 + 0.49 = 0.82 in. water.

All data required for a first estimate of T_2 are now available. Substituting into equations (44) and (48),

$$T_2 = 530 \frac{28.5}{29.5} \cdot \frac{1}{0.884} \left[5.2\ (1.64 - 0.82) + 0.884\right] = 2980°F$$

$$E = \frac{0.295\ (2980 - 530) + 266}{1205} \times 100 = 82\%$$

In estimating terms for the efficiency calculation, the efficiency and outlet temperature were assumed as 80 percent and 3000°R,

respectively. Since the calculated and assumed values differ only slightly, the calculations need not be repeated.

APPENDIX C

DERIVATIONS

Heat Flux Derivation

For the conduction of heat in an isotropic solid, the following general equation applies

$$\rho C_p \frac{\partial T}{\partial t} = \text{div } (k \text{ grad. } T) \tag{15}$$

or, expressed in cylindrical coordinates,

$$\rho C_p \frac{\partial T}{\partial t} = \frac{1}{r}\left[\frac{\partial}{\partial r}(kr \frac{\partial T}{\partial r}) + \frac{\partial}{\partial \theta}\left(\frac{k}{r} \frac{\partial T}{\partial \theta}\right) + \frac{\partial}{\partial x}(kr \frac{\partial T}{\partial x})\right] \tag{16}$$

For the geometry used in this experiment, the following assumptions can be made.

$$\frac{\partial T}{\partial t} = 0, \qquad \frac{\partial T}{\partial x} = 0, \text{ and } \qquad \frac{\partial T}{\partial \theta} = 0$$

By also assuming an isotropic solid and a constant, average thermal conductivity, a reduced equation is obtained

$$\frac{\partial^2 T}{\partial r^2} + \frac{1}{r} \frac{\partial T}{\partial r} = 0 \tag{17}$$

The general solution,

$$T = b_1 \ln r + b_2 \tag{18}$$

can be expressed in terms of known temperatures at any two points (T_1, r_1) and (T_2, r_2) as

$$\frac{T - T_1}{T_2 - T_1} = \frac{\ln \frac{r}{r_1}}{\ln \frac{r_2}{r_1}} \tag{19}$$

The flux at any point in the wall is given by

$$\frac{q}{A} = k_{av}\left(\frac{dT}{dr}\right) = -\frac{k_{av}}{r}\ \frac{T_2 - T_1}{\ln (r_2/r_1)} \tag{20}$$

The flux at the inside surface is most easily evaluated from the data using extrapolated inside and outside surface temperatures. The final expression becomes

$$(q/A)_S = \frac{k_{av}}{r_S}\ \frac{T_S - T_o}{\ln (r_o/r_S)} \tag{21}$$

Resonant Frequency

The following derivation for the resonant frequency of a gas column is adapted from Jost[26].

Consider a gas column in a doubly open tube with an interface separating regions of hot and cold gases.

The one-dimensional wave equations describing the motion in the two gases are

$$\frac{\partial^2 y_1}{\partial t^2} = a_1^2 \frac{\partial^2 y_1}{\partial x^2}\ ,\ \frac{\partial^2 y_2}{\partial t^2} = a_2^2 \frac{\partial^2 y_2}{\partial x^2} \tag{22}$$

in which the subscripts 1 and 2 refer to the unburned and burned gases respectively, and y is the particle displacement in the x direction.

If y varies as $\cos (2\pi ft)$, the above equations become

$$\frac{\partial^2 y_1}{\partial x^2} + \frac{4\pi^2 f^2 y_1}{a_1^2} = 0,\quad \frac{\partial^2 y_2}{\partial x^2} + \frac{4\pi^2 f^2 y_2}{a_2^2} = 0 \tag{23}$$

The solutions for these equations are

$$y_1 = \left(C_1 \cos \frac{2\pi fx}{a_1} + B_1 \sin \frac{2\pi fx}{a_1}\right) \cos (2\pi ft) \qquad (24)$$

$$y_2 = \left(C_2 \cos \frac{2\pi f(L-x)}{a_2} + B_2 \sin \frac{2\pi f(L-x)}{a_2}\right) \cos (2\pi ft) \qquad (25)$$

where (L-x) is the distance in the x direction for the burned gas.

For a doubly open pipe, a velocity antinode exists at both ends giving the boundary conditions

$$\frac{\partial y_1}{\partial x} = 0 \text{ when } x = 0, \qquad \frac{\partial y_2}{\partial x} = 0 \text{ when } x = L$$

Applying the boundary conditions, $B_1 = B_2 = 0$

The wave equations now become

$$y_1 = C_1 \cos \frac{2\pi fx}{a_1} \cos (2\pi ft) \qquad (26)$$

$$y_2 = C_2 \cos \frac{2\pi f(L-X)}{a_2} \cos (2\pi ft) \qquad (27)$$

At the intersection of these two waves, displacement components and intensity components are assumed to be equal for both media. This yields

$$y_1 = y_2$$

$$p_1\gamma_1 \frac{\partial y_1}{\partial x} = p_2\gamma_2 \frac{\partial y_2}{\partial x} \quad \text{(see reference 26)}$$

Applying these conditions to the two wave equations gives

$$C_1 \cos \frac{2\pi fx}{a_1} = C_2 \cos \frac{2\pi f(L-x)}{a_2} \qquad (28)$$

$$-C_1 \frac{p_1\gamma_1}{a_1} \sin \frac{2\pi fx}{a_1} = C_2 \frac{p_2\gamma_2}{a_2} \sin \frac{2\pi f(L-x)}{a_2} \qquad (29)$$

The difference between p_1 and p_2 is very small in most flames and can be neglected. Dividing the above equations yields the equation for vibration frequency

$$-a_1\gamma_1 \tan \frac{2\pi f(L-x)}{a_2} = a_2\gamma_2 \tan\frac{2\pi fx}{a_1} \qquad (30)$$

Pressure Amplitude

In the derivation of tube frequency, it was shown that the theoretical particle movement due to standing sound waves in a tube is given by

1) $$y = C_1 \cos \frac{2\pi fx}{a_1} \cos 2\pi ft \qquad (31)$$

The particle velocity, v, and the maximum particle velocity amplitude, $|v|$, can then be expressed as

2) $$v = \frac{\partial y}{\partial t} = 2\pi f\, C_1 \cos \frac{2\pi fx}{a_1} \sin 2\pi ft \qquad (32)$$

3) $$|v| = 2\pi f\, C_1 \cos \frac{2\pi fx}{a_1} \qquad (33)$$

The pressure amplitude of the wave at any point, $\overline{P}$, is found from thermodynamic considerations[44]

4) $$\overline{P} = P - P_o = P_o\gamma \frac{\partial y}{\partial x} \qquad (34)$$

Substituting for $\partial y/\partial x$ gives

5) $$\overline{P} = P_o\gamma \frac{2\pi fC_1}{a_1} \sin \frac{2\pi fx}{a_1} \cos 2\pi ft \qquad (35)$$

and the maximum pressure amplitude is

6) $$|\overline{P}| = P_o\gamma \frac{2\pi fC_1}{a_1} \sin \frac{2\pi fx}{a_1} \qquad (36)$$

Dividing the expressions for maximum pressure and maximum velocity amplitude results in

$$\frac{|\bar{P}|}{|v|} = \frac{P_o\gamma}{a_1} \frac{\sin(2\pi fx/a_1)}{\cos(2\pi fx/a_1)} = \frac{P_o\gamma}{a_1} \tan\frac{2\pi fx}{a_1} \qquad (37)$$

To explain the unusual rates of heat transfer in Runs 75 and 76, it was postulated that the maximum pressure amplitude was sufficient to produce a maximum particle velocity which was equal to or exceeded the flow velocity past the flame holder.

The calculations are summarized below.

$$|P| = |v| \frac{P_o\gamma}{a_1} \tan \frac{2\pi fx}{a_1} \qquad (38)$$

Flow rate = 2.95 SCFM

Flow area at flame holder = 0.00246 ft.^{2}

$\therefore |v| = \frac{2.95}{60 \times 0.00246} = 20.0$ ft/sec.

a_1 = 1120 ft/sec. (at 70°F)

P_o = 14.7 psia = 2115 lbs/ft.^{2}

γ = 1.4

For Run 75:

L_t = 36 in, L_b = 9 in.

$x = L_t - L_b$ = 27 in. = 2.25 ft.

f = 450 cycles /sec.

$$\therefore |P| = 20.0 \frac{2115\ (1.4)}{1120} \tan \frac{2\pi\ (450)(2.25)}{1120}$$

$$= 36.4 \text{ lb/ft}^2 = 159 \text{ decibels}$$

For Run 76:

L_t = 42 in, L_b = 9 in

x = 33 in. = 2.75 ft.

f = 395 cycles/sec.

$$\therefore |P| = 20.0 \frac{2115\ (1.4)}{1120} \tan \frac{2\pi\ (395)(2.75)}{1120}$$

$$= 10.2 \text{ lb/ft}^2 = 148 \text{ decibels}$$

Combustion Efficiency

The general mass, momentum, and energy relations can be reduced by reasonable assumptions to the following one-dimensional form

Mass: $$\rho_1 u_1 A_1 = \rho_2 u_2 A_2 \tag{39}$$

Momentum: $$\left(P_1 + \frac{\rho_1 u_1^2}{g_c}\right) A_1 - F_D = \left(\frac{P_2 + \rho_2 u_2^2}{g_c}\right) A_2 \tag{40}$$

Energy: $$\bar{C}_{p_1} (T_1 - T_o) + \frac{u_1^2}{2g_c} + Q_r^{(T_o)} - Q_t = \bar{C}_{p_2}(T_2 - T_o) + \frac{u_2^2}{2g_c} \tag{41}$$

A detailed derivation of these equations is presented by Adamson[76].

The assumptions made in deriving these equations are

1) The flow is steady
2) Thermal diffusion is neglected
3) μ' is negligible compared to μ
4) C_{p_s} = constant
5) There are no gradients in velocity, temperature, or pressure at either stations 1 or 2.

Assumptions 1, 2, and 3 are quite valid. By evaluating C_{p_s} at a mean temperature between T_o and T_1 or T_2, the error introduced through assumption 4 is minimized. In the experiments, stations 1 and 2 are located upstream of the flame-holder and at the exit of the tube, respectively. Upstream at the flame holder, conditions are uniform, but gradients do exist at the tube exit. Since reaction rates are decreasing at the exit, the gradients are not severe. The equations were also solved without assumption 5. Calculations indicated that the results of the more rigorous procedure differed negligibly from the approximation.

At atmospheric pressure and high temperature, the ideal gas law can be applied in the form

$$P = \frac{\rho R_o T}{\bar{M}} \qquad \text{or} \qquad T = \frac{\bar{P}\bar{M}}{\rho R_o}$$

From this it follows that

$$\frac{T_2}{T_1} = \frac{P_2}{P_1} \frac{\rho_1}{\rho_2} \frac{\bar{M}_2}{\bar{M}_1} \tag{42}$$

The mass and momentum equations can be combined to give

$$\frac{\rho_1}{\rho_2} = \frac{u_2 A_2}{u_1 A_1} = \frac{g_c A_2}{\rho_1 u_1^2 A_1} \left[P_1 - P_2 \frac{A_2}{A_1} - \frac{F_D}{A_1} + \frac{\rho_1 u_1^2}{g_c} \right] \tag{43}$$

Substituting in the expression for temperature ratio gives

$$\frac{T_2}{T_1} = \frac{P_2}{P_1} \frac{\bar{M}_2}{\bar{M}_1} \frac{g_c}{\rho_1 u_1^2} \frac{A_2}{A_1} \left[P_1 - P_2 \frac{A_2}{A_1} - \frac{F_D}{A_1} + \frac{\rho_1 u_1^2}{g_c} \right] \tag{44}$$

The energy equation can be solved for the heat released due to chemical reaction:

$$Q_r^{(T_o)} = \bar{C}_{p_2} (T_2 - T_o) - \bar{C}_{p_1} (T_1 - T_o) + \frac{u_2^2}{2g_c} - \frac{u_1^2}{2g_c} + Q_t \tag{45}$$

In the experiments, T_1 was maintained at about 70°F. The reference temperature, T_o, is then conveniently chosen as 70°F. The kinetic energy terms are also much smaller than the exit sensible heat and heat transfer terms. The above expression can then be reduced with negligible error to

$$Q_r^{(T_o)} = \bar{C}_{p_2} (T_2 - T_o) + Q_t \tag{46}$$

Substituting for T_2 yields

(47)

$$Q_r^{(T_o)} = \bar{C}_{p_2}\left[\left(T_1 \frac{P_2}{P_1} \frac{M_2}{M_1} \frac{g_c}{\rho_1 u_1^2} \frac{A_2}{A_1}\right)\left(P_1 - P_2 \frac{A_2}{A_1} - \frac{F_D}{A_1} \frac{\rho_1 u_1^2}{g_c}\right) - T_o\right] + Q_t$$

The combustion efficiency is defined as the ratio of the heat released by chemical reaction to the heat which would be released if combustion were complete.

$$E = \frac{Q_r^{(T_o)}}{Q_R^{(T_o)}} = \frac{\bar{C}_{p_2}(T_2 - T_o) + Q_t}{Q_R^{(T_o)}} \qquad (48)$$

Effect of Thermocouple Holes

The effect of the thermocouple holes on the heat flux through the isolated sector can be estimated from conformal mapping techniques. The approximate conditions of the problem are

1) $T = T_S$ at $r = 485$ mils

2) $T = T_o$ at $r = 970$ mils

3) $\frac{\partial T}{\partial L} = 0$ at $L = \pm \frac{1}{2}$ inch

4) $\frac{\partial T}{\partial \theta} = 0$ at $\theta = \pm \frac{\pi}{6}$ radians

5) 42 mil diameter anisotropic holes extending to radial depths of 570, 750, and 920 mils

The mapping procedure is illustrated in Figure 44. A longitudinal hole at a radius of 580 mils will have the greatest effect on the heat flux. The middle and upper holes will be neglected in the analysis. The following summary of the derivation has been adapted from Churchill[9].

Under steady state conditions, the heat conduction equation in cylindrical coordinates is

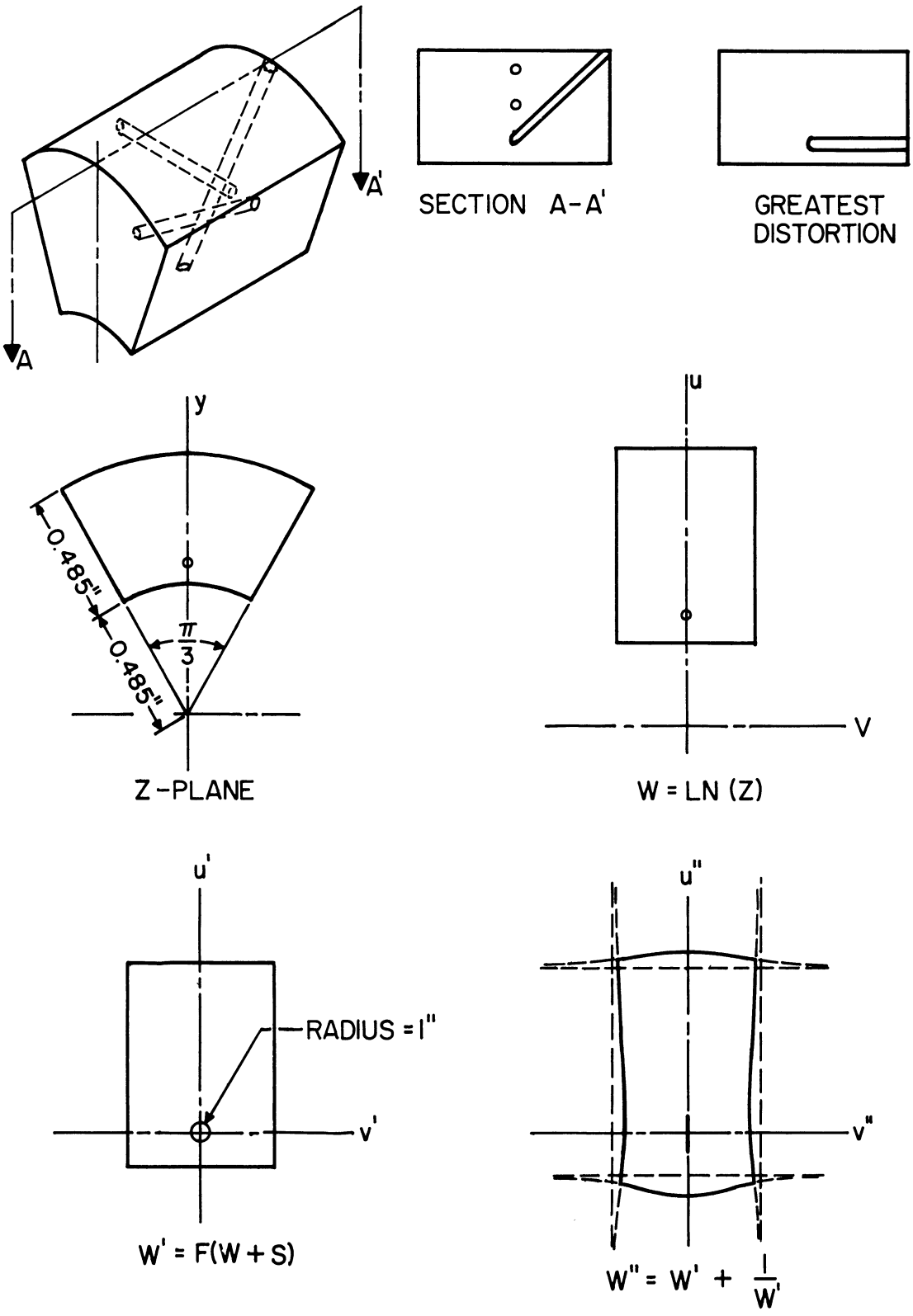

Figure 44. Illustration of Conformal Mapping Procedure.

$$\frac{\partial^2 T}{\partial r^2} + \frac{1}{r}\frac{\partial^2 T}{\partial \theta^2} + \frac{\partial^2 T}{\partial x^2} = 0 \qquad (49)$$

The conformal transformation W = ln Z transforms the above equation to

$$\frac{\partial^2 T}{\partial u^2} + \frac{\partial^2 T}{\partial V^2} + \frac{\partial^2 T}{\partial x^2} = 0 \qquad (50)$$

where u = ln r and V = θ.

This transformation converts the annular sector into a rectangular box. Assuming longitudinal conduction is negligible, the problem is reduced to two dimensions.

Application of the transformation W' = F(W + S) results in an expansion of every point in the W plane by the factor F, followed by a horizontal translation through the distance S. With F = 13.45 and S = 6.35, the hole is enlarged to unit radius and is centered at the origin.

The conformal transformation

$$W'' = W' + \frac{1}{W'}$$

collapses the unit circle into the u" axis from u" = -2 to u" = +2, and changes the boundary of the rectangular region into the approximately-rectangular region shown in Figure 44. A dotted image of the W' plane is superimposed for comparison. The curvature of the W" plane is exaggerated for purposes of illustration.

If the region in the W" plane is approximated by a rectangle with the same average coordinates, the solution for the maximum flux is

$$q'' = \frac{2k\, V_1'' \,(T_S - T_o)}{u_S'' - u_o''} \qquad (51)$$

where u_S'', u_o'', and V_1'' are the average coordinates. A similar solution can be formulated for the W' plane under the assumption that no hole is present. In this case, the flux becomes

$$q' = \frac{2k\, V_1' \,(T_S - T_o)}{u_S' - u_o'} \tag{52}$$

Dividing the heat flux equations give

$$\frac{q''}{q'} = \frac{q \text{ holes}}{q \text{ no holes}} = \frac{V''}{V'} \quad \frac{(u_S' - u_o')}{(u_S'' - u_o'')} \tag{53}$$

The relation between points in the various planes are

$$u' = F\,(\ln r + S)$$

$$V' = F\theta$$

$$u'' = u'\left(1 + \frac{1}{u'^2 + V'^2}\right)$$

$$V'' = V'\left(1 - \frac{1}{u'^2 + V'^2}\right)$$

Applying these relationships to the coordinates of important points gives the following table

θ	r	u'	V'	u"	V"
0	485	-2.29	0	-2.73	0
0	970	7.13	0	7.27	0
$\pi/6$	485	-2.29	7.04	-2.33	6.91
$\pi/6$	570	0	7.04	0	6.89
$\pi/6$	970	7.13	7.04	7.19	6.96

The coordinates of the approximate rectangle in the W" plane will be taken at the average of the maximum and minimum values in the above table. Thus, the average coordinates are $u_S'' = -2.53$, $u_o'' = 7.24$,

and $V_1'' = 6.93$. Substituting these values into the heat flux expression results in

$$\frac{q \text{ holes}}{q \text{ no holes}} = \frac{6.93}{7.04} \frac{(-2.29 - 7.13)}{(-2.53 - 7.24)} = 0.95$$

Hence the maximum reduction in heat flux is 5 percent when the holes are filled with perfect insulation. Since the deepest thermocouple slopes upward and the thermocouple assembly is not a perfect insulator, the actual reduction in flux should be considerably less than the maximum of 5 percent.

APPENDIX D

PROPERTIES OF MATERIALS AND CALIBRATIONS

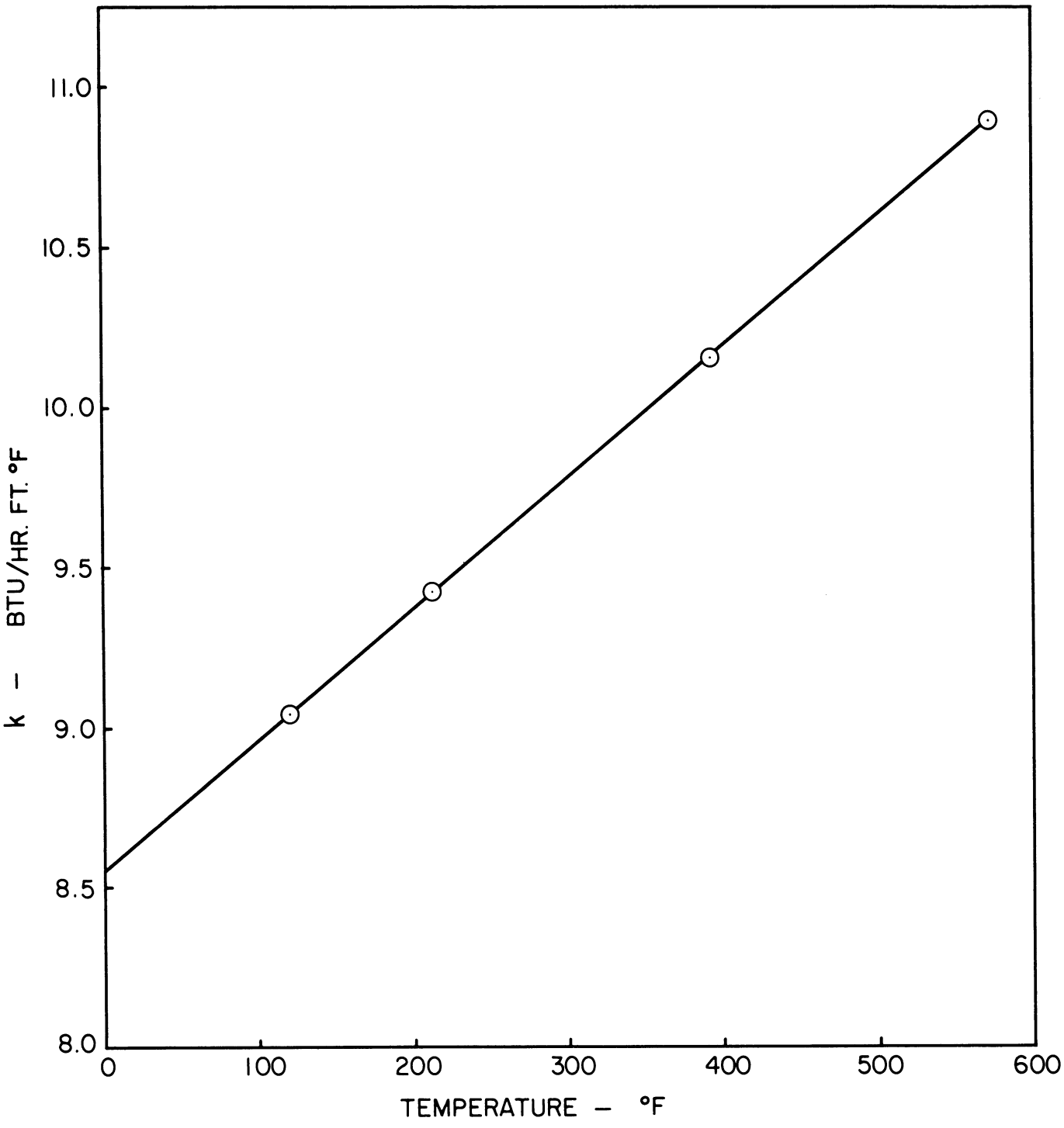

Figure 45. Thermal Conductivity of Type 304 Stainless Steel.

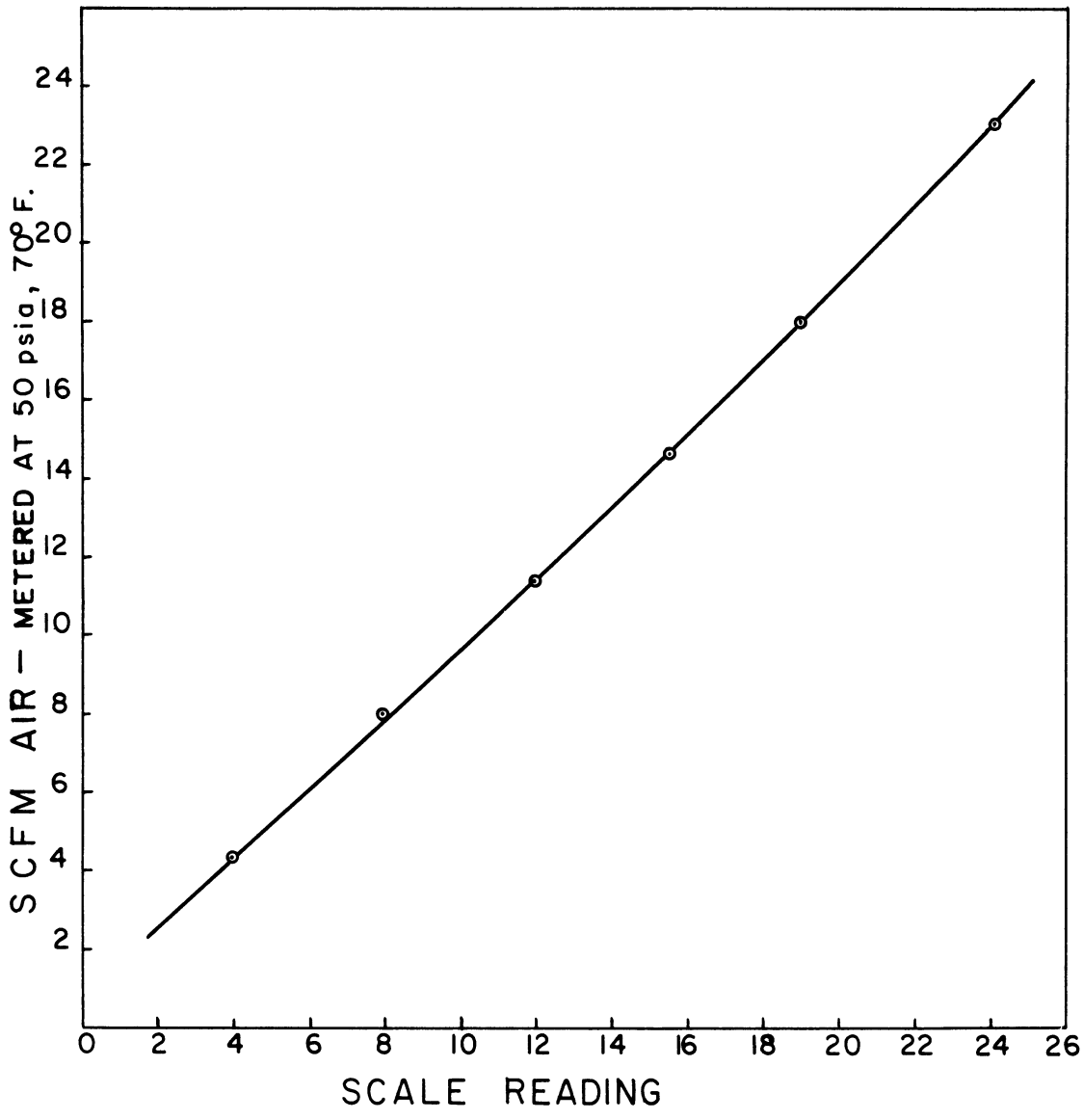

Figure 46. Calibration Curve for Low Flow Range Air Rotameter.

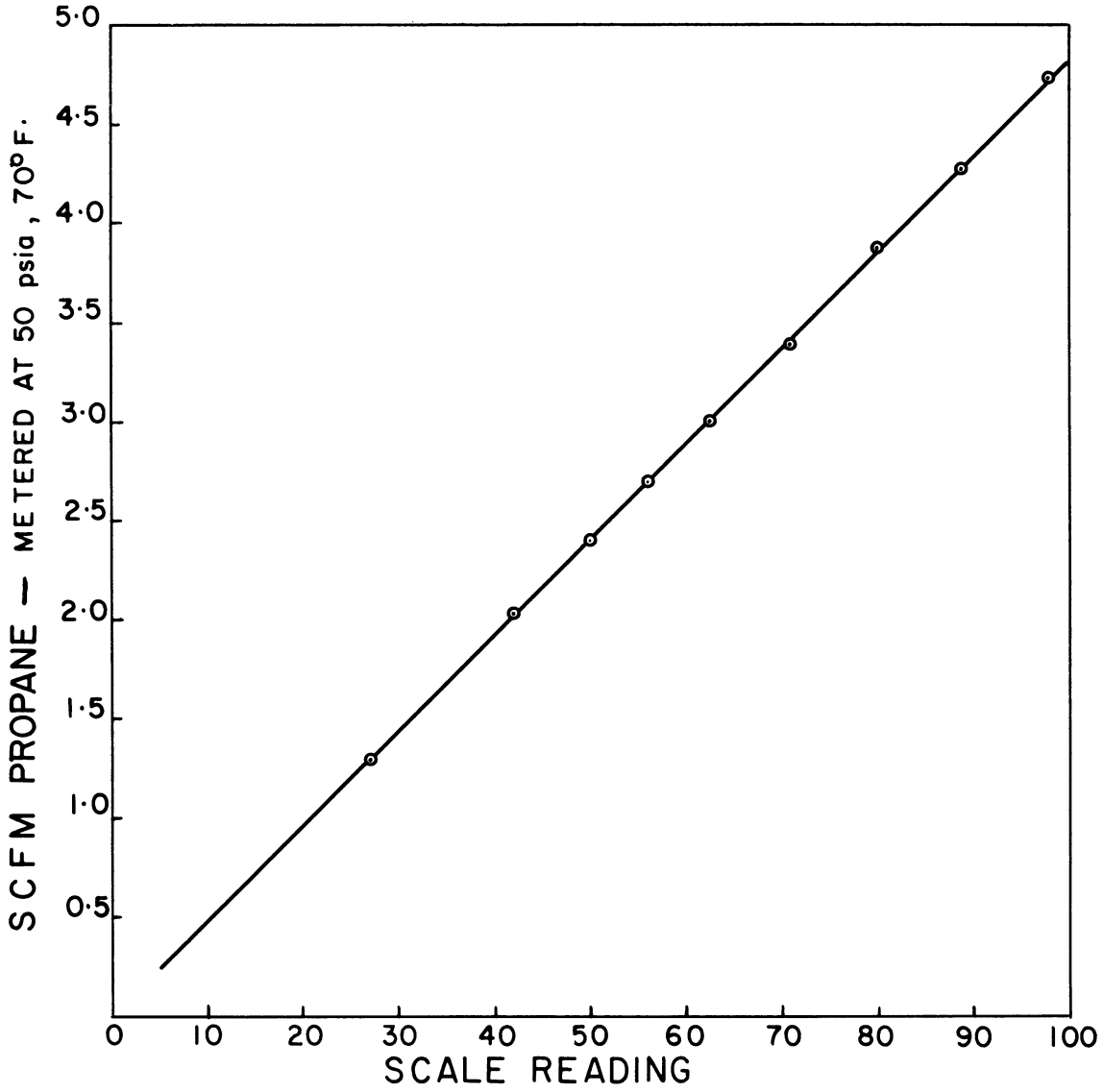

Figure 47. Calibration Curve for High Flow Range Propane Rotameter.

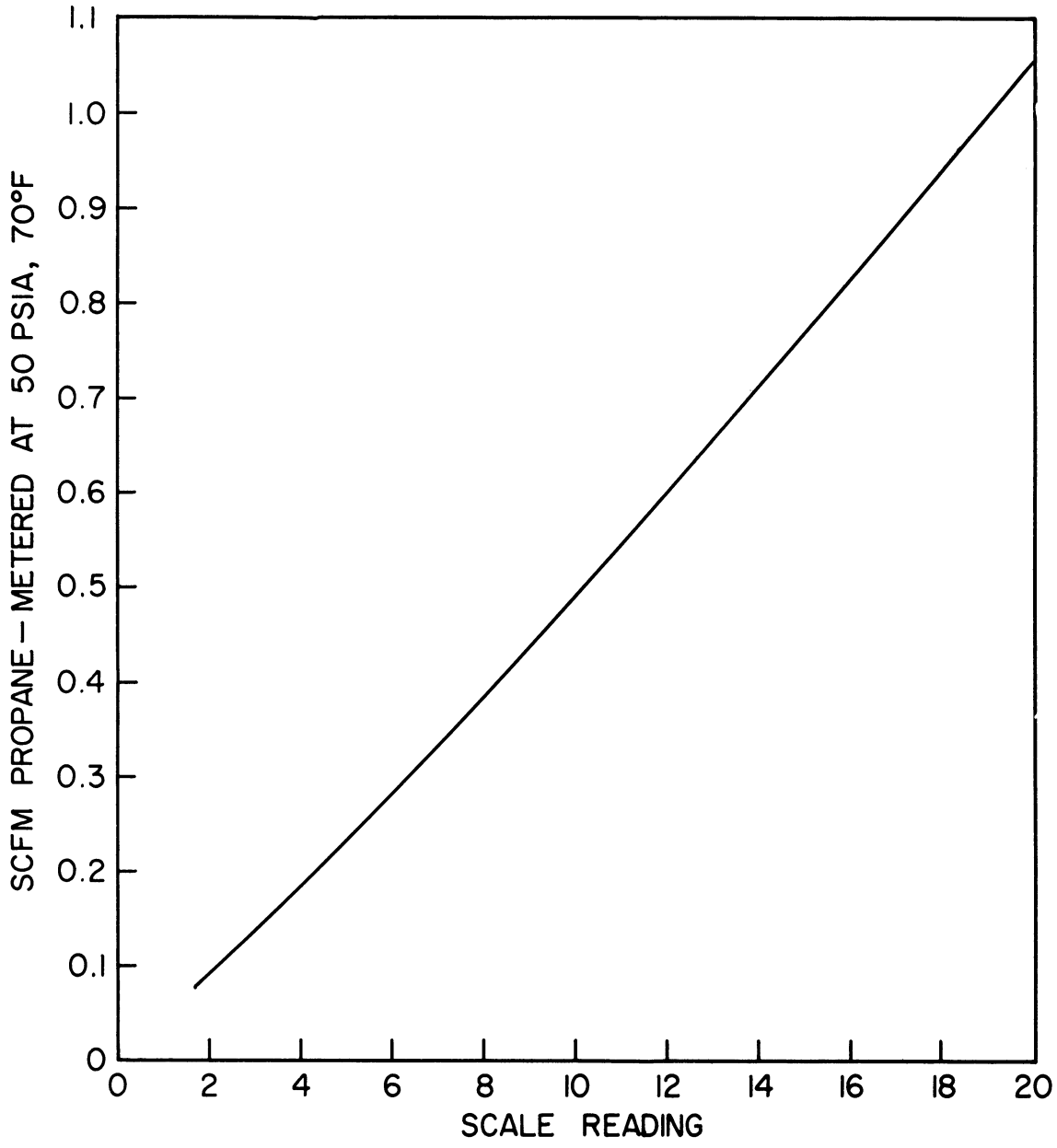

Figure 48. Calibration Curve for Low Flow Range Propane Rotameter.

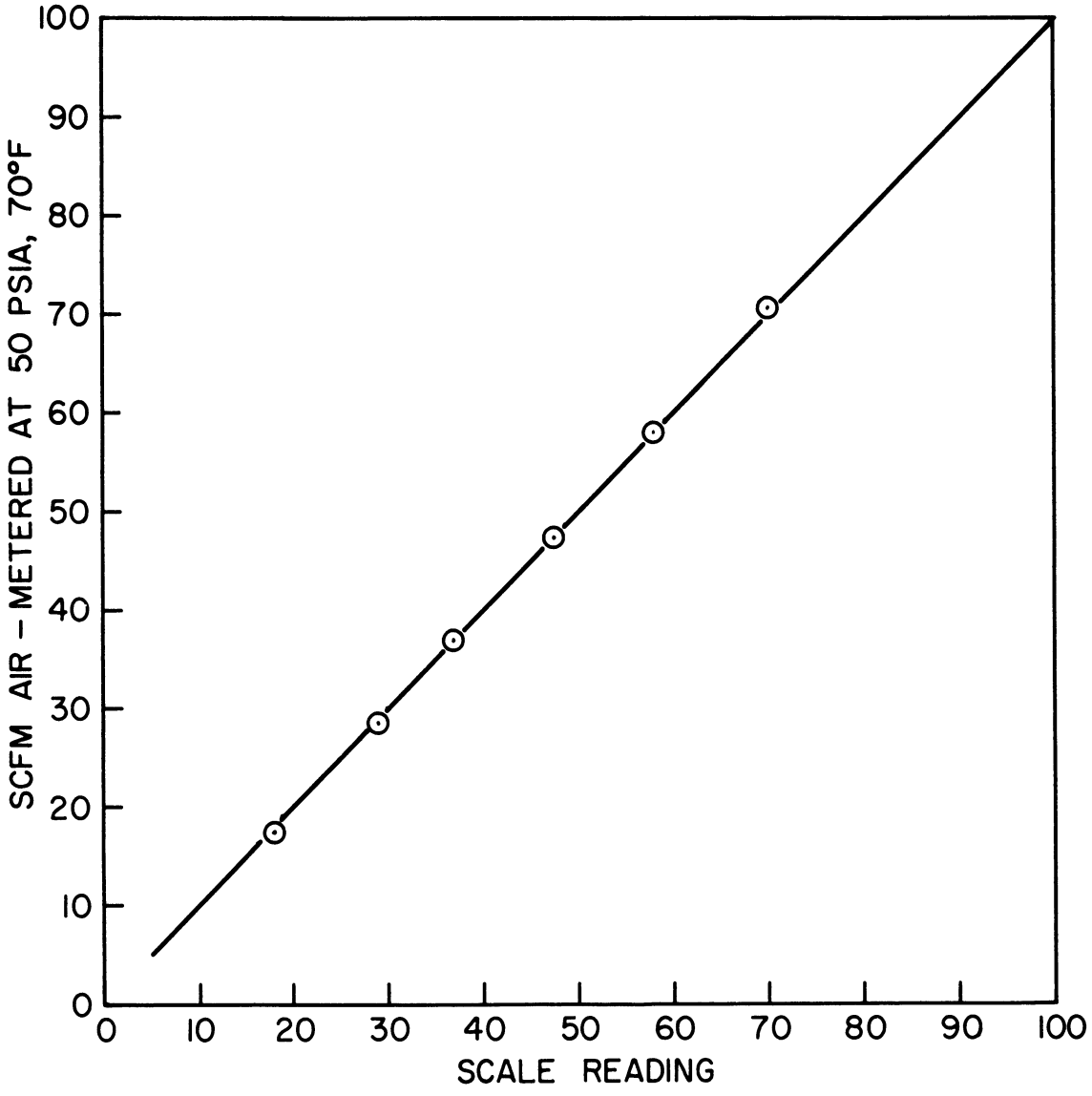

Figure 49. Calibration Curve for High Flow Range Air Rotameter.

APPENDIX E

SOURCES OF EQUIPMENT AND MATERIALS

Item	Source (Company)	Type
Supply Systems:		
Propane	Gallup-Silkworth Co.	Commercial
Air	Building Service System	95 psig
Calcium Chloride	Mallinkrodt Chemical Co.	4 mesh dessicant quality
Pressure Regulators	Moore Products Co.	42-50, 42-100
Rotameters	Fischer and Porter Co.	Figure 735
Thermometers	Consolidated Ashcroft Hancock Co.	Liquid
Pressure Gauges	Champion Gauge Co.	Bourdon
Rupture Disc.	Frangible Discs, Inc.	Union
Heat Transfer Test Unit:		
Stainless steel tube	Babcock-Wilcox Co.	304
Special thermocouples	Aero Research	Chromel-alumel, 36 gage, M_gO insulation
Thermocouple wire	Thermo-Electric Co.	Chromel-alumel, 16 gage; Copper-constantan, 24 gage.
Silicone resin	Dow-Corning Co.	Type 994
Rotary thermocouple selector switch	Minneapolis-Honeywell Regulator Co.	#911A1A-36
Precision potentiometer	Leeds and Northrup Co.	Portable type 8662
Manometer	Meriam Instrument Co.	U type

BIBLIOGRAPHY

1. Avery, W. H., and R. W. Hart, Ind. Eng. Chem. 45, 1634 (1953)

2. Baines, W. D., and E. G. Peterson, Trans. A.S.M.E. 73, 467 (1951)

3. Barrere, M., and A. Mestre, "Selected Combustion Problems," (Butterworth, London, 1954) p. 426.

4. Berman, Kurt, and S. H. Cheney, Jr., J. Am. Rocket Soc. 23 89 (1953).

5. Blackshear, P. L. Jr., Sixth Symposium (International) on Combustion (Reinhold, New York, 1956) p. 512.

6. Blackshear, P. L., Jr., W. D. Rayle, and L. K. Tower, NACA TN 3567 (1955).

7. Boden, R. H., Trans. ASME 73, 385 (1951).

8. Boys, S. F., and J. Corner, Proc. Roy Soc. (London) A 197, 90 (1949)

9. Churchill, S. W. "Convective Heat Transfer from a Gas Stream at High Temperature to a Cylinder Normal to the Flow," Ph.D. Thesis, University of Michigan 1953.

10. Damkohler, G., Z. Electrochem 46, 601 (1940)

11. DeZubay, A. E., Aero Digest 61, 54 (1950)

12. Dunlap, R. A., "Resonance of a Flame in a Parallel Walled Combustion Chamber," University of Michigan, Rept. No. UMM-43, March 1950.

13. Dunlap, R. A., "An Investigation Into Resonance in Ramjet-Type Burners," AF Technical Report 6588, University of Michigan, October 1950.

14. Fenn, J. B., H. B. Forney,, and R. C. Garmon, Ind. Eng. Chem. 43, 1663 (1951).

15. Gordon, R., J. Am. Rocket Soc. 22, 65 (1950).

16. Greenfield, S., J. Aero Sci. 18, 512 (1951).

17. Hahnemann, H., and L. Ehret, NACA TM 1271 (1950).

18. Hammaker, F. G. Jr., and T. E. Hampel, Am. Gas Assoc. Labs., Research Rept. No. 1255 (1956).

19. Havemann, H. A., J. Indian Inst. Sci. 37B, 58, 121, (1955).

20. Havemann, H. A., and N. N. Narayan Rao, Nature (London) 174, 41 (1954).

21. Hilsenrath, J., et al. National Bureau of Standards Circular 564 (1955).

22. Hirschfelder, J. O., "Heat Transfer in Chemically Reacting Gas Mixtures," WIS-ONR-18, Naval Research Lab., University of Wisconsin (1956).

23. Hirschfelder, J. O., and C. F. Curtiss, Third Symposium on Combustion, Flame, and Explosion Phenomena (Williams and Wilkins Co., Baltimore, 1949) p. 121.

24. Jackson, E. G., and J. K. Kilham, Ind. Eng. Chem. 48, 2077 (1956)

25. Jenson, W. P., Jet Propulsion 26, 499 (1956).

26. Jost, W., "Explosion and Combustion Processes in Gases," (McGraw-Hill, New York, 1946).

27. Karlovitz, B., National Bureau of Standards Ciruclar No. 523 (1954) p. 523.

28. Karlovitz, B., D. W. Denniston, Jr., and F. E. Wells, J. Chem. Phys. 19, 541 (1951).

29. Kaskan, W. E., Fourth Symposium (International) on Combustion (Williams and Wilkins, Baltimore, 1953) p. 575.

30. Kaskan, W. E., and A. E. Noreen, Trans, ASME 77, 885 (1955).

31. Kilham, J. K., Third Symposium on Combustion, Flame, and Explosion Phenomena, (Williams and Wilkins, Baltimore, 1949) p. 733.

32. Kippenham, C. J., and H. O. Croft, Trans. ASME 74, 1151 (1952).

33. Kubanskii, P. N., Zh. Tekh. Fiz. 22, 585, 593 (No. 4, 1952).

34. Lemlich, R., Ind. Eng. Chem. 47, 1175 (1955).

35. Linke, W., Zetschrift V. D. I. 95, 1179 (1953).

36. Longwell, J. P., Fourth Symposium (International) on Combustion (Williams and Wilkins, Baltimore, 1953) p. 90.

37. Longwell, J. P., Combustion Researches and Reviews (Butterworth, London, 1955), p. 58.

38. Longwell, J. P., E. E. Frost, and M. A. Weiss, Ind. Eng. Chem. 45, 1629 (1953).

39. Longwell, J. P., and M. A. Weiss, Ind. Eng. Chem. 47, 1634 (1955).

40. Loshaek, S., R. S. Fein, and H. L. Olsen, J. Acoust. Soc. Am. 21, 605 (1949).

41. Martinelli, R. C., Trans. ASME 65, 789 (1943).

42. McAdams, W. H., "Heat Transmission" (McGraw-Hill, New York, 1954).

43. Moore, F. K., and S. H. Maslen, NACA TN 3152 (1954).

44. Morse, P. M., Vibration and Sound, (McGraw-Hill, New York, 1948).

45. Mullen, J. W., J. B. Fenn, and R. C. Garmon, Ind. Eng. Chem. 43, 195 (1951).

46. Nicholson, H. M., and J. P. Fields, Third Symposium on Combustion, Flame, and Explosion Phenomena (Williams and Wilkins, Baltimore, 1949) p. 44.

47. Perry, J. H., "Chemical Engineers Handbook", (McGraw-Hill, New York, 1950).

48. Petrein, R. J., J. P. Longwell, and M. A. Weiss, Jet Propulsion 26, 81 (1956).

49. Putnam, A. A., and W. R. Dennis, Trans. ASME 75, 15 (1953).

50. Putnam, A. A. and W. R. Dennis, Fourth Symposium (International) on Combustion (Williams and Wilkins, 1953) p. 566

51. Putnam, A. A., and W. R. Dennis, Trans. ASME 77, 875 (1955).

52. Putnam, A. A., and W. R. Dennis, ASME Paper No. 55-5A-48 (1955).

53. Putnam, A. A., and W. R. Dennis, Sixth Symposium (International) on Combustion (Reinhold, N. Y., 1957) p. 493.

54. Rayleigh, Lord, "The Theory of Sound," Vol II (Dover Publ., 1945).

55. Richardson, E. G., "Dynamics of Real Fluids" (Arnold, London, 1950) p. 39.

56. Rogers, D. E., Personal Communication, University of Michigan, 1957.

57. Rogers, D. E., and F. E. Marble, Jet Propulsion 26, 456 (1956).

58. Ross, P. A., Jet Propulsion 28, 123 (1958).

59. Rossini, F. D., et al., National Bureau of Standards Circular 500.

60. Scadron, M. D., and I. Warshawsky, NACA TN 2599 (1952).

61. Schmidt, E., H. Steinicke, and U. Neubert, Fourth Symposium (International) on Combustion (Williams and Wilkins, 1953) p. 658.

62. Scurlock, A. C., Meteor Report No. 19, Massachusetts Institute of Technology, May 1948.

63. Shorin, S. N., and K. N. Pravoverov, Izvest. Akad. Nauk. S.S.S.R., Otdel. Tekh. Nauk. 1953, 1122.

64. Smith, R. P., and D. F. Sprenger, Fourth Symposium (International) on Combustion, (Williams and Wilkins, 1953) p. 893.

65. Spalding, D. B., Aircraft Eng. 25, 264 (1953).

66. Summerfield, M., "Heat Transfer Symposium," University of Michigan, 1952, p. 151.

67. Summerfield, M., S. H. Reiter, V. Kebely, and R. W. Mascolo, Jet Propulsion 25, 377 (1955).

68. Sutton, G. P., J. British Interplanetary Soc. 15, 192 (1956).

69. Tailby, S. R., and M. A. Saleh, Trans. Inst. Chem. Eng. (London) 31, 36 (1953).

70. Timofeev, V. N., and V. A. Uspenskii, Izvest. Akad. Nauk. S.S.S.R., Otdel. Tekh. Nauk. 1956, No. 9, p. 111.

71. Tischler, A. O. and T. Male, Proceedings of the Gas Dynamics Symposium on Aerothermochemistry, Northwestern University (1956) p. 71.

72. Topper, L., Ind. Eng. Chem., 46, 2551 (1954).

73. Truman, J. C., and R. T. Newton, Ind. Eng. Chem. 47, 1183 (1955).

74. Tsien, H. S., J. Applied Mechanics 73, 188 (1951).

75. Weir, Alex Jr., D. E. Rogers, and R. E. Cullen, University of Michigan Report UMM-74 (Sept. 1950).

76. Weir, Alex Jr., T. C. Adamson, and R. B. Morrison, "Combustion," Notes for a summer session course, University of Michigan, 1955.

77. West, F. B., and A. T. Taylor, Chem. Eng. Prog. 48, 39 (1952).

78. Westenberg, A. A., W. G. Berl, and J. L. Rice, Proceedings of the Gas Dynamics Symposium on Aerothermochemistry, Northwestern University (1956) p. 211.

79. Wilkerson, E. C., and J. B. Fenn, Fourth Symposium (International) on Combustion, (Williams and Wilkins, 1953) p. 749.

80. Williams, G. C., H. C. Hottel, and A. C. Scurlock, Third Symposium on Combustion, Flame, and Explosion Phenomena (Williams and Wilkins, 1949) p. 21.

81. Williams, G. C., P. T. Woo, and C. W. Shipman, Sixth Symposium (International) on Combustion (Reinhold, 1957) p. 427.

82. Winter, E. F., Fuel 34, 409 (1955).

83. Zelinski, J. J., W. T. Baker, L. J. Matthews III, and E. C. Bagnell, Proceedings of the Gas Dynamics Symposium on Aerothermochemistry, Northwestern University (1956) p. 179.

84. Zellnik, H. E., "Heat Transfer from Hot Gases Inside Circular Tubes," Ph.D. Thesis, University of Michigan, 1956.

85. Ziebland, H., J. Brit. Interplan. Soc. 14, 249 (1955).

86. Zukoski, E. E., and F. E. Marble, Proceedings of the Gas Dynamics Symposium on Aerothermochemistry, Northwestern University (1956), p. 205.